Title
Defining Antiviral T Cell Responses Elicited by Vaccines versus Infection in HIV-1 and in SARS-CoV-2

Author
Taus, Ellie Abigail

Publication Date
2022

Peer reviewed|Thesis/dissertation

UNIVERSITY OF CALIFORNIA

Los Angeles

Defining Antiviral T Cell Responses Elicited by Vaccines versus Infection in HIV-1 and in SARS-CoV-2

A dissertation submitted in partial satisfaction of the requirements for the degree of Doctor of Philosophy in Molecular and Medical Pharmacology

by

Ellie Abigail Taus

2022

ABSTRACT OF THE DISSERTATION

Defining Antiviral T Cell Responses
Elicited by Vaccines versus Infection
in HIV-1 and in SARS-CoV-2

by

Ellie Abigail Taus
Doctor of Philosophy in Molecular and Medical Pharmacology
University of California, Los Angeles, 2022
Professor Otto Orlean Yang, Co-Chair
Professor Donald Barry Kohn, Co-Chair

Viruses have plagued humanity for thousands of years, but it is only in the last few centuries that we have even begun to develop vaccines and therapeutics to manage them. While we now have myriad vaccines that reduce death and suffering hugely compared to even half a century ago, millions of people still die every year from viral infections—some of which are preventable given current vaccines. Part of this is attributable to inequities that persist globally, but many deaths still result from diseases that we have been unable to control adequately.

The main issues in producing effective vaccines derive from two factors: inability to induce an adequate immune response, and the ability of the pathogen to avoid an

immune response. In many cases, such as HIV-1, certain flu strains, and hepatitis C virus, both are an issue. In HIV-1, a high tolerance for mutations allows for rapid escape from antibodies, which are adequate to prevent infection for many other pathogens. Conversely, we do not have methods to reliably generate T cell responses capable of broad recognition, and it is unknown whether doing so would even suffice. However, to approach more mechanistic explanations of how particular conditions affect an immune response, it is valuable to study the results of all vaccine trials, failed or otherwise. To this end, I characterize the antiviral capabilities of $CD8^+$ cytotoxic T lymphocyte (CTL) clones that were elicited by the Mrk/Ad5 vaccine, a recombinant adenoviral vector that introduced single variants of the HIV-1 *gag, pol*, and *nef* genes. By testing their ability to kill and suppress virus-infected cells, I found that most clones were able to efficiently target the sequence used in the vaccine, but each exhibited very limited antiviral functions when tested against common epitope variants.

The most recent pandemic, caused by SARS-CoV-2, has killed millions in a span of a few years, despite public health measures and rapid development of vaccines. A common issue seen in both SARS-CoV-2 vaccination and after infection is an apparent rapid waning of immune responses. As T cells are very important in containing and clearing most viral infections, it is crucial to characterize their responses in these contexts. By testing responses against SARS-CoV-2 structural proteins, I characterize the distribution of CTL targeting, the immunodominance of this targeting, and the persistence of different T cell responses elicited in either natural infection or SARS-CoV-2 mRNA vaccination.

The dissertation of Ellie Abigail Taus is approved.

Ting-Ting Wu

Gay M. Crooks

Donald Barry Kohn, Committee Co-Chair

Otto Orlean Yang, Committee Co-Chair

University of California, Los Angeles

2022

TABLE OF CONTENTS

LIST OF FIGURES & TABLES

ACKNOWLEDGEMENTS

I would first like to thank my advisor, Dr. Otto O. Yang, for everything he's done for me over the years. He has made time for me when I've had questions, has freely given additional guidance when I've asked for it, and has been compassionate when I have struggled. He does not suffer foolishness, and I very much appreciate that as well. I am also grateful for the time, patience, and guidance of the other members of my committee: Dr. Gay Crooks, Dr. Don Kohn, and Dr. Ting-Ting Wu.

I would like to express my gratitude to Emily Fitch, whose competence is truly a blessing upon the Pharmacology department.

I appreciate all the help, guidance, support, and advice from everyone who has been part of the Yang lab while I have been a member. I only wish I could've baked for you all more.

The love and support of I have received over the years from friends and family have helped me get through—at times really trudging along. Emani, Karen, Dow, Carolina, Lisa, Rex, so many more… thank you and I love you all.

Mom and dad, your unconditional love has helped me in times when I felt lost. I'd especially like to thank Xiuli Wang for introducing me to the fascinating world of immunology and encouraging me to be a researcher.

I would also like to acknowledge the role that certain forms of entertainment have had in helping me in the last number of years, either through enduring boredom or just lifting my mood… Got7, my favorite podcasts (the history chicks, two dope queens, couples therapy, getting curious, all of Nicole Byer's material…), and the countless clips

of standup comedy from James Acaster, Naomi Ekperigin, Daniel Sloss, Hari Kondabolu, Tom Segura, Dara O'Briain, and so many others.

I am also incredibly grateful for everyone who has generously participated in trials and provided samples for this research—it is only possible with their help.

I would like to acknowledge the resources provided by the UCLA AIDS Institute and the James B. Pendleton Trust, as well as the following sources for funding my work:

- NIH U01 AI068618 subcontract, "Delineating Potential CTL Failure Mechanisms of the STEP Trial," 6/1/2008-5/31/2011, Subcontract **P.I. Yang**, P.I. McElrath
- AIDS Healthcare Foundation Grant, "Identifying and Closing Gaps in TCR Coverage of HIV-1 Escape," 5/1/2013-4/30/2018, **P.I. Yang**
- NIH R01 DE025166, "Dissection of HIV-1 CTL Escape Pathways," 9/13/2014-8/31/2019, **P.I. Yang**

Chapter 3 of this dissertation is a modified version of the following publication:

Taus E, Hofmann C, Ibarrondo FJ, Hausner MA, Fulcher JA, Krogstad P, Ferbas KG, Tobin NH, Rimoin AW, Aldrovandi GM, Yang OO. Dominant $CD8^+$ T Cell Nucleocapsid Targeting in SARS-CoV-2 Infection and Broad Spike Targeting From Vaccination. Front Immunol. 2022 Feb 22;13:835830. doi: 10.3389/fimmu.2022.835830. PMID: 35273611; PMCID: PMC8902813.

Chapter 4 of this dissertation is a modified version of the following:

Taus E, Hofmann C, Ibarrondo FJ, Hausner MA, Krogstad P, Ferbas KG, Tobin NH, Rimoin AW, Aldrovandi GM, Yang OO. Persistence of Spike-Specific Memory T cells months out from mRNA vaccination in Healthy, Vaccinated Individuals. In preparation.

VITA

Education

UC Berkeley, Berkeley, California

- B.A. Molecular and Cellular Biology, Immunology emphasis, May 2013
- Latin minor

Research Experience

PhD Candidate: Dr. Otto Yang Lab, Dept. of Molecular & Medical Pharmacology, UCLA

- Research areas: $CD8^+$ T cell antiviral activity, specificity, and responses in vaccination and infection

Research Associate I: Dr. Steve Forman Lab, Dept. of Cancer Immunotherapeutics and Tumor Immunology, City of Hope: July 2013-June 2015, 40hr/wk

- Supervisor: Dr. Xiuli Wang
- Research area: CAR T cell therapy in hematological cancers

Undergraduate Researcher: Dr. Greg Barton Lab, UC Berkeley: September 2011-May 2013

- Research area: expression and trafficking of endosomal TLRs and their associated molecules

Summer Intern Researcher: Dr. Steve Forman Lab, Dept. of Cancer Immunotherapeutics and Tumor Immunology, City of Hope: June-August 2011, June-August 2012

- Supervisor: Dr. Xiuli Wang
- Research area: CAR T cell therapy in hematological cancers

Publications

Taus E, Hofmann C, Ibarrondo FJ, Hausner MA, Fulcher JA, Krogstad P, Ferbas KG, Tobin NH, Rimoin AW, Aldrovandi GM, Yang OO. Dominant $CD8^+$ T Cell Nucleocapsid Targeting in SARS-CoV-2 Infection and Broad Spike Targeting From Vaccination. Front Immunol. 2022 Feb 22;13:835830. doi: 10.3389/fimmu.2022.835830. PMID: 35273611; PMCID: PMC8902813.

Taus E, Hofmann C, Ibarrondo FJ, Gong LS, Hausner MA, Fulcher JA, Krogstad P, Ferbas KG, Weiskopf D, Sette A, Tobin NH, Rimoin AW, Aldrovandi GM, Yang OO. Rapid Contraction of Circulating SARS-CoV-2-Specific T Cells but Persistent Memory after mRNA Vaccination Compared to Infection. In preparation.

Ibarrondo FJ, Hofmann C, Fulcher JA, Goodman-Meza D, Mu W, Hausner MA, Ali A, Balamurugan A, **Taus E**, Elliott J, Krogstad P, Tobin NH, Ferbas KG, Kitchen SG, Aldrovandi GM, Rimoin AW, Yang OO. Primary, Recall, and Decay Kinetics of SARS-CoV-2 Vaccine Antibody Responses. ACS Nano. 2021 Jun 23. doi: 10.1021/acsnano.1c03972. Epub ahead of print. PMID: 34159781.

Wang X, Wong CW, Urak R, **Taus E**, Aguilar B, Chang WC, Mardiros A, Budde LE, Brown CE, Berger C, Forman SJ, Jensen MC. Comparison of naïve and central memory derived $CD8^+$ effector cell engraftment fitness and function following adoptive transfer. Oncoimmunology. 2015 Aug 20;5(1):e1072671. doi: 10.1080/2162402X.2015.1072671. PMID: 26942092; PMCID: PMC4760301.

Munoz A*, Urak R*, **Taus E**, Hsieh C, Jin K, Lin SH, Priceman SJ, Clark MC, Forman SJ, Wang X. Dexamethasone Enhances CAR T Cell Persistence and Function by Upregulating Interleukin 7 Receptor. Submitted.

Chapter 1: Introduction

Brief History of Vaccines

The history of vaccines is remarkably recent. Public health measures have produced astounding successes in reducing infectious diseases despite the fact that the vast majority of vaccines have only been around since the mid-twentieth century.

In 1798, Edward Jenner first tested the use of what was thought to be cowpox virus for inoculation in humans as a means to protect against smallpox. As it proved to be highly effective and quite safe, many consider this to be the first vaccine. Although Jenner receives the bulk of the credit, there were also others who made similar observations and attempts at around the same time. Additionally, for centuries prior to this, people in other parts of the world had been reducing the dangers associated with smallpox infection through a process called variolation. Variolation entailed inoculating a person with a small amount of residue taken from a smallpox lesion to induce a milder form of the disease, though not without risk. While the 1-2% mortality rate of variolation is unimaginably high relative to later vaccines, this was drastically lower than the 30% mortality rate of smallpox that one would face without variolation. Lady Mary Wortley Montagu, after encountering widespread use of the technique in the Ottoman Empire, introduced variolation into Western Europe nearly 80 years before Jenner tested cowpox as an inoculating agent (1,2).

The next vaccine was not developed until nearly 100 years after Jenner's smallpox vaccine, when Louis Pasteur developed a live attenuated vaccine for rabies. In the first half of the twentieth century, vaccines came out for several additional diseases. As the tools and techniques to study vaccines have advanced, the rate of vaccine research and development has accelerated.

Between 1990 and 2020, the global mortality rates for both the under-5 and 5- to 9-year-old age groups decreased by 60-61%. Effective vaccination campaigns have contributed greatly to this by preventing deaths from childhood diseases such as measles, diptheria, and pertussis (3,4). Despite these impressive strides, inequity and vaccine hesitancy threaten continued progress in these areas.

To date, no pathogen has been countered as effectively as the target of the very first vaccine—smallpox—which was officially declared eradicated in 1980. While the global initiative to eradicate polio through vaccination has come very close, humanity has yet to replicate this enormous achievement. Effective vaccines have remained elusive for several infectious diseases, perhaps most notoriously for the human immunodeficiency virus (HIV-1), where myriad approaches have all failed despite nearly 40 years of sustained efforts (5,6). Historically, many vaccines were developed empirically and turned out to be relatively ‘easy targets’ to immunize against. However, many pathogens have defied numerous vaccination strategies, and new diseases continue to emerge.

These challenges are driving the development of novel vaccine platforms, as well as further study into immunology, host-microbe interactions, and molecular biology. Many modern vaccinologists hope that a deeper understanding of these mechanisms will allow for ‘rational design’ of vaccines—that is, the ability to more accurately predict how to generate protection and reliably manipulate immune responses.

Vaccine Types

Vaccines are biological products or derivatives that are used to elicit immune memory capable of providing some degree of protection against a pathogen without requiring natural exposure to the pathogen. Efficacy and a high level of safety are absolute requirements for a vaccine, but additional practical factors, like scalability, cost, infrastructure, and patient adherence can also affect the decisions in vaccine regimens (7). The emergence of new diseases, ongoing challenges in creating effective and/or durable immunity, and interest in expanding the use of vaccines beyond protection from pathogens, have driven innovation in all aspects of vaccines (8).

All vaccines contain a biological or biological-derivative antigenic component that defines the specificity of a vaccine. This is the primary target of the immune response and the antigen that the immune system should respond to upon exposure to pathogen if the vaccine effectively produces immunological memory. The second vaccine ever developed was a live attenuated virus to vaccinate against rabies. To this day, live-attenuated viruses remain a useful vaccine platform for many diseases, including the measles, mumps, and rubella (MMR) vaccine (9), though particular live-attenuated vaccines can pose risks to immunocompromised individuals. There are many forms of non-living biological elements of vaccines, including killed whole organism, toxoid, subunit vaccines made with proteins or polysaccharides, virus-like particles, viral vectors, and DNA- or RNA-based vaccines (7). There are also experimental vaccination platforms being developed, with particular interest in cell-based vaccination in the realm of cancer treatments (10,11). See **Table 1-S1** for examples of approved vaccines for each platform and established or proposed correlates of protection for each vaccine.

The biological component is the core of a vaccine and the element which directs the specificity of the immune response. However, the ability to effectively raise an immune response or influence the type of immune response depends on several factors, which has become increasingly apparent in recent decades as a greater number of vaccination platforms and regimens are clinically tested.

Focusing in on approaches used in SARS-CoV-2 and HIV-1 vaccines illustrates many of the challenges that impede optimal immunization as well as strategies that are/have been tested to overcome them. In depth characterization of the outcome of every vaccine trial can teach us valuable lessons about how the immune system responds to particular stimuli, even—or perhaps especially—when the outcome is not as expected.

A consistent struggle across SARS-CoV-2 vaccines has been a rapid waning of the antibody-mediated protection from infection (12,13). Certain vaccines produce lifelong (14,15), or at least multiyear-long immunity, while others require periodic or even frequent boosting (16,17). Trials with SARS-CoV-2 vaccines have also highlighted the difficulty in eliciting an effective response across all ages (18). Risks due to COVID-19 increase with age, but increased age also tends to be associated with greater difficulty in generating new immune responses. Several vaccines that are administered in a series, such as the HPV (19) and HBV vaccines (20), already have set scheduling to optimize immunity. COVID-19 vaccination has also brought the effects of dose scheduling to the fore, as extended intervals between doses has been observed to result in improved antibody titers (21).

In HIV-1, scientists have attempted several approaches in clinical trials: some vaccine trials have aimed to exclusively elicit T cell-based responses, some have sought to drive entirely antibody-based immune responses, and some have pursued both (6). While broadly neutralizing antibodies do arise in HIV-infected subjects, this only occurs in a minority of cases, where they can take years to develop and are always quickly escaped within an infected individual (22,23). Nevertheless, some researchers are investigating potential ways to manipulate B cell responses and affinity maturation by sequential administration of different epitopes to direct specific changes in the hopes of quickly and consistently raising anti-HIV-broadly neutralizing antibodies (bNAbs) by vaccination (24–26). It is unclear whether it would be possible to achieve such a result reliably, but the difficulty of overcoming HIV-1 requires creative approaches to immune manipulation, and might prove useful for developing vaccines against other pathogens.

Mutations in Viruses

Most viruses that target animals go through a similar sequence of events during an infection cycle: first there is attachment, followed by penetration, uncoating, replication, assembly, and finally, release of new virions. Mutations in viral genomes are introduced within an infected cell and can occur through different mechanisms.

Mutations can affect several characteristics of a virus, including alterations in virulence (27), tropism (28,29), and drug sensitivity (30,31). Another important consequence of mutations the ability to evade immune responses, either memory responses from prior infection and/or vaccination, as well as ongoing immune responses within a host organism.

Orthomyxoviridae, the virus family that includes Alphainfluenzaviruses, Betainfluenzaviruses, and Gammainfluenzaviruses, contain RNA genomes that are divided into six to eight fragments. The co-occurrence of different strains of flu viruses can result in recombination of these fragments. This can lead to flu viruses jumping between different species of animals, with potentially heavy consequences for the affected population. This drastic change in a virus's genome is known as antigenic shift, a phenomenon mainly seen in influenzaviruses.

In contrast to antigenic shift, antigenic drift occurs in most viruses. Antigenic drift is a phenomenon wherein mutations are introduced in smaller units, often changes in a single nucleotide. The rate at which these mutations are introduced, however, varies widely between virus species. Most viruses encode their own enzymes that are involved in aspects of genome replication. Mutation rates vary greatly between the enzymes of different virus species, with selective pressures driving error rates that are most beneficial to a virus species over time. Therefore, some types of viruses have extremely stable genomes, while others are very dynamic and can introduce massive diversity very quickly.

$CD8^+$ Cytotoxic T Lymphocytes and Viral Infections

$CD8^+$ Cytotoxic T Lymphocytes (CTL) are one of the fundamental components of the adaptive immune system and are particularly important in fighting and clearing viral infections (32). CTL can directly kill virus-infected cells (33), such as cells infected with HIV-1 or SARS-CoV-2. Research into CTL activity in fighting HIV-1 hints at the potential tool they may be in ultimately developing vaccines for challenging targets. While the

CTL response is not curative, evidence from genome-wide association studies (34), clinical correlations (35–40), animal models (41,42), and in vitro testing (43) all point to CD8+ cytotoxic T lymphocytes (CTL) as the main actors of the immune system controlling viremia in HIV-1-infected individuals.

When a cell becomes infected with a virus, the virus introduces proteins into the cell, both within the virion itself and expressed after infection. Proteins within the cytoplasm of cells are regularly processed in the proteasome into peptide fragments, which are then loaded onto Major Histocompatibility Complex class I (MHC-I) molecules within the cell before being transported to the cell surface where they can be surveyed by T cells (44). A person's HLA (the human form of MHC) haplotype determines which epitopes a human is able to present to CTL, and thus limits the potential scope of responses an individual can develop (45,46).

T cells recognize infected cells through their T cell receptors, or TCR. The TCR interacts with the peptide-MHC complex in a "lock-and-key" mechanism, where the interaction has to be of a certain affinity in order for it to trigger signaling by the TCR (47,48). When mutations are introduced in sequences targeted by CTL, viruses can escape recognition. This can occur through altering the interaction between the TCR and pMHC, or by interfering with any of the steps that lead up to the epitope being presented on the cell surface (38,39,43,49,50).

An initial exposure to cognate antigen combines with additional immune signals to drive naïve CTL to mature and undergo exponential clonal expansion. As the drivers of this response diminish, the responding T cell population contracts to a much smaller, long-lived population of primarily memory cells (51). The timeline over which the kinetics

of this response play out varies, as does the magnitude of the response (52). Upon repeat exposure to antigen, they (as well as CD4+ memory T cells (53)) can become activated more easily and undergo clonal expansion much more rapidly (54). While the persistence of different memory T cells may vary, there is evidence that specific memory CD4+ and CD8+ antiviral T cell populations can endure for decades, if not a lifetime (14).

Overview of the Dissertation

The overarching goal of my research has been, and will continue to be, elucidating the development and mechanisms of immune responses. This dissertation presents my research characterizing T cell responses that have been elicited in different contexts: a T cell-based vaccine for HIV-1, recovery from SARS-CoV-2 infection, and SARS-CoV-2 mRNA vaccination in healthy subjects.

In **Chapter 2**, I test the antiviral capacities of CTL clones derived from HIV-negative individuals who received the Mrk/Ad5 vaccine, a recombinant adenovirus-vectored vaccine. Seeking to help explain the failure of this vaccine despite its ability to elicit HIV-specific T cells, I determine the ability of these clones to kill and suppress virus-infected cells, as well as exploring their ability to recognize common epitope variants.

In **Chapter 3**, I characterize T cell responses in COVID-19-convalescent individuals shortly after SARS-CoV-2 infection and in the following months. In addition to determining the prevalence of T cell responses, I map CTL targeting across the viral structural proteins to determine patterns of immunodominance in natural infection. I

follow up on this by performing similar analyses on CTL from individuals recently vaccinated against SARS-CoV-2 to show that immunogenicity and immunodominance against the spike protein are similar between infection and vaccination.

In **Chapter 4**, I further define the T cell immune response to SARS-CoV-2 mRNA vaccination in healthy subjects by evaluating the kinetics and decay/persistence of vaccine-elicited T cells. By testing longitudinal samples of expanded CTL against peptide pools, I see rapid peaks and declines in spike-specific CTL very shortly after vaccination. To check for the presence of memory T cells, I develop a technique to enrich spike-specific T cells *in vitro* using the mRNA-1273 SARS-CoV-2 vaccine and am able to show the persistence of memory cells several months after vaccination.

Vaccine Platform	Examples of Successful Vaccines	Established Correlates/Surrogates of protection
Live attenuated	Measles, oral polio vaccine, yellow fever	Measles: microneutralization Yellow fever & polio: neutralization by antibodies
Killed whole organism	Pertussis, polio, influenza	Influenza: hemagglutination inhibition; pertussis: ELISA against toxin
Toxoid	Diphtheria, tetanus	Diphtheria & tetanus: toxin neutralization (antibody-based)
Subunit (e.g. protein, polysaccharide)	HBV, typhoid, meningococcal	HBV: ELISA; meningococcal: bactericidal activity from antibodies
Virus-like particle	HPV	Not defined
Outer membrane vesicle	Group B meningococcal	meningococcal: bactericidal activity from antibodies
Protein-polysaccharide conjugate	*H. influenzae* type B, pneumococcal	*H. influenzae* type B: ELISA of antibodies
Viral vectored	Ebola	Not defined, seems to involve both humoral & cellular immune responses
Nucleic Acid (RNA+ lipid coat or DNA)	SARS-CoV-2	Neutralization titer (for mRNA vaccination)
Bacterial vectored	*Experimental	N/A
Antigen-presenting cell	*Experimental	N/A

Table 1-S1: The first column shows many of the vaccine platforms currently in use or under investigation. The second column contains examples of important vaccines for each vaccine platform. Immunological responses to vaccines are monitored and analyzed for certain measurements that highly correlate with vaccine efficacy—the correlates of protection. The third column indicates the test used to determine the likelihood that an individual will have protection based on previously defined values.

Table adapted from the following sources: Pollard and Bijker, Nat. Rev. Immun. 2021 (7); Plotkin, CVI, 2010 (55); Plotkin, Vaccine, 2020 (56).

REFERENCES

1. Nature Milestones in Vaccines [Internet]. [cited 2022 Jul 18]. Available from: https://www.nature.com/immersive/d42859-020-00005-8/index.html

2. Smallpox: Variolation [Internet]. U.S. National Library of Medicine; [cited 2022 Jul 18]. Available from: https://www.nlm.nih.gov/exhibition/smallpox/sp_variolation.html

3. Immunization coverage [Internet]. [cited 2022 Jul 18]. Available from: https://www.who.int/news-room/fact-sheets/detail/immunization-coverage

4. Child mortality and causes of death [Internet]. [cited 2022 Jul 18]. Available from: https://www.who.int/data/gho/data/themes/topics/topic-details/GHO/child-mortality-and-causes-of-death

5. Martin AR, Siliciano RF. Progress Toward HIV Eradication: Case Reports, Current Efforts, and the Challenges Associated with Cure. Annu Rev Med. 2016;67(1):215–28.

6. Tomaras GD, Plotkin SA. Complex immune correlates of protection in HIV-1 vaccine efficacy trials. Immunol Rev. 2017 Jan 1;275(1):245–61.

7. Pollard AJ, Bijker EM. A guide to vaccinology: from basic principles to new developments. Nat Rev Immunol. 2021 Feb;21(2):83–100.

8. Kumar A, Meldgaard TS, Bertholet S. Novel Platforms for the Development of a Universal Influenza Vaccine. Front Immunol. 2018;9:600.

9. Measles-Mumps-Rubella (MMR) Vaccine Information Statement | CDC [Internet]. 2022 [cited 2022 Jul 26]. Available from: https://www.cdc.gov/vaccines/hcp/vis/vis-statements/mmr.html

10. Roy S, Sethi TK, Taylor D, Kim YJ, Johnson DB. Breakthrough concepts in immune-oncology: Cancer vaccines at the bedside. J Leukoc Biol. 2020 Oct;108(4):1455–89.

11. Song Q, Zhang CD, Wu XH. Therapeutic cancer vaccines: From initial findings to prospects. Immunol Lett. 2018 Apr;196:11–21.

12. Ibarrondo FJ, Hofmann C, Fulcher JA, Goodman-Meza D, Mu W, Hausner MA, et al. Primary, Recall, and Decay Kinetics of SARS-CoV-2 Vaccine Antibody Responses. ACS Nano. 2021 Jul 27;15(7):11180–91.

13. Goldberg Y, Mandel M, Bar-On YM, Bodenheimer O, Freedman L, Haas EJ, et al. Waning Immunity after the BNT162b2 Vaccine in Israel. N Engl J Med. 2021 Dec 9;385(24):e85.

14. Hammarlund E, Lewis MW, Hansen SG, Strelow LI, Nelson JA, Sexton GJ, et al. Duration of antiviral immunity after smallpox vaccination. Nat Med. 2003 Sep;9(9):1131–7.

15. Who. Vaccines and vaccination against yellow fever: WHO Position Paper, June 2013--recommendations. Vaccine. 2015 Jan 1;33(1):76–7.

16. Burdin N, Handy LK, Plotkin SA. What Is Wrong with Pertussis Vaccine Immunity? The Problem of Waning Effectiveness of Pertussis Vaccines. Cold Spring Harb Perspect Biol. 2017 Dec 1;9(12):a029454.

17. Milligan R, Paul M, Richardson M, Neuberger A. Vaccines for preventing typhoid fever. Cochrane Database Syst Rev. 2018 May 31;5:CD001261.

18. Collier DA, Ferreira IATM, Kotagiri P, Datir R, Lim E, Touizer E, et al. Age-related immune response heterogeneity to SARS-CoV-2 vaccine BNT162b2. Nature. 2021 Jun 30;1–9.

19. Lei J, Ploner A, Elfström KM, Wang J, Roth A, Fang F, et al. HPV Vaccination and the Risk of Invasive Cervical Cancer. N Engl J Med. 2020 Oct 1;383(14):1340–8.

20. CDC. Hepatitis B - Vaccination of Adults | CDC [Internet]. Centers for Disease Control and Prevention. 2022 [cited 2022 Aug 4]. Available from: https://www.cdc.gov/hepatitis/hbv/vaccadults.htm

21. Flaxman A, Marchevsky NG, Jenkin D, Aboagye J, Aley PK, Angus B, et al. Reactogenicity and immunogenicity after a late second dose or a third dose of ChAdOx1 nCoV-19 in the UK: a substudy of two randomised controlled trials (COV001 and COV002). Lancet Lond Engl. 2021 Sep 11;398(10304):981–90.

22. Burton DR, Hangartner L. Broadly Neutralizing Antibodies to HIV and Their Role in Vaccine Design. Annu Rev Immunol. 2016;34(1):635–59.

23. Wei X, Decker JM, Wang S, Hui H, Kappes JC, Wu X, et al. Antibody neutralization and escape by HIV-1. Nature. 2003 Mar 20;422(6929):307–12.

24. Sadanand S, Suscovich TJ, Alter G. Broadly Neutralizing Antibodies Against HIV: New Insights to Inform Vaccine Design. Annu Rev Med. 2016;67(1):185–200.

25. Sok D, Le KM, Vadnais M, Saye-Francisco KL, Jardine JG, Torres JL, et al. Rapid elicitation of broadly neutralizing antibodies to HIV by immunization in cows. Nature. 2017 Aug;548(7665):108–11.

26. Cirelli KM, Carnathan DG, Nogal B, Martin JT, Rodriguez OL, Upadhyay AA, et al. Slow Delivery Immunization Enhances HIV Neutralizing Antibody and Germinal Center Responses via Modulation of Immunodominance. Cell. 2019 May 16;177(5):1153-1171.e28.

27. Mandary MB, Poh CL. Changes in the EV-A71 Genome through Recombination and Spontaneous Mutations: Impact on Virulence. Viruses. 2018 Jun 12;10(6):E320.

28. Rothenburg S, Brennan G. Species-Specific Host-Virus Interactions: Implications for Viral Host Range and Virulence. Trends Microbiol. 2020 Jan;28(1):46–56.

29. Naffakh N, Tomoiu A, Rameix-Welti MA, van der Werf S. Host restriction of avian influenza viruses at the level of the ribonucleoproteins. Annu Rev Microbiol. 2008;62:403–24.

30. Giacomelli A, Pezzati L, Rusconi S. The crosstalk between antiretrovirals pharmacology and HIV drug resistance. Expert Rev Clin Pharmacol. 2020 Jul;13(7):739–60.

31. Li DK, Chung RT. Overview of Direct-Acting Antiviral Drugs and Drug Resistance of Hepatitis C Virus. Methods Mol Biol Clifton NJ. 2019;1911:3–32.

32. Nikolich-Zugich J, Slifka MK, Messaoudi I. The many important facets of T-cell repertoire diversity. Nat Rev Immunol. 2004 Feb;4(2):123–32.

33. Yang OO, Kalams SA, Rosenzweig M, Trocha A, Jones N, Koziel M, et al. Efficient lysis of human immunodeficiency virus type 1-infected cells by cytotoxic T lymphocytes. J Virol. 1996 Sep 1;70(9):5799–806.

34. International HIV Controllers Study, Pereyra F, Jia X, McLaren PJ, Telenti A, de Bakker PIW, et al. The major genetic determinants of HIV-1 control affect HLA class I peptide presentation. Science. 2010 Dec 10;330(6010):1551–7.

35. Koup RA, Safrit JT, Cao Y, Andrews CA, McLeod G, Borkowsky W, et al. Temporal association of cellular immune responses with the initial control of viremia in primary human immunodeficiency virus type 1 syndrome. J Virol. 1994 Jul;68(7):4650–5.

36. Borrow P, Lewicki H, Hahn BH, Shaw GM, Oldstone MB. Virus-specific CD8+ cytotoxic T-lymphocyte activity associated with control of viremia in primary human immunodeficiency virus type 1 infection. J Virol. 1994 Sep;68(9):6103–10.

37. Borrow P, Lewicki H, Wei X, Horwitz MS, Peffer N, Meyers H, et al. Antiviral pressure exerted by HIV-1-specific cytotoxic T lymphocytes (CTLs) during primary infection demonstrated by rapid selection of CTL escape virus. Nat Med. 1997 Feb;3(2):205–11.

38. Geels MJ, Cornelissen M, Schuitemaker H, Anderson K, Kwa D, Maas J, et al. Identification of sequential viral escape mutants associated with altered T-cell responses in a human immunodeficiency virus type 1-infected individual. J Virol. 2003 Dec;77(23):12430–40.

39. Jamieson BD, Yang OO, Hultin L, Hausner MA, Hultin P, Matud J, et al. Epitope escape mutation and decay of human immunodeficiency virus type 1-specific CTL responses. J Immunol Baltim Md 1950. 2003 Nov 15;171(10):5372–9.

40. Ndhlovu ZM, Kamya P, Mewalal N, Kløverpris HN, Nkosi T, Pretorius K, et al. Magnitude and Kinetics of CD8+ T Cell Activation during Hyperacute HIV Infection Impact Viral Set Point. Immunity. 2015 Sep 15;43(3):591–604.

41. Kuroda MJ, Schmitz JE, Charini WA, Nickerson CE, Lifton MA, Lord CI, et al. Emergence of CTL coincides with clearance of virus during primary simian immunodeficiency virus infection in rhesus monkeys. J Immunol Baltim Md 1950. 1999 May 1;162(9):5127–33.

42. Barouch DH, Kunstman J, Kuroda MJ, Schmitz JE, Santra S, Peyerl FW, et al. Eventual AIDS vaccine failure in a rhesus monkey by viral escape from cytotoxic T lymphocytes. Nature. 2002 Jan 17;415(6869):335–9.

43. Yang OO, Sarkis PTN, Ali A, Harlow JD, Brander C, Kalams SA, et al. Determinants of HIV-1 Mutational Escape From Cytotoxic T Lymphocytes. J Exp Med. 2003 May 19;197(10):1365–75.

44. Germain RN. MHC-dependent antigen processing and peptide presentation: providing ligands for T lymphocyte activation. Cell. 1994 Jan 28;76(2):287–99.

45. Haskins K, Kubo R, White J, Pigeon M, Kappler J, Marrack P. The major histocompatibility complex-restricted antigen receptor on T cells. I. Isolation with a monoclonal antibody. J Exp Med. 1983 Apr 1;157(4):1149–69.

46. Adams JJ, Narayanan S, Birnbaum ME, Sidhu SS, Blevins SJ, Gee MH, et al. Structural interplay between germline and adaptive recognition determines TCR-peptide-MHC cross-reactivity. Nat Immunol. 2016 Jan;17(1):87–94.

47. Gudmundsdottir H, Wells AD, Turka LA. Dynamics and Requirements of T Cell Clonal Expansion In Vivo at the Single-Cell Level: Effector Function Is Linked to Proliferative Capacity. J Immunol. 1999 May 1;162(9):5212–23.

48. Pettmann J, Huhn A, Abu Shah E, Kutuzov MA, Wilson DB, Dustin ML, et al. The discriminatory power of the T cell receptor. Graw F, Taniguchi T, editors. eLife. 2021 May 25;10:e67092.

49. Iglesias MC, Almeida JR, Fastenackels S, Bockel DJ van, Hashimoto M, Venturi V, et al. Escape from highly effective public CD8+ T-cell clonotypes by HIV. Blood. 2011 Aug 25;118(8):2138–49.

50. Appay V, Iglesias MC. Antigen sensitivity and T-cell receptor avidity as critical determinants of HIV control. Curr Opin HIV AIDS. 2011 May;6(3):157–62.

51. Murali-Krishna K, Altman JD, Suresh M, Sourdive DJD, Zajac AJ, Miller JD, et al. Counting Antigen-Specific CD8 T Cells: A Reevaluation of Bystander Activation during Viral Infection. Immunity. 1998 Feb 1;8(2):177–87.

52. Akondy RS, Monson ND, Miller JD, Edupuganti S, Teuwen D, Wu H, et al. The Yellow Fever Virus Vaccine Induces a Broad and Polyfunctional Human Memory CD8+ T Cell Response. J Immunol Baltim Md 1950. 2009 Dec 15;183(12):7919–30.

53. Rogers PR, Dubey C, Swain SL. Qualitative changes accompany memory T cell generation: faster, more effective responses at lower doses of antigen. J Immunol Baltim Md 1950. 2000 Mar 1;164(5):2338–46.

54. Wherry EJ, Teichgräber V, Becker TC, Masopust D, Kaech SM, Antia R, et al. Lineage relationship and protective immunity of memory CD8 T cell subsets. Nat Immunol. 2003 Mar;4(3):225–34.

55. Plotkin SA. Correlates of Protection Induced by Vaccination. Clin Vaccine Immunol. 2010 Jul;17(7):1055–65.

56. Plotkin SA. Updates on immunologic correlates of vaccine-induced protection. Vaccine. 2020 Feb 24;38(9):2250–7.

Chapter 2: Limited Antiviral Cross-Reactivity to HIV-1 Epitope Variants by CD8+ Cytotoxic T Lymphocytes Elicited by the Merck/rAd5 Vaccine

INTRODUCTION

The human immunodeficiency virus (HIV-1), the causative agent of acquired immunodeficiency syndrome (AIDS), was first identified in 1983 (40). Despite initial optimism that this might allow for the swift development of prophylactic and curative interventions, humanity has yet to develop either a preventive vaccine or a broadly applicable cure for infection with HIV-1. Approximately 79.3 million people have been infected with HIV-1 to date, resulting in an estimated 36.3 million deaths. As of 2020, there were roughly 37.7 million people living with HIV-1 (PLWH) worldwide (1).

The development of several extremely effective antiretroviral therapy (ART) drugs has reduced an HIV-1 diagnosis, which was once a death sentence for many, to an infection that can be well-controlled in most people with proper and consistent medications (2). However, as of mid-2020, there were still around 9.5 million PLWH who did not have access to ART, including almost half of children aged 14 and under (3). Additionally, at any given time, many people are not aware of their HIV-1 status. In 2020, over 6 million people were unaware of their HIV+ status, and the number has likely only increased as the COVID-19 pandemic interfered with all aspects of HIV-1 outreach, education, and treatment (3,4). Widespread and effective use of antiretrovirals poses many challenges, including enormous financial burden (with universal ART estimated to cost up to 8% of a country's GDP in highest-burden countries (5)), patient adherence, overcoming stigma, and basic access to healthcare (6). In 2020, there were 680,000 deaths from AIDS-related illnesses, and despite progress in reducing infection rates, there were approximately 1.5 million new infections (3).

Both preventive vaccines and curative treatments for HIV-1 are of enormous import to public health. While there have been several vaccine trials aimed at providing protective immunity against HIV-1, an effective vaccine has proven elusive. A major barrier in the development of either a preventive vaccine or curative intervention is the lack of naturally occurring protective immunity to emulate, as well as inherent challenges posed by the virus, including latency and lack of sequence conservation (6).

Evidence from genome-wide association studies (7), clinical correlations (8–13), animal models (14,15), and in vitro testing (16) all point to CD8+ cytotoxic T lymphocytes (CTL) as the main actors of the immune system controlling HIV-1 viremia in infected individuals. Based on these data, there have been efforts to provide protective immunity by inducing CTL responses in uninfected individuals (17,18). The HIV Vaccine Trial Network (HVTN) attempted to do so in trials using a recombinant adenovirus type 5 (rAd5) vector carrying single sequences of *gag*, *pol*, and *nef* portions of the HIV-1 genome (the Merck rAd5, or Mrk/Ad5 vaccine). The vaccine generated HIV-specific CTL in the majority of vaccinated individuals as determined by IFN-ɣ ELISpot (19), a technique which involves adding supraphysiologic amounts of exogenous peptide to cells *in vitro* to detect the presence of cells that can recognize the particular peptide(s) added. However, while this assay detects cells that can respond to a given antigen, the high levels of peptide that are typically used may mean that a positive IFN-ɣ ELISpot result is not necessarily predictive of antiviral capacity (16,20,21).

Despite being able to elicit CTL that could recognize portions of HIV, the vaccine failed either end goal of preventing infection or lowering viral setpoint in those who

subsequently became infected (19,22,23). While the vaccine did not produce the desired outcome, a study by Rolland *et al.* produced compelling evidence that CTL elicited by the vaccine were able to apply selective pressure on HIV-1 sequences (24). Among study participants from both the placebo and vaccine group who subsequently became infected with HIV, researchers compared the founder sequences (the variant of HIV-1 which established the infection) against the sequence used in the vaccine. The sequences in gag, a more conserved portion of HIV, were found to be significantly more divergent between sequences of the vaccinated-infected group and the vaccine sequence compared to the sequences in the placebo group relative to the vaccine sequence. This divergence can be explained by a so-called sieve effect, wherein pre-existing CTL might prevent certain variants from establishing infections. The suggestion that CTL induced by this vaccine might be capable of exerting selective pressure raises the possibility that increasing the breadth of targeting to cover more variants, or potentially directing immune responses to the “right” targets, could lead to an effective vaccine.

Given that the immunogenicity of the Mrk/Ad5 vaccine was primarily established through IFN-ɣ ELISpot, we wanted to test the functional capabilities of CTL clones elicited by this vaccine. We first examined the ability of these clones to kill cells infected with virus bearing the vaccine variant of their cognate epitope, then test their ability to kill and suppress a panel of common clade B variants of that epitope.

RESULTS

CTL elicited by the Mrk/Ad5 vaccine are able to kill virus-infected cells

We first assessed the ability of six CTL clones to kill cells infected with replicative HIV-1 bearing their cognate (index) epitope. **Table 2-S2** contains a summary of CTL clone designation, targeting, and naming in this chapter. These clones had originally been identified through responses to peptide by IFN-ɣ ELISpot and were only isolated out of PBMC after initial peptide stimulation and expansion. As they were known to respond to the vaccine variant of peptide that had elicited them, we first tested their ability to target viruses bearing the vaccine variant. Chromium release killing assays were set up against HLA-matched, HIV-permissive target cells which were either uninfected without the addition of peptide, uninfected with exogenous peptide of the vaccine variant (index) epitope added, or infected with a replicative NL4-3-M20A HIV-1 strain bearing the vaccine variant. Three CTL clones targeting the A*24-restricted KW9 Gag epitope (KYKLKHIVW) were able to kill virus-infected cells, although clone H8-10.4T-KW9 had relatively low levels of specific lysis compared to the other two clones targeting that epitope (19.0% in contrast to 82.2% and 54.6% for clones H8-3.17T-KW9 and H8-3.30T-KW9, respectively, at an effector-to-target ratio of 5:1) **(Fig. 2-1A).** Two CTL clones targeting the B*27-restricted WF9 Nef epitope (WRFDSKLAF) were also able to kill virus-infected cells **(Fig. 2-1B),** and one CTL clone targeting the B*27-restricted QR9 epitope (QRGNFRNQR) was tested and also exhibited killing of cells infected with NL4-3-M20A virus bearing the vaccine variant **(Fig. 2-1C)**.

Vaccine-derived CTL clones exhibit limited cross-reactivity against epitope variants despite high killing efficiency of vaccine variant.

Killing efficiency translates a CTL's ability to kill peptide-loaded cells into its antiviral capability. To test this, we first infected HLA-matched HIV-permissive target cell lines with replicative NL4-3-M20A bearing particular epitope variants. Once target cells were adequately infected (>70% by flow cytometry), chromium release killing assays were performed. Uninfected target cells were used to determine background lysis by CTL against the cell line and to check for alloreactivity, while target cells loaded with high levels of index peptide were used to determine the theoretical maximal killing by a CTL. The QR9 variants tested here total to approximately 54.3% of common clade by variants, though we were also unable to test a common variant that represents approximately 9% of QR9 clade B variants, as we were unable to make productive virus with NL4-3 bearing that variant. This is likely due to a lack of compensatory mutations. As for WF9, the ten variants we used in these assays totaled to 84.4% of clade B HIV-1 sequences, while KW9 variants totaled to 27.4% (see **Tables 2-1 and 2-S1**).

All killing efficiency assays included the HIV-subject-derived S1-3.23-SL9 clone as a control (shown in **Fig 2-2A** only), as it targets an area that is unmutated between the tested viruses and thus should demonstrate similar killing efficiency against all viruses tested.

All three of the vaccine-derived KW9 Gag CTL clones killed cells infected with vaccine KW9, but with uneven efficiency **(Fig 2-2A)**. H8-10.4T-KW9 had moderately reduced killing efficiency (42%) for the vaccine-variant relative to the other two clones (69% for H8-3.30T-KW9 and ≥100% efficiency for H8-3.17T-KW9 at E:T of 5:1). On the

other hand, the killing efficiency against a common clade B KW9 variant with a K1Q substitution caused all three clones a drastic reduction in recognition. Only the H8-3.17T-KW9 clone maintained modest killing efficiency, although it still represented an approximately 5-fold reduction relative to killing efficiency against virus with vaccine KW9.

When tested against a large panel of clade B epitope variants, two vaccine-derived CTL clones targeting WF9 Nef showed good killing efficiency against the vaccine variant. Surprisingly, both clones actually had higher killing efficiency against an epitope variant with a K6R substitution (85% efficiency against K6R vs 57% efficiency against the vaccine variant for H7-1.4-WF9, 68% efficiency against K6R vs 49% efficiency against the vaccine variant for H7-1.4-WF9). However, neither clone exhibited efficient killing against any of the other eight variants tested **(Fig. 2-2B).**

Similarly, a QR9 Gag vaccine-derived CTL clone had high killing efficiency against cells infected with virus bearing the vaccine variant of QR9 and one additional variant, with an R9K substitution, while losing recognition against the remaining four variants tested. The killing efficiency of the R9K variant was reduced relative to the index epitope, but was still very high, both at an E:T of 5:1 and of 1:1 **(Fig. 2-2C)**. Taken together, the data suggest that CTL clones tested exhibit highly efficient killing against viruses bearing the index epitope but display limited ability to kill against viruses bearing epitope variants.

<u>Patterns of virus suppression against epitope variants by vaccine-derived CTL clones are consistent with limited cross-reactivity seen in killing efficiency</u>

The CTL clones and viruses used to test inhibition of viral growth **(Fig. 2-3)** were the same as those used to test killing efficiency **(Fig. 2-2)**, except with the inclusion of an additional QR9 Gag CTL clone, H7-10.7-QR9 **(Fig. 2-3B)**. To determine maximum possible growth (and represent the absence of inhibition) for a given set of conditions (virus strain, target cell, MOI), infected cells were plated without CTL. The concentration of virus in supernatants, as measured by levels of the HIV-1 p24 protein by ELISA, is compared proportionately between conditions. In wells which were cultured with T cells, minimal or no reduction in p24 levels suggests lack of recognition, while clearer reductions are attributed to antiviral activity of the T cells. Based on our lab's experiences, we arbitrarily consider a diminution of one log or more in supernatant p24 concentration to be a reliable indicator of viral suppression in this assay.

In all instances, vaccine-derived CTL were able to suppress growth of virus bearing the vaccine sequence **(Fig. 2-3).** However, clone H8-10.4T-KW9 exhibited poor suppression relative to other clones **(Fig. 2-3A)**, which aligns with its poorer killing efficiency **(Fig. 2-2A)**. The QR9 Gag clone tested for killing efficiency, H7-3.1-QR9, displayed equivalent patterns of targeting as demonstrated in **Fig. 2-2C**. However, an additional QR9 clone, H7-10.7-QR9 was only able to suppress virus bearing the vaccine variant of QR9.

As in the killing efficiency assays, the HIV-subject-derived S1-3.23-SL9 clone was used as a control to show effective viral suppression, and in most cases was able to suppress virus by one log or more relative to the no CTL condition (shown in **Fig 2-3 B&C).**

DISCUSSION

The CTL clones used for the experiments in this study derive from healthy, HIV-negative individuals who developed CTL responses to a limited repertoire of HIV-1 epitopes in response to Mrk/Ad5 vaccination. HLA haplotype determines which epitopes a human is able to present to CTL, and thus limits the potential scope of responses an individual can develop, as well as limiting the potential for shared epitope-targeting between individuals (25,26). Due to high polymorphism of HLA, it can be challenging to find individuals within a small cohort who develop responses to the same epitope. This factor limited our ability to compare clonal targeting profiles directly and determined which epitopes we ultimately explored in this study.

Killing efficiency translates the ability of a CTL clone to kill peptide-loaded cells into its antiviral capability. It is a measurement that is specific to each TCR and pMHC complex. Testing CTL against healthy, HLA-matched cells that have been pre-loaded with high levels of exogenous cognate peptide represents targeting under optimal conditions, providing the theoretical maximum level of specific lysis that a given TCR can effect. The often supraphysiological levels of exogenously added peptides in such assays allow for detection of T cell responses that might be of little relevance under physiological conditions, as it bypasses antigen processing and ignores differences in levels of expression of viral proteins in an infected cell. Our lab (27,31) and others (41) have shown that a CTL clone can ‘recognize’ a peptide or peptide variant in one assay (*e.g.*, release of IFN-ɣ in an ELISpot or killing of exogenous peptide-loaded cells) that it cannot ‘recognize’ in another (*e.g.*, killing infected cells or suppressing virus). Lysis of peptide-loaded cells does indicate recognition of a peptide-MHC complex by a TCR, but

killing efficiency closely correlates to antiviral activity, accounting for target cell infectivity and the variables of antigen processing and epitope presentation. In fact, Bennett *et al.* found that TCR avidity is linearly correlated with killing efficiency, which is in turn linearly correlated with suppression efficiency (27). There is, however, a minimum threshold of avidity (measured against exogenous peptide-loaded cells) to confer killing or suppressive capacity. As killing efficiency is more representative of *in vivo* conditions, it can help to delineate the utility of a CTL, and viral inhibition helps contextualize CTL function further.

In this chapter, we tested the antiviral capabilities of vaccine-elicited CTL clones targeting three HIV-1 epitopes. All CTL clones exhibited a killing efficiency of 42% or greater against cells infected with the vaccine variant of their cognate epitope, meaning they all have the ability to kills cells infected with virus bearing the sequence used in vaccination. In this regard, the vaccine was successful. However, examining the cross-reactivity and inhibition of viral growth exhibited by these clones may provide a useful insight into a shortcoming of this vaccine-mediated immunity.

The patterns of virus suppression and killing efficiency generally agreed across CTL clones and variants for WF9 and QR9. These data showed both WF9 clones were able to effectively target viruses bearing the vaccine sequence and a variant containing the K6R substitution. However, they were also tested against 8 additional common variants and were unable to efficiently kill or suppress any of those. According to the Los Alamos National Laboratory database, the 10 variants tested in WF9 assays represent 84.4% of clade B sequences (**Table 2-S1**), while the two WF9 variants that these CTL effectively targeted represent only 15.9% of sequences.

Similarly, QR9 variants tested represent 54.3% of clade B sequences, while the one variant suppressed by H7-10.7-QR9 represents 33.85% of sequences, and the two variants recognized by H7-3.1-QR9 make up 36.2% of sequences. We were unable to make productive virus with the third most frequent QR9 variant (8.9% of sequences), likely owing to a missing compensatory mutation in NL4-3.

Although the three clones targeting KW9 were only tested against two variants, these clones exhibited a range of efficacy against the vaccine sequence, suggesting that this epitope requires highly efficient killing by CTL in order to be efficacious. While H8-3.17T-KW9 had extremely efficient killing and suppression of index KW9, the H8-10.4T-KW9 clone had much lower killing efficiency and very little suppressive capacity, with the H8-3.30T-KW9 clone being intermediate in both regards.

The H8-3.17T-KW9 clone had greater than 100% killing efficiency in virus bearing the vaccine sequence relative to cells loaded with the equivalent peptide at 1ug/ml. This could signify that levels of KW9 presentation on infected cells are actually even greater than on exogenously-loaded cells (at 1ug/ml). It has previously been shown that clones with greater killing efficiency have TCR with greater sensitivity to the pMHC complex (relative to other clones that target the same epitope) (27). Since the data from the H8-3.17T-KW9 clone suggest that this epitope is presented at very high levels, it would follow that the other two clones have decreasing sensitivity, to the point where antiviral capacity is minimal. Of course, seeing killing efficiency above 100% could also be due to the fact that *in vitro* experiments are not perfect models. The specific lysis against uninfected cells loaded with exogenous peptide (72% average) and cells infected with vaccine KW9 virus (82%) both represent very high levels, and

higher lysis in the uninfected cells could have been due to some combination of increased susceptibility to lysis in infected cells or other factors that produce a margin of error in such assays. However, even if the magnitudes of the numbers are not completely accurate, the relative efficacy between clones and across epitope variants still hold.

In Gorin *et al.*, our lab previously demonstrated a technique of testing CTL clones against virus libraries containing all possible single- and about half of all double-amino acid mutants of their cognate epitopes (29). Follow up research (30) used this method to compare clones targeting the B*2705-restricted KK10 Gag 263-272 epitope (KRWIILGLNK), an epitope which is associated with delayed progression to AIDS in the absence of antiretroviral therapy. When testing a CTL clone derived from a Mrk/Ad5 vaccine recipient, we found this clone could effectively apply selective pressure against the vaccine variant of the epitope, as well as several other relatively 'fit' variants. However, it applied low selective pressure on two of the 'fittest' variants. KK10-specific TCRs derived from two different HIV+ subjects were available for comparison by this method and indicated much higher selective pressure on these two variants. While limited, these data suggest that the CTL elicited by the Mrk/Ad5 vaccine are effective in targeting virus bearing the vaccine variant of their cognate epitope, but exhibit limited breadth of targeting against other common epitope variants.

Likely due to the challenging nature of working with T cell clones, there are limited data on cross-reactivity against which the results presented in this chapter might be compared. However, Bennett *et al.* tested killing efficiency and viral inhibition in five CTL clones derived from HIV-1-infected individuals (27). These clones exhibited wide

diversity in their degree of cross-reactivity for epitope variants (summarized in **Table 2-S3**). Killing efficiency for three clones targeting A*02-restricted SL9 Gag (SLYNTVATL) overall exhibited much greater cross-reactivity, with killing efficiency of 50% or greater in 2 of 6, 4 of 6, and 5 of 6 tested variants, and killing efficiency of at least 20% in a total of 4 of 6, 5 of 6, and 5 of 6 tested variants. On the other hand, two clones targeting two other epitopes displayed more limited breadth: a clone targeting RL10 Rev (RPAEPVPLQL) had a killing efficiency greater than 50% for 3 of 11 tested variants, and a killing efficiency greater than 20% for one additional variant. The clone targeting the IV9 epitope (ILKEPVHGH) in reverse transcriptase exhibited a killing efficiency greater than 50% for only one of 16 tested variants, with a killing efficiency greater than 20% for one additional variant.

The data presented in this chapter indicate that the Mrk/Ad5 vaccine was able to elicit CTL with high antiviral efficacy across all three epitopes. However, these CTL clones exhibit limited breadth, and likely target well under 50% of circulating clade B HIV-1 epitope variants. Additionally, results from the H8-10.4T-KW9 clone suggest that the vaccine also elicited some CTL that have poor efficacy against even virus bearing the vaccine sequence. When compared to the data from Bennett *et al.*, and taken together with the disparity in selection seen between infection and vaccine-derived CTL in the KK10 library assay from Gorin *et al.*, the cross-reactivity of the Mrk/Ad5-elicited CTL appears to be more limited. However, these observations would clearly benefit from testing additional CTL clones specific for other epitopes, as well as direct comparison of clones which target the same epitope but are elicited by natural HIV-1 infection and the Mrk/Ad5 vaccine (28).

As different areas of the HIV-1 genome vary in their tolerance for mutations, theories have emerged around this to suggest possible routes to CTL-based immunity. Gorin *et al.* illustrated how some epitopes result in smaller or larger targets and found this likely to be an element of what makes a particular CTL response 'effective,' such as what is seen in 'elite controllers' **(supplemental figure 2-S1).** If an indispensable portion of the virus can be adequately targeted by CTL, this could theoretically prevent an infection from establishing. The SL9 Gag epitope is an immunodominant epitope restricted to HLA-A*02, the most common HLA allele. Although many people with HLA-A*02 are likely to develop a response to SL9 when exposed to HIV-1 or whole Gag, looking at the size of the SL9 'target' (*i.e.,* the number of fit and viable variants that would need to be targeted) can help frame the challenges of eliciting an adequate immune response without attempting to control for certain variables. Relative to the other two epitopes, SL9 has many options for mutating that allow it to remain relatively fit. There are two main approaches for dealing with the variability of HIV-1: 1) aim for a smaller target (*i.e.,* a portion of HIV-1 that cannot change easily), and 2) induce an immune response that can respond more broadly to variants. The Mrk/Ad5 vaccine aimed to elicit a CTL-based immune response, but did not direct that response with any precision (beyond limiting it to *gag*, *pol*, and *nef*). In fact, follow up research from the STEP trial (which used the same vaccine) on the distribution of targeting found significant skewing of vaccine-elicited CTL responses to less conserved regions (44). There is ongoing research investigating the feasibility, applicability, and efficacy of directing immune responses to particularly conserved regions of HIV-1 (43,45,47).

It's likely that the most effective immune response will be tailored towards 'easier' targets with fewer options for immune escape, but it will probably be even more important to have methods to reliably induce cross-reactive CTL responses. In the example of an A*02 individual who is vaccinated without regard for directing the response, there's a decent chance they will end up mounting a CTL response against SL9. If nothing is done to ensure that this response is highly cross-reactive, it seems a foregone conclusion that the vaccine-induced SL9 response will not provide any meaningful protection. An effective cross-reactive response could be achieved by inducing several distinct clones that target the same epitope, or through fewer clones that can individually target more broadly. Research into potential mechanisms to achieve this through vaccination have also been underway (46). Data presented in this chapter suggest that the Mrk/Ad5 vaccine elicited strong responses against the sequence used in the vaccine, but likely did little to induce cross-reactivity against variants.

As the rAd5 vector was able to elicit highly specific CTL responses that appear capable of antiviral activity, it could potentially still be a useful vaccine platform against relatively stable pathogens. As a basis for an HIV-1 vaccine, however, it was severely lacking. An effective vaccine for HIV-1 will require some very specific characteristics. A more profound understanding of the interactions between CTL and HIV-1, as well as CTL with different vaccine types, will doubtless be crucial for the strategic development of an effective vaccine for HIV-1.

MATERIALS & METHODS

Selection of CTL clones and epitopes used in this study

The CTL clones used for the experiments in this study are isolated from healthy, HIV-negative individuals who received the Mrk/Ad5 vaccine and developed CTL responses. We were limited to testing the epitopes that subjects developed CTL responses to, which mostly varied between donors due to the genetic polymorphism of MHC. Additionally, certain epitopes were restricted to HLA types for which we were unable to find HLA-matched HIV-permissive cells. The sequences for the index epitopes matched the sequence used in the Mrk/Ad5 vaccine, and additional variants for testing were chosen based on frequency among HIV-1 Clade B sequences found on the Los Alamos National Laboratory Database **(Table 2-1).**

Generating replicative HIV-1 viruses containing epitope variants of interest

Epitope variants (listed in **Table 2-1**) were generated using the QuikChange Site-Directed Mutagenesis Kit (Agilent, Santa Clara, CA) in either a p83-10.M20A or p83-2.1 plasmid, as appropriate, before being transformed into Stellar competent cells (Takara-Clontech, Kusatsu, Japan). These plasmids, described previously (32), divide the genome of the CXCR4-tropic HIV-1 molecular clone NL4-3 (33) into two portions to facilitate molecular cloning in bacteria by preventing recombination through the HIV-1 LTRs. The p83-10 plasmid used in these experiments contains a Nef M20A mutation that diminishes Nef's ability to downregulate HLA-A and HLA-B presentation on infected cells (34,35). Restoring pMHC presentation on the cell surface allows for optimal detection of virus inhibition for comparison (42). After confirming mutations by

sequencing, the p83 plasmid bearing the mutation(s) was electroporated into T1 cells with the p83 plasmid containing the alternate half of the HIV-1 genome, resulting in supernatants containing full-length replicative NL4-3. Viruses were titered in the HIV-permissive C8166 cell line.

HIV-permissive cell lines

Replicative viruses were produced in T1 cells (36). After the HLA-restrictions for minimal epitopes were determined, target cells were chosen based on HIV-permissiveness and expression of the appropriate HLA molecule. T1 cells transduced to stably express HLA-A*24 were used as target cells for HLA-A*24 KW9 Gag 28-36; untransduced T1 cells were used as target cells for HLA-B*40 KL9 Gag 481-489; T1 cells transduced to stably express HLA-B*27 were used as target cells for both HLA-B*27 QR9 Gag 379-387 and HLA-B*27 WF9 Gag 183-191.

Isolation and culture of vaccine-elicited CTL clones

CTL clones were generated by limiting dilution cloning of peptide-stimulated PBMC derived from subjects who had received the Mrk/Ad5 vaccine. CTL clones were maintained in complete RPMI 1640 medium (supplemented with 10% fetal bovine serum (FBS), L-glutamine, HEPES buffer, and antibiotic) with recombinant human IL-2 at 50U/ml (NIH AIDS Reagent Repository Program) (R10-50). Clones were restimulated periodically or when thawing by adding irradiated PBMC from healthy donors and 12F6 anti-CD3 antibody clone (at 200ng/ml). All CTL clones were checked by chromium

release assay (CRA) to be active against HLA-matched target cells loaded with cognate peptide at least 8 days after stimulation and prior to use in any functional assays.

Chromium Release Assay

Cell killing was measured in chromium release assays, as previously described (27,37). Briefly, target cells were labeled with ^{51}Cr and incubated with or without peptide before washing. Synthetic peptides were purchased from Sigma-Aldrich (St. Louis, MO) and used at a concentration of 1ug/ml. Virus-infected cells were incubated without peptide as targets for determining lysis and calculating killing efficiency. Uninfected target cells were also chromated without the addition of peptide for use as targets to measure for any alloreactivity. Cells were plated at an E:T of 1:1 or 5:1 and incubated at 37°C for 3.5-4 hours before supernatants were transferred to LumaPlates (PerkinElmer) for quantification on a Microbeta microscintillation counter (Wallac). All conditions were set up in at least duplicate and averaged, with the exception of spontaneous release (chromated target cells + medium) and maximum lysis (chromated target cells + Triton-X at 2.5% final concentration) conditions that were plated in quadruplicate.

Calculating Specific Lysis and Killing Efficiency

Calculations were made as previously described (27). Replicates of spontaneous release were averaged, and the resulting value was subtracted from all other samples. Specific Lysis was calculated by dividing the average of background-subtracted values by the background-subtracted maximum lysis. To calculate killing efficiency: maximum lysis values were adjusted by the percent infectivity of the target cells, as determined by

intracellular flow cytometry staining (Flow Cytometry Fixation & Flow Cytometry permeabilization/wash buffer from R&D Systems) for HIV-1 p24 (KC57-RD1 antibody from Beckman Coulter). The background-subtracted average of sample values was divided by the adjusted maximum lysis value, and the resulting value was divided into the specific lysis of the index epitope for matching conditions (*i.e.* the same target cell line and CTL clone, plated at equivalent E:T ratios). Calculations summarized as follows: (specific lysis against cells infected with virus *n*) / (specific lysis of exogenous peptide-loaded uninfected cells x % infectivity of cells infected with virus *n*).

Virus Suppression Assay

Assays testing the ability of CTL clones to suppress replicative virus were performed as previously described (27,38). Briefly, target cells were infected at a multiplicity of infection (MOI) of 0.01 with previously titered replicative virus strains and plated at $5x10^4$/well in 96 well flat-bottom plates, either without or with ($1.25x10^4$ effector cells) CTL. Supernatants were collected at days 3, 6, and 9 or days 4, 6, and 8, and replenished with fresh R10-50. Levels of p24 in collected supernatants were quantified using a p24 ELISA kit (Xpress Bio, Frederick, MD).

Epitope	Epitope Location	HLA Restriction	Vaccine Sequence	Variant	LANL Clade B Frequency	Frequency Rank
QR9	Gag 379-387	B*27	QRGNFRNQR	---------	33.85%	1
				-K-------	13.93%	2
				--------K	2.32%	4
				-K----S--	1.51%	5
				-K---K---	1.41%	7
				-----KG--	1.26%	8
WF9	Nef 183-191	B*27	WRFDSKLAF	---------	0.75%	15
				-K---R---	46.27%	1
				-----R---	15.16%	2
				-K---H---	6.28%	3
				-K---S---	4.39%	4
				-K-------	3.34%	5
				-K---L---	2.50%	6
				-K---R--Y	2.15%	7
				-K---R--L	1.80%	8
				-K---T---	1.71%	9
KW9	Gag 28-36	A*24	KYKLKHIVW	---------	20.64%	2
				Q--------	6.71%	5
KL9	Gag 481-489	B*40	KELYPLASL	---------	33.50%	1

Table 2-1: List of HIV-1 index epitopes and variants. Frequency and frequency ranking of epitope variants were found using the Los Alamos National Laboratory (LANL) HIV-1 sequence database QuickAlign tool (39). Data was summarized by subtype. Both frequency and frequency rank in this table are relative to total clade B sequences which cover that epitope.

A

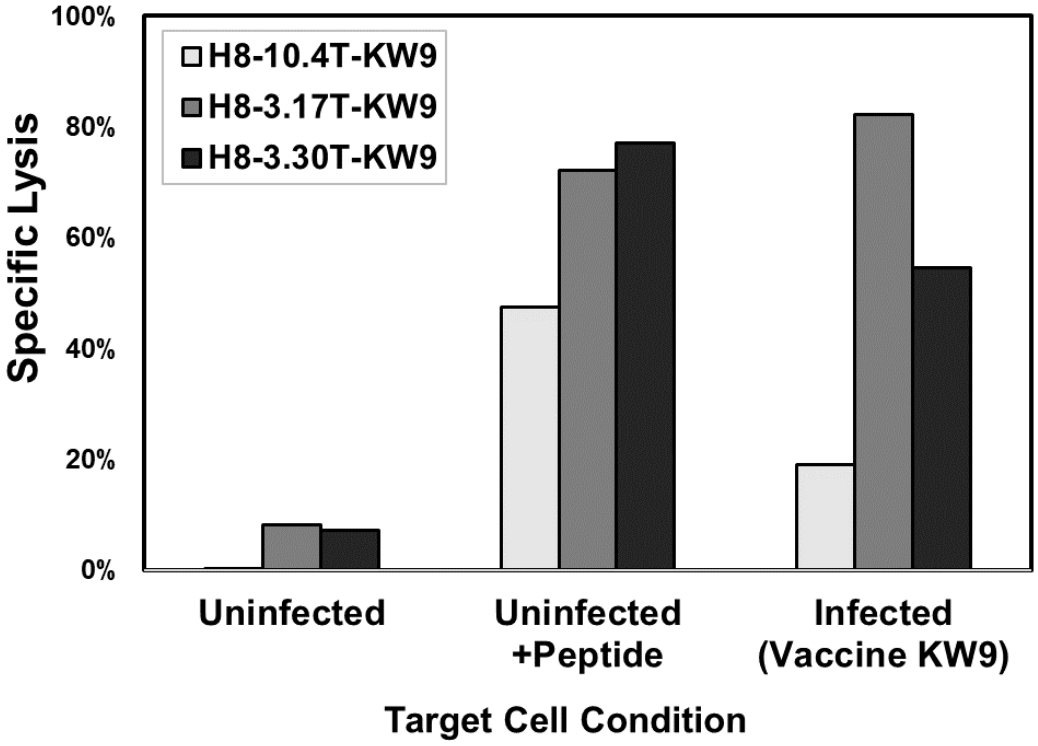
100%
80%
60%
40%
20%
0%
Specific Lysis
H8-10.4T-KW9
H8-3.17T-KW9
H8-3.30T-KW9
Uninfected
Uninfected +Peptide
Infected (Vaccine KW9)
Target Cell Condition

B

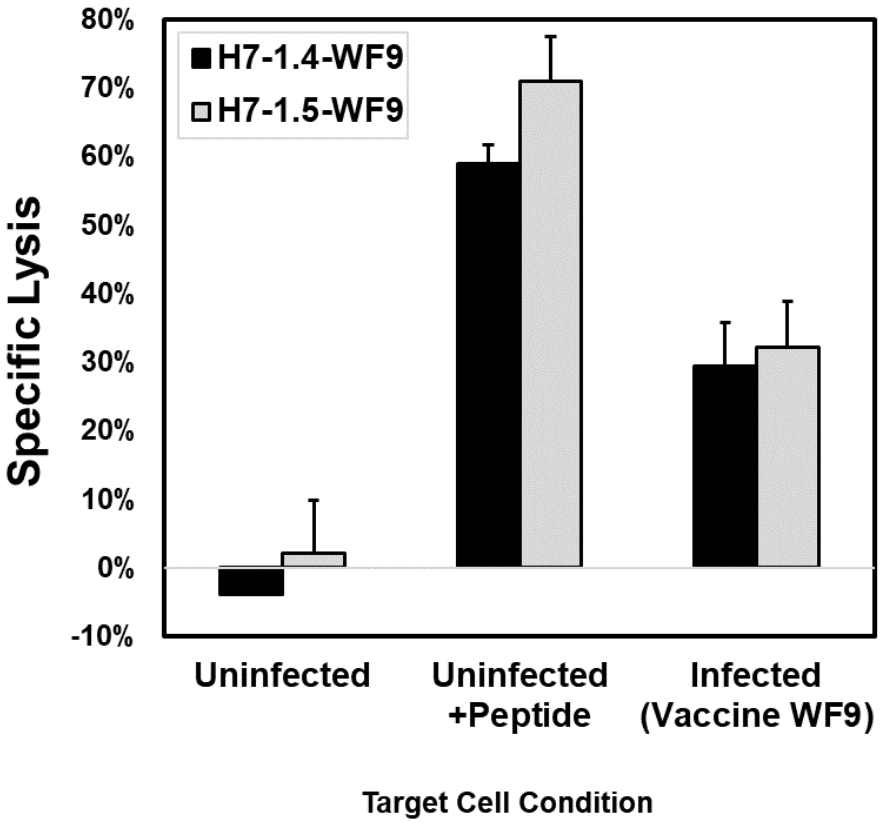
80%
70%
60%
50%
40%
30%
20%
10%
0%
-10%
Specific Lysis
H7-1.4-WF9
H7-1.5-WF9
Uninfected
Uninfected +Peptide
Infected (Vaccine WF9)
Target Cell Condition

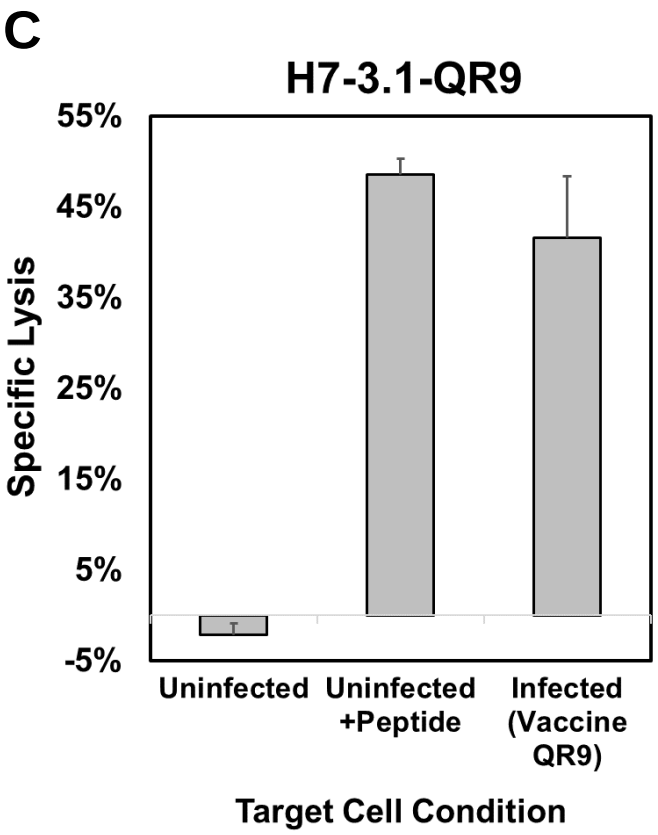

Figure 2-1: Vaccine-elicited CTL clones are able to kill virus-infected cells. (A-C) Six CTL clones were tested by Chromium release assay against HLA-matched, HIV-permissive target cells. Target cell conditions were as follows: uninfected without the addition of peptide, uninfected with added exogenous peptide of the vaccine variant, or infected with a replicative NL4-3 HIV-1 strain bearing the vaccine variant. Three CTL clones target the A*24-restricted KW9 Gag epitope (KYKLKHIVW) **(A)**; two CTL clones target the B*27-restricted WF9 Nef epitope (WRFDSKLAF) **(B)**; one CTL clone targets the B*27 QR9 epitope (QRGNFRNQR) **(C)**. Data shown with an effector-to-target ratio of 5:1. Bars represent the mean specific lysis; error bars represent the standard deviation between two experimental replicates **(B,C)**.

A

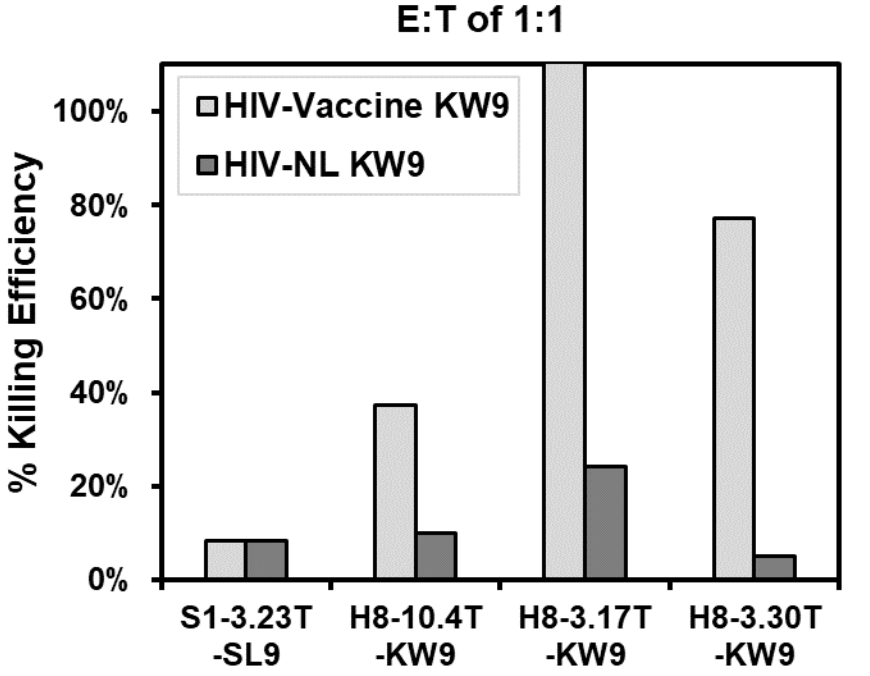
E:T of 1:1
HIV-Vaccine KW9
HIV-NL KW9
% Killing Efficiency
100%
80%
60%
40%
20%
0%
S1-3.23T -SL9
H8-10.4T -KW9
H8-3.17T -KW9
H8-3.30T -KW9

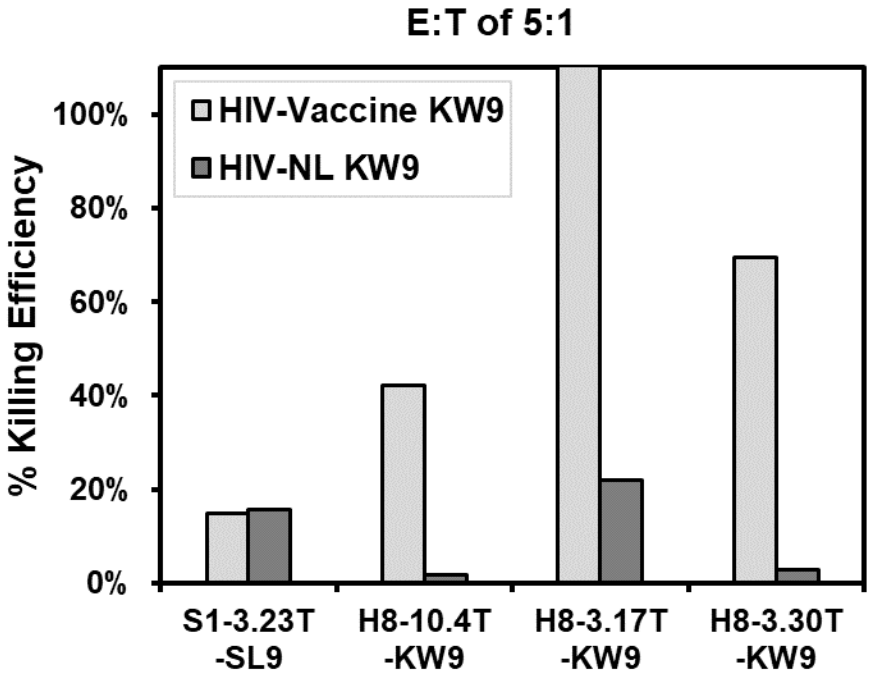
E:T of 5:1
HIV-Vaccine KW9
HIV-NL KW9
% Killing Efficiency
100%
80%
60%
40%
20%
0%
S1-3.23T -SL9
H8-10.4T -KW9
H8-3.17T -KW9
H8-3.30T -KW9

B

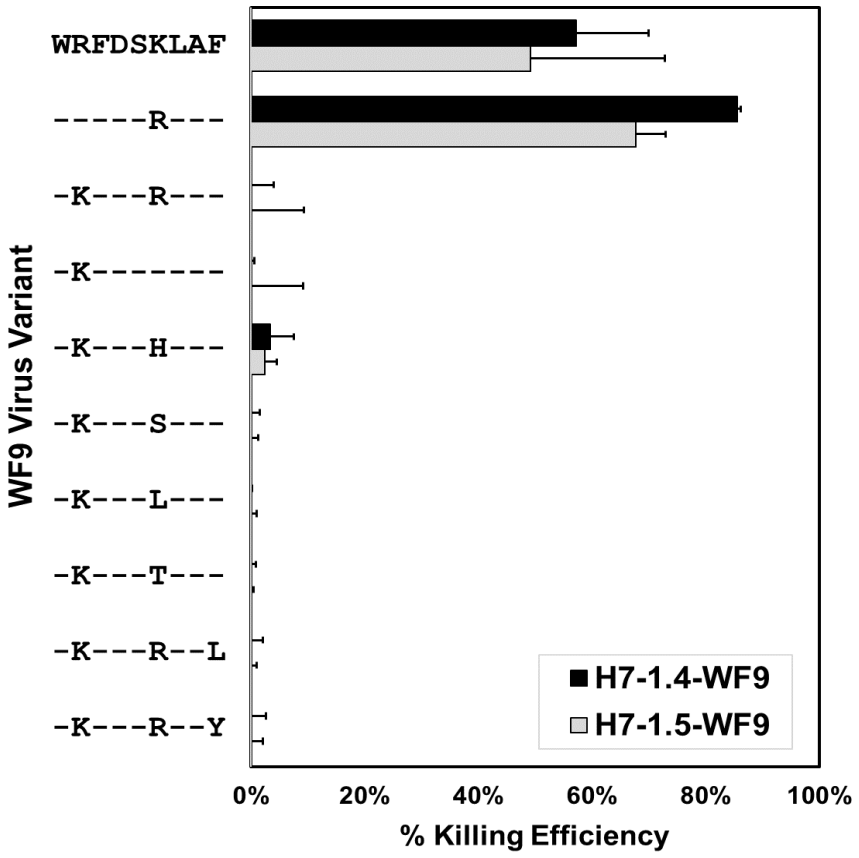
WRFDSKLAF
-----R---
-K---R---
-K-------
-K---H---
-K---S---
-K---L---
-K---T---
-K---R--L
-K---R--Y
WF9 Virus Variant
H7-1.4-WF9
H7-1.5-WF9
0%
20%
40%
60%
80%
100%
% Killing Efficiency

C

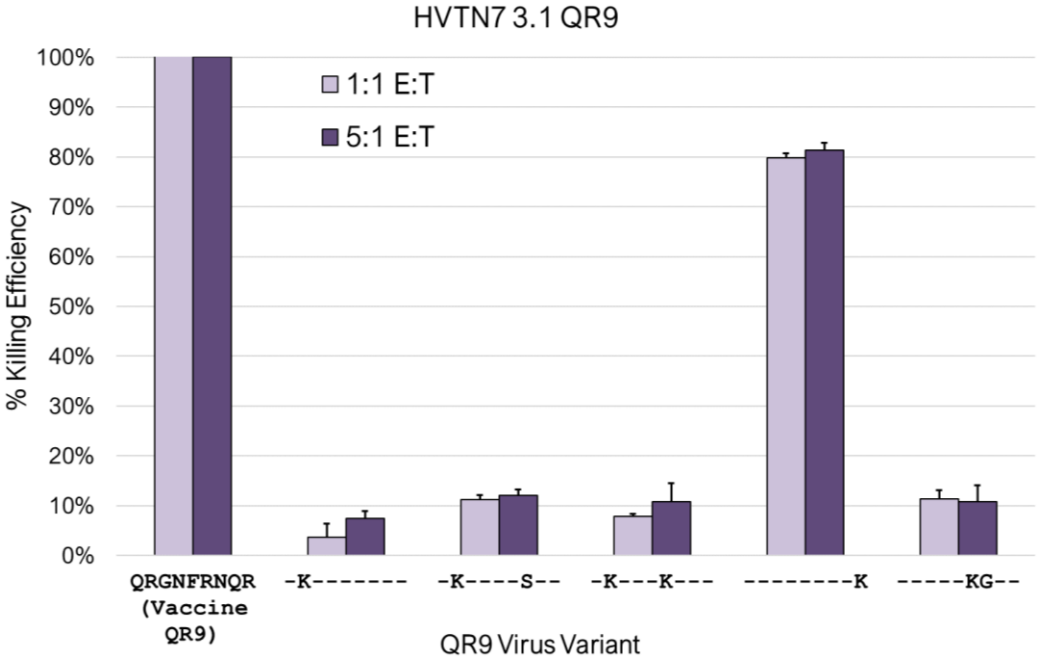
HVTN7 3.1 QR9
100%
90%
80%
70%
60%
50%
40%
30%
20%
10%
0%
1:1 E:T
5:1 E:T
% Killing Efficiency
QRGNFRNQR (Vaccine QR9)
-K-------
-K----S--
-K---K---
--------K
-----KG--
QR9 Virus Variant

Figure 2-2: Infected-cell killing efficiency by vaccine-elicited CTL against multiple epitope variants. Killing efficiency was measured by comparing specific lysis against virus-infected cells to specific lysis against an index epitope in chromium release assays. Killing efficiency is shown for different epitope variants, with calculations made in each case relative to peptide killing of the vaccine/index variant at the same effector-to-target (E:T) ratio **(A-C).** Killing efficiency by three KW9 Gag CTL clones for the vaccine variant and one other KW9 variant; S1-3.23-SL9 clone use as inter-virus control. Shown at E:T of 1:1 (top) and 5:1 (bottom) **(A).** Killing efficiency by two WF9 Nef clones for the vaccine variant and nine other WF9 variants, shown at E:T of 5:1 **(B).** Killing efficiency by one QR9 Gag clone at E:T of 1:1 and 5:1 for the vaccine variant and five other QR9 variants **(C).** Bars represent the mean calculated killing efficiency; error bars represent the standard deviation between two experimental replicates **(B,C)**.

A

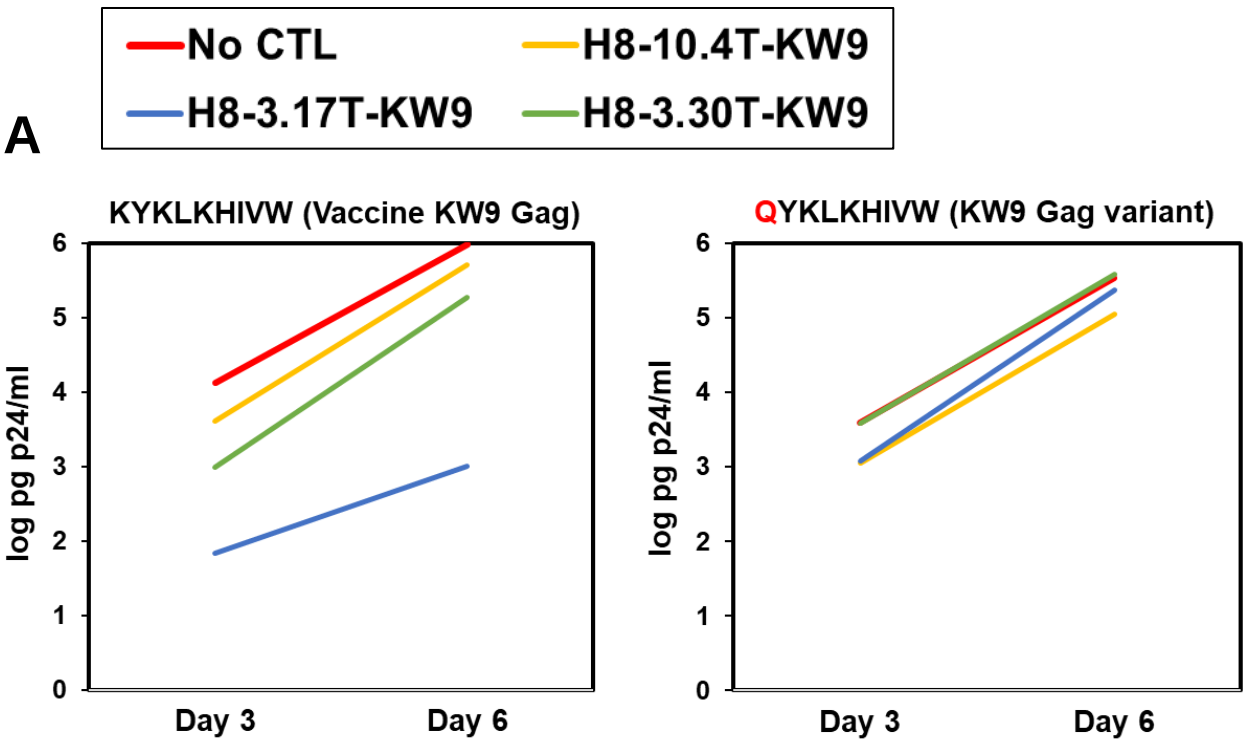
No CTL
H8-10.4T-KW9
H8-3.17T-KW9
H8-3.30T-KW9
KYKLKHIVW (Vaccine KW9 Gag)
QYKLKHIVW (KW9 Gag variant)
log pg p24/ml
0
1
2
3
4
5
6
Day 3
Day 6

B

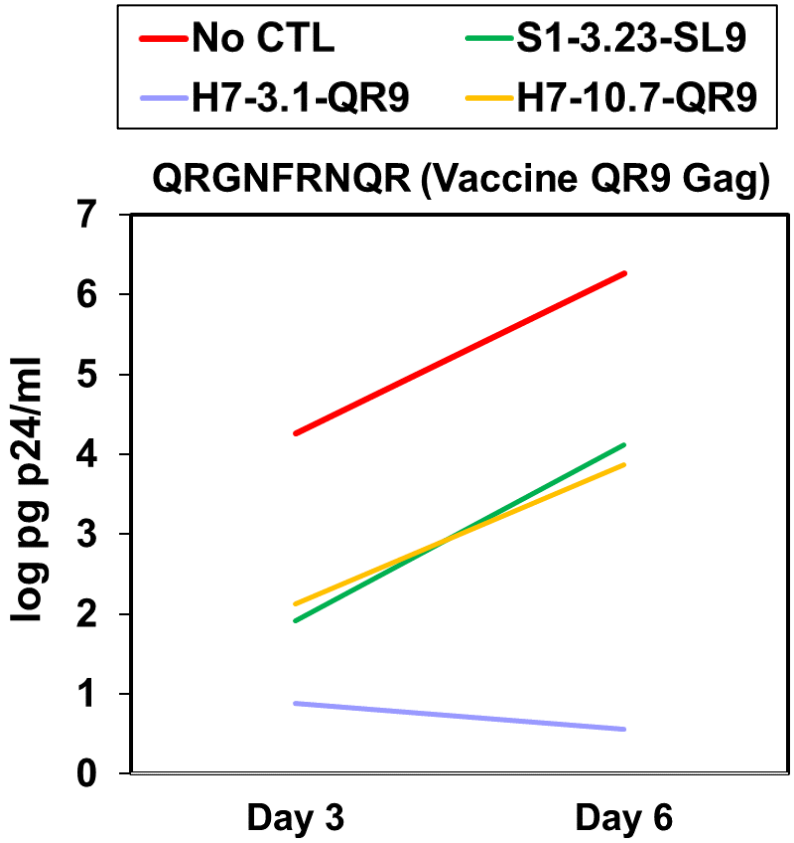
No CTL
S1-3.23-SL9
H7-3.1-QR9
H7-10.7-QR9
QRGNFRNQR (Vaccine QR9 Gag)
log pg p24/ml
0
1
2
3
4
5
6
7
Day 3
Day 6

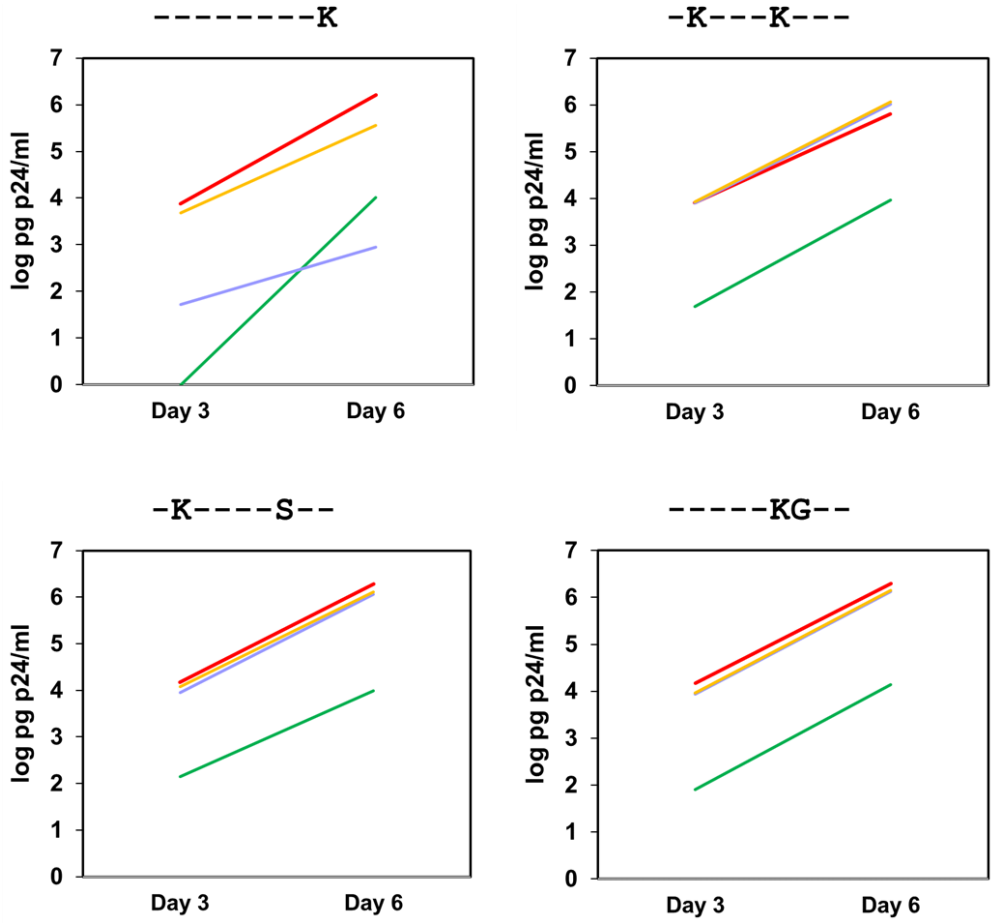
--------K
-K---K---
-K----S--
-----KG--
log pg p24/ml
0
1
2
3
4
5
6
7
Day 3
Day 6

C


No CTL
S1-3.23-SL9
H7-1.4-WF9
H7-1.5-WF9

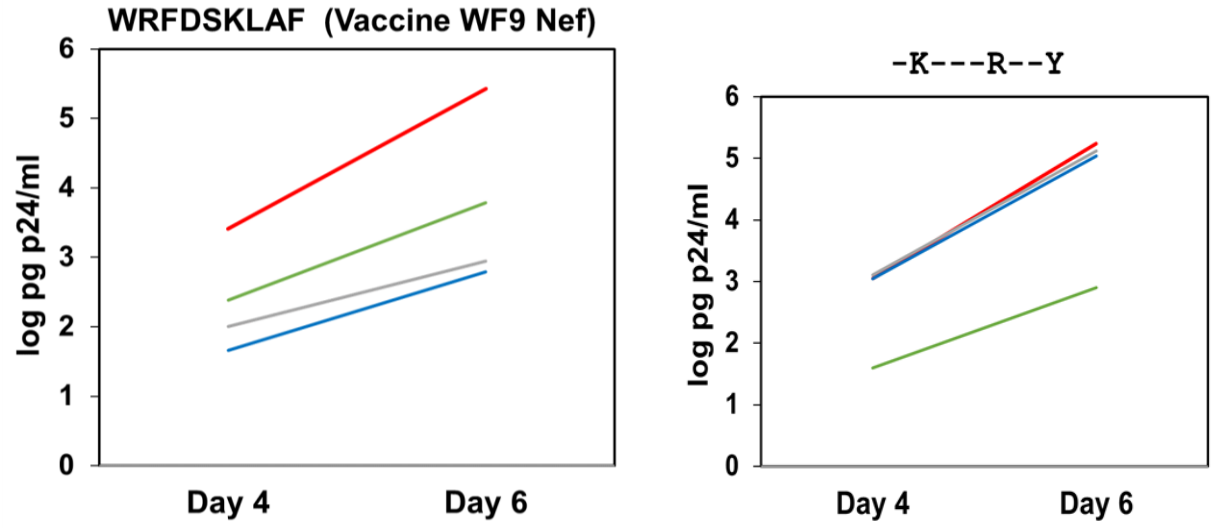
WRFDSKLAF (Vaccine WF9 Nef)
-K---R--Y
log pg p24/ml
0
1
2
3
4
5
6
Day 4
Day 6

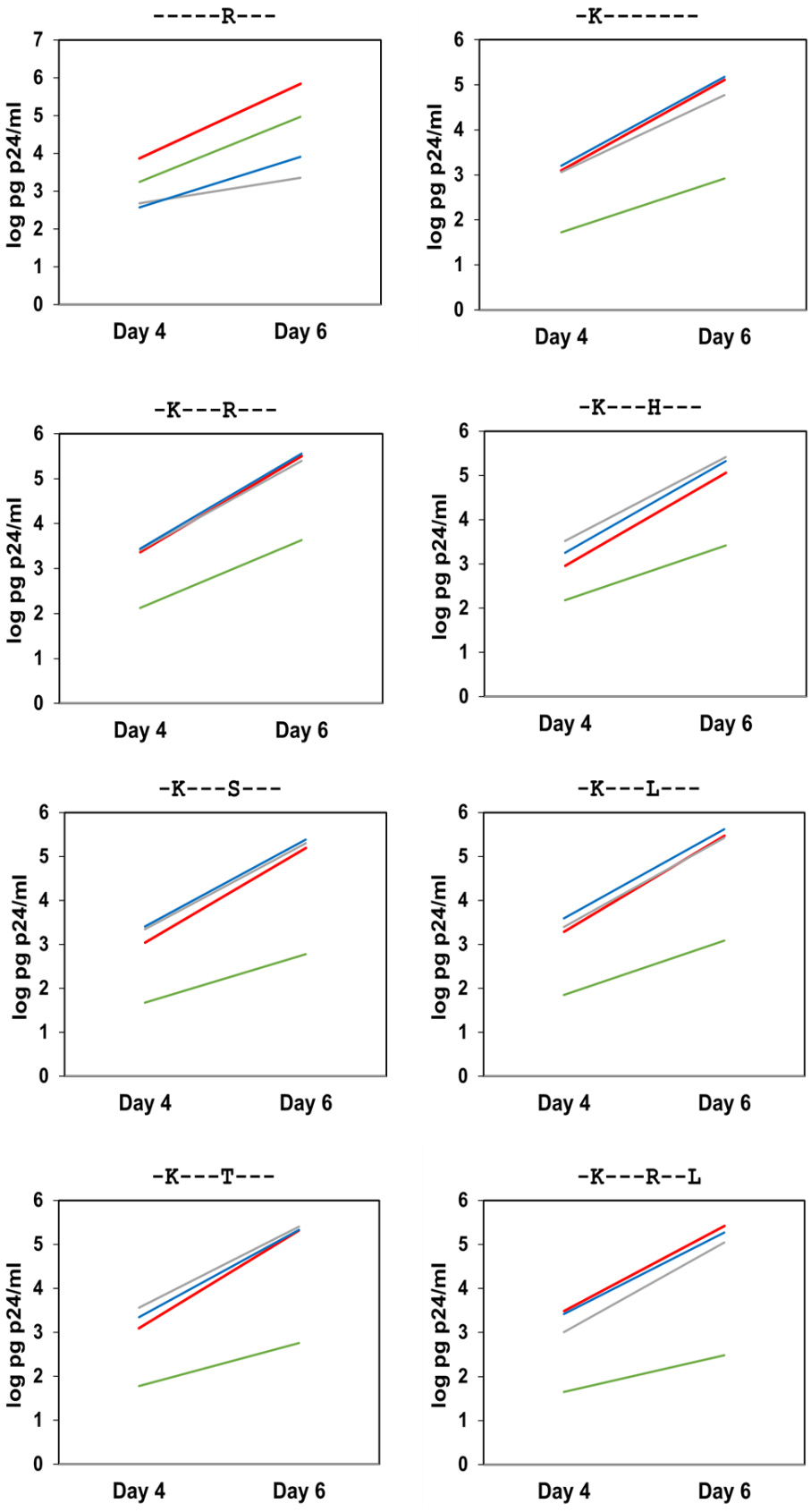
-----R---
-K-------
-K---R---
-K---H---
-K---S---
-K---L---
-K---T---
-K---R--L
log pg p24/ml
Day 4
Day 6

Figure 2-3: Suppression of replicative HIV-1 variants by vaccine-elicited CTL. Each plot represents the levels of a particular virus strain at two collection timepoints (X-axis, in days since infection), with each line in the plot representing the culturing conditions. The Y-axis reads log-scale concentrations (pg/ml) of the HIV-1 p24 protein found in supernatant as measured by p24-ELISA. Measurements of this protein are used to quantify the approximate number of HIV-1 virions present. All coculture experiments are run in triplicate (mean data shown). “No CTL” control wells (shown in red) for each virus represent the theoretical maximum growth for that strain. Other lines represent virus levels under CTL pressure, with the particular CTL clone indicated in the legend. All CTL are derived from HIV-negative, Mrk/Ad5-vaccinated subjects, with the exception of the HIV-subject-derived S1-3.23-SL9 clone **(B & C),** which was included in some assays as a positive control for CTL suppression. Target cells were infected with replicative NL4-3 containing the index epitope or substituted variant, as indicated at the top of each graph. All viruses were made in a backbone containing an M20A mutation in Nef. Fully functional Nef can cause significantly reduced expression of HLA-A and HLA-B on the surface of an infected cell, abrogating recognition by a large percentage of TCRs. The M20A mutation eliminates this function of Nef, allowing for more typical pMHC presentation on the cell surface. The M20A Nef mutation has been shown to have no effect on killing efficiency, but it reduces confounding, epitope-specific effects that Nef can introduce, so removing it allows for optimal detection of differences in viral inhibition (34,35,42). Graphs illustrate measured virus levels under the following conditions: three vaccine-derived CTL clones targeting A*24-restricted KW9 (Gag 28-36) tested against index epitope and one variant **(A)**; two vaccine-derived CTL clones

targeting B*27-restricted QR9 Gag (379-387) tested against index epitope and five variants **(B)**; two vaccine-derived CTL clones targeting B*27-restricted WF9 Nef (183-191) tested against index epitope and nine variants **(C)**.

Epitope	Epitope Location	Total Coverage of Variants Tested	Total Coverage of 2 Most Frequent Variants	Total Coverage of 10 Most Frequent Variants
QR9	Gag 379-387	54.3%	47.8%	67.1%
WF9	Nef 183-191	84.4%	61.4%	84.8%
KW9	Gag 28-36	27.4%	45.1%	84.1%

Table 2-S1: Frequency of tested and most prevalent epitopes variants among circulating Clade B HIV-1 variants.

Cognate Epitope	Epitope Abbreviation	Protein	Amino Acids	MHC-1 Restriction	CTL Clone Designation	Clone Name Used throughout
KYKLKHIVW	KW9	Gag	28-36	A*2402	HVTN00008-KW9-10.4T	H8-10.4T-KW9
					HVTN00008-KW9-3.17T	H8-3.17T-KW9
					HVTN00008-KW9-3.30T	H8-3.30T-KW9
QRGNFRNQR	QR9	Gag	379-387	B*27	HVTN00007-QR9-3.1	H7-3.1-QR9
					HVTN00007-QR9-10.7	H7-10.7-QR9
WRFDSKLAF	WF9	Nef	183-191	B*27	HVTN00007-WF9-1.4	H7-1.4-WF9
					HVTN00007-WF9-1.5	H7-1.5-WF9
SLYNTVATL	SL9	Gag	77-85	A*0201	S00001-SL9-3.23T	S1-3.23-SL9

Table 2-S2: Summary of the CTL clones used in Chapter 2. Clones targeting KW9, QR9, and WF9 were all generated from HIV-1-negative subjects who received the Mrk/Ad5 vaccine. The clone targeting SL9 was generated from a chronically HIV-1-infected individual.

A

Epitope	Epitope Protein	Index Seq.	Shorthand Clone ID	Total# of seq. tested	#seq. ≥≈50% efficiency	#seq. ≥≈20% efficiency	% High effic.	% Low to High effic.
SL9	Gag	SLYNTVATL	3.23	6	2	2	33.3%	66.7%
SL9	Gag	SLYNTVATL	10.18T	6	4	1	66.7%	83.3%
SL9	Gag	SLYNTVATL	1.9	6	5	0	83.3%	83.3%
RL10	Rev	RPAEPVPLQL	3.22	11	3	1	27.3%	36.4%
IV9	RT	ILKEPVHGV	68A62	16	1	1	6.3%	12.5%

B

Epitope	Epitope Protein	Index Seq.	Shorthand Clone ID	Total# of seq. tested	#seq. ≥≈50% efficiency	#seq. ≥≈20% efficiency	% High effic.	% Low to High effic.
SL9	Gag	SLYNTVATL	3.23	6	3	1	50.0%	66.7%
SL9	Gag	SLYNTVATL	10.18T	6	2	2	33.3%	66.7%
RL10	Rev	RPAEPVPLQL	3.22	11	3	1	27.3%	36.4%

Table 2-S3: Summary from Bennett *et al.* of infected-cell killing efficiency. (A) and virus suppression **(B)** by CTL clones derived from HIV-1-infected persons (27).

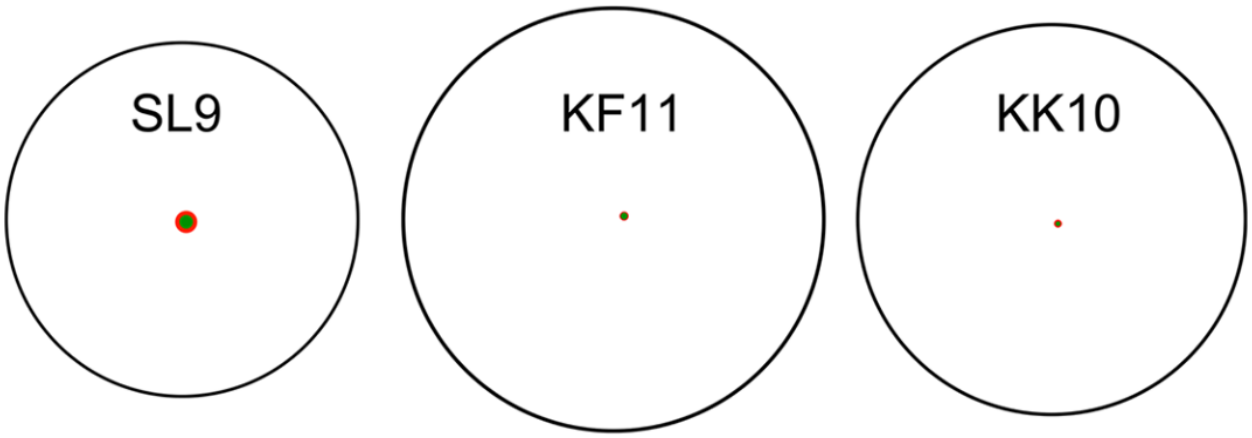

Supplemental Figure 2-S1: Variable fitness constraints of different CTL-targeted epitopes in HIV-1. From Gorin *et al.*, Plos Path, 2017 (reference 29). Areas of the graphs represent numerical proportions. The outer circles represent all possible single and double amino acid variants within each epitope; the area within the red (including the green) circles represents all variants that were considered viable, and green (innermost) circles represent viable variants that were susceptible to the CTL clones tested.

References

1. November 30 CSH gov D last updated:, 2021. Global Statistics [Internet]. HIV.gov. 2021 [cited 2022 Jul 24]. Available from: https://www.hiv.gov/hiv-basics/overview/data-and-trends/global-statistics

2. Phanuphak N, Gulick RM. HIV treatment and prevention 2019: current standards of care. Curr Opin HIV AIDS. 2020 Jan;15(1):4–12.

3. Global HIV & AIDS statistics — Fact sheet [Internet]. [cited 2022 Jul 24]. Available from: https://www.unaids.org/en/resources/fact-sheet

4. Brown LB, Spinelli MA, Gandhi M. The interplay between HIV and COVID-19: summary of the data and responses to date. Curr Opin HIV AIDS. 2021 Jan;16(1):63–73.

5. Kavanagh M, Cohn J, Mabote L, Meier BM, Williams B, Russell A, et al. Evolving Human Rights and the Science of Antiretroviral Medicine. Health Hum Rights. 2015 Jun 11;17(1):E76-90.

6. Martin AR, Siliciano RF. Progress Toward HIV Eradication: Case Reports, Current Efforts, and the Challenges Associated with Cure. Annu Rev Med. 2016;67(1):215–28.

7. International HIV Controllers Study, Pereyra F, Jia X, McLaren PJ, Telenti A, de Bakker PIW, et al. The major genetic determinants of HIV-1 control affect HLA class I peptide presentation. Science. 2010 Dec 10;330(6010):1551–7.

8. Koup RA, Safrit JT, Cao Y, Andrews CA, McLeod G, Borkowsky W, et al. Temporal association of cellular immune responses with the initial control of viremia in primary human immunodeficiency virus type 1 syndrome. J Virol. 1994 Jul;68(7):4650–5.

9. Borrow P, Lewicki H, Hahn BH, Shaw GM, Oldstone MB. Virus-specific CD8+ cytotoxic T-lymphocyte activity associated with control of viremia in primary human immunodeficiency virus type 1 infection. J Virol. 1994 Sep;68(9):6103–10.

10. Borrow P, Lewicki H, Wei X, Horwitz MS, Peffer N, Meyers H, et al. Antiviral pressure exerted by HIV-1-specific cytotoxic T lymphocytes (CTLs) during primary infection demonstrated by rapid selection of CTL escape virus. Nat Med. 1997 Feb;3(2):205–11.

11. Geels MJ, Cornelissen M, Schuitemaker H, Anderson K, Kwa D, Maas J, et al. Identification of sequential viral escape mutants associated with altered T-cell responses in a human immunodeficiency virus type 1-infected individual. J Virol. 2003 Dec;77(23):12430–40.

12. Jamieson BD, Yang OO, Hultin L, Hausner MA, Hultin P, Matud J, et al. Epitope escape mutation and decay of human immunodeficiency virus type 1-specific CTL responses. J Immunol Baltim Md 1950. 2003 Nov 15;171(10):5372–9.

13. Ndhlovu ZM, Kamya P, Mewalal N, Kløverpris HN, Nkosi T, Pretorius K, et al. Magnitude and Kinetics of CD8+ T Cell Activation during Hyperacute HIV Infection Impact Viral Set Point. Immunity. 2015 Sep 15;43(3):591–604.

14. Kuroda MJ, Schmitz JE, Charini WA, Nickerson CE, Lifton MA, Lord CI, et al. Emergence of CTL coincides with clearance of virus during primary simian immunodeficiency virus infection in rhesus monkeys. J Immunol Baltim Md 1950. 1999 May 1;162(9):5127–33.

15. Barouch DH, Kunstman J, Kuroda MJ, Schmitz JE, Santra S, Peyerl FW, et al. Eventual AIDS vaccine failure in a rhesus monkey by viral escape from cytotoxic T lymphocytes. Nature. 2002 Jan 17;415(6869):335–9.

16. Yang OO, Sarkis PTN, Ali A, Harlow JD, Brander C, Kalams SA, et al. Determinants of HIV-1 Mutational Escape From Cytotoxic T Lymphocytes. J Exp Med. 2003 May 19;197(10):1365–75.

17. Tomaras GD, Plotkin SA. Complex immune correlates of protection in HIV-1 vaccine efficacy trials. Immunol Rev. 2017 Jan 1;275(1):245–61.

18. Shiver JW, Fu TM, Chen L, Casimiro DR, Davies ME, Evans RK, et al. Replication-incompetent adenoviral vaccine vector elicits effective anti-immunodeficiency-virus immunity. Nature. 2002 Jan 17;415(6869):331–5.

19. Buchbinder SP, Mehrotra DV, Duerr A, Fitzgerald DW, Mogg R, Li D, et al. Efficacy assessment of a cell-mediated immunity HIV-1 vaccine (the Step Study): a double-blind, randomised, placebo-controlled, test-of-concept trial. Lancet. 2008 Nov 29;372(9653):1881–93.

20. Yang OO. Will we be able to ‘spot’ an effective HIV-1 vaccine? Trends Immunol. 2003 Feb 1;24(2):67–72.

21. Balamurugan A, Ng HL, Yang OO. Cross-Reactivity against Multiple HIV-1 Epitopes Is Characteristic of HIV-1-Specific Cytotoxic T Lymphocyte Clones. J Virol. 2018 Aug 15;92(16):e00617-18.

22. Gray G, Buchbinder S, Duerr A. Overview of STEP and Phambili trial results: two phase IIb test-of-concept studies investigating the efficacy of MRK adenovirus type 5 gag/pol/nef subtype B HIV vaccine. Curr Opin HIV AIDS. 2010 Sep;5(5):357–61.

23. Fitzgerald DW, Janes H, Robertson M, Coombs R, Frank I, Gilbert P, et al. An Ad5-Vectored HIV-1 Vaccine Elicits Cell-mediated Immunity but does not Affect Disease Progression in HIV-1–infected Male Subjects: Results From a Randomized Placebo-Controlled Trial (The Step Study). J Infect Dis. 2011 Mar 15;203(6):765–72.

24. Rolland M, Tovanabutra S, deCamp AC, Frahm N, Gilbert PB, Sanders-Buell E, et al. Genetic impact of vaccination on breakthrough HIV-1 sequences from the STEP trial. Nat Med. 2011 Mar;17(3):366–71.

25. Price DA, Brenchley JM, Ruff LE, Betts MR, Hill BJ, Roederer M, et al. Avidity for antigen shapes clonal dominance in CD8+ T cell populations specific for persistent DNA viruses. J Exp Med. 2005 Nov 21;202(10):1349–61.

26. Venturi V, Price DA, Douek DC, Davenport MP. The molecular basis for public T-cell responses? Nat Rev Immunol. 2008 Mar;8(3):231–8.

27. Bennett MS, Ng HL, Dagarag M, Ali A, Yang OO. Epitope-Dependent Avidity Thresholds for Cytotoxic T-Lymphocyte Clearance of Virus-Infected Cells. J Virol. 2007 May 15;81(10):4973–80.

28. Bennett MS, Joseph A, Ng HL, Goldstein H, Yang OO. Fine-tuning of T-cell receptor avidity to increase Hiv epitope variant recognition by cytotoxic T lymphocytes. Aids. 2010 Nov 13;24(17):2619–28.

29. Gorin AM, Du Y, Liu FY, Zhang TH, Ng HL, Hofmann C, et al. HIV-1 epitopes presented by MHC class I types associated with superior immune containment of viremia have highly constrained fitness landscapes. PLOS Pathog. 2017 Aug 7;13(8):e1006541.

30. Gorin A. Defining The Fitness Landscape of HIV-1 Escape from CD8+ Cytotoxic T-Lymphocytes [Internet] [Ph.D.]. [United States -- California]: University of California, Los Angeles; [cited 2022 Aug 1]. Available from: https://www.proquest.com/pqdtglobal/docview/1891352439/abstract/A50DDC587DBC41EFPQ/1

31. Bennett MS, Ng HL, Ali A, Yang OO. Cross-Clade Detection of HIV-1—Specific Cytotoxic T Lymphocytes Does Not Reflect Cross-Clade Antiviral Activity. J Infect Dis. 2008 Feb 1;197(3):390–7.

32. Ali A, Jamieson BD, Yang OO. Half-genome human immunodeficiency virus type 1 constructs for rapid production of reporter viruses. J Virol Methods. 2003 Jun 30;110(2):137–42.

33. Adachi A, Gendelman HE, Koenig S, Folks T, Willey R, Rabson A, et al. Production of acquired immunodeficiency syndrome-associated retrovirus in human and

nonhuman cells transfected with an infectious molecular clone. J Virol. 1986 Aug;59(2):284–91.

34. Ali A, Lubong R, Ng H, Brooks DG, Zack JA, Yang OO. Impacts of epitope expression kinetics and class I downregulation on the antiviral activity of human immunodeficiency virus type 1-specific cytotoxic T lymphocytes. J Virol. 2004 Jan;78(2):561–7.

35. Ali A, Pillai S, Ng H, Lubong R, Richman DD, Jamieson BD, et al. Broadly increased sensitivity to cytotoxic T lymphocytes resulting from Nef epitope escape mutations. J Immunol Baltim Md 1950. 2003 Oct 15;171(8):3999–4005.

36. Salter RD, Howell DN, Cresswell P. Genes regulating HLA class I antigen expression in T-B lymphoblast hybrids. Immunogenetics. 1985;21(3):235–46.

37. Yang OO, Kalams SA, Rosenzweig M, Trocha A, Jones N, Koziel M, et al. Efficient lysis of human immunodeficiency virus type 1-infected cells by cytotoxic T lymphocytes. J Virol. 1996 Sep 1;70(9):5799–806.

38. Adnan S, Balamurugan A, Trocha A, Bennett MS, Ng HL, Ali A, et al. Nef interference with HIV-1-specific CTL antiviral activity is epitope specific. Blood. 2006 Nov 15;108(10):3414–9.

39. QuickAlign [Internet]. [cited 2022 Jul 18]. Available from:https://www.hiv.lanl.gov/content/sequence/QUICK_ALIGNv2/QuickAlign.html?sample_input=1

40. Barré-Sinoussi F, Chermann JC, Rey F, Nugeyre MT, Chamaret S, Gruest J, et al. Isolation of a T-lymphotropic retrovirus from a patient at risk for acquired immune deficiency syndrome (AIDS). Science. 1983 May 20;220(4599):868–71.

41. Valentine LE, Piaskowski SM, Rakasz EG, Henry NL, Wilson NA, Watkins DI. Recognition of Escape Variants in ELISPOT Does Not Always Predict CD8+ T-Cell Recognition of Simian Immunodeficiency Virus-Infected Cells Expressing the Same Variant Sequences. Journal of Virology. 2008 Jan 1;82(1):575–81.

42. Chen DY, Balamurugan A, Ng HL, Cumberland WG, Yang OO. Epitope targeting and viral inoculum are determinants of Nef-mediated immune evasion of HIV-1 from cytotoxic T lymphocytes. Blood. 2012 Jul 5;120(1):100–11.

43. Yang OO, Ali A, Kasahara N, Faure-Kumar E, Bae JY, Picker LJ, et al. Short Conserved Sequences of HIV-1 Are Highly Immunogenic and Shift Immunodominance. J Virol. 2015 Jan 15;89(2):1195–204.

44. Li F, Finnefrock AC, Dubey SA, Korber BTM, Szinger J, Cole S, et al. Mapping HIV-1 Vaccine Induced T-Cell Responses: Bias towards Less-Conserved Regions and Potential Impact on Vaccine Efficacy in the Step Study. PLoS One [Internet]. 2011

Jun 10 [cited 2017 Sep 16];6(6). Available from: http://www.ncbi.nlm.nih.gov/pmc/articles/PMC3112144/

45. Yang OO, Daar ES, Ng HL, Shih R, Jamieson BD. Increasing CTL targeting of conserved sequences during early HIV-1 infection is correlated to decreasing viremia. AIDS Res Hum Retroviruses. 2011 Apr;27(4):391–8.

46. Korber B, Hraber P, Wagh K, Hahn BH. Polyvalent vaccine approaches to combat HIV-1 diversity. Immunol Rev. 2017 Jan;275(1):230–44.

47. Brennan CA, Ibarrondo FJ, Sugar CA, Hausner MA, Shih R, Ng HL, et al. Early HLA-B*57-Restricted CD8+ T Lymphocyte Responses Predict HIV-1 Disease Progression. J Virol. 2012 Oct 1;86(19):10505–16.

Chapter 3: Dominant CD8+ T Cell Nucleocapsid Targeting in SARS-CoV-2 Infection and Broad Spike Targeting from Vaccination

INTRODUCTION

The correlates of immune protection against SARS-CoV-2 are still being defined (1,2). Antibodies likely prevent or lessen early infection (3–5) but have little capacity to ameliorate established severe infection (6–8). The mRNA vaccines afford protection from disease after a single dose before detectable neutralizing antibodies, indicating importance of cellular immunity (2,9). Likely both antibodies and T cells have important roles, separately or in concert.

A global Th1 T cell profile correlates with positive outcome after infection (10), including bias of virus-specific T cells (11–14). Development of virus-specific cellular immunity correlates to recovery from infection (12,15). Given the protective role of CD8+ T cells in many viral infections, SARS-CoV-2-specific CD8+ T cells (16–19) may be particularly important for preventing severe disease. Antiviral CD8+ T cell frequency and breadth have not been clearly defined in most studies, most of which have used single pools of predicted epitopes from across the proteome and/or unseparated PBMC for qualitative evaluations.

SARS-CoV-2 vaccines protect against serious illness and death (20,21). There have been increasing observations of vaccinated persons becoming infected, associated with viral spike mutations mediating antibody resistance (22–25). Despite these breakthrough infections, vaccination still protects against severe illness or death, further underscoring the importance of cellular immunity (9,26). To date, however, CD8+ T cell responses against the vaccine have not been compared in detail to natural infection.

Here we confirm the overall Th1 profile of SARS-CoV-2-specific T cells and examine the targeting of spike, nucleocapsid, matrix, and envelope proteins by the CD8+ T cell subset in persons recovered from recent SARS-CoV-2 infection. The stability of these responses is evaluated, as well as boosting after vaccination. In SARS-CoV-2-naïve individuals, vaccine-elicited antiviral CD8+ T cell targeting is compared to that from natural infection.

RESULTS

After Infection, CD4+ T Cell Responses Against SARS-CoV-2 Are Predominately IFN-ɣ-Expressing

Virus-specific T cell responses in 25 persons early after COVID19 (mean 29.8 days after symptom onset, range 15-49 days) were assessed by intracellular cytokine staining after stimulating PBMC with pooled peptides. These peptides spanned the spike protein and included predicted CD4+ T cell epitopes across the proteome (spike and CD4 “megapools”) (27). CD4+ T cells were assessed for IL-2, IFN-ɣ, IL-4, IL-10, and IL-17 production (**Figure 3-S1** and **Figures 3-1A, 3-B**). IFN-ɣ production predominated, with a mean of 0.030% positive cells (17/25, 68% of persons above 0.01%). IL-2 responses were lower, with a mean of 0.010% (12/25, 48% of persons above 0.01%). Most cells producing IL-2 also produced IFN-ɣ; the mean percentage of cells producing either was 0.033% (18/25, 72% of persons above 0.01%). Few virus-specific CD4+ T cells produced IL-10, IL-17, or IL-4 (means 0.003%, 0.002%, and 0.007%, respectively). None of these responses correlated to concurrent anti-RBD antibody levels (**Fig. 3-2**).

CD8$^+$ T Cell Responses Against SARS-CoV-2 Are Also Predominately IFN-ɣ-Expressing

The CD8+ T cell subset in PBMC was evaluated in parallel (**Figure 3-S1** and **Figures 3-1C, 3-D**). The response was mostly limited to IFN-ɣ, with a mean of 0.053% positive cells (17/25 or 68% above 0.01%). IL-2 responses were minimal, with a mean of 0.001% (6/25 or 18% of persons above 0.01%). Again, IL-2 production mostly overlapped IFN-ɣ production; the mean percentage of cells producing either was 0.054% positive cells (18/25, 72% of persons above 0.01%). There were minimal IL-17, IL-10, or IL-4 responses (means 0.002%, 0.004%, and 0.012%, respectively), but a few individuals had significant IL-4 responses (6/26, 23% of persons above 0.01%). None of these responses correlated to anti-RBD antibody levels (**Figure 3-S2**). Testing of intracellular cytokine responses using pooled peptides of predicted CD8+ minimal epitopes from across the SARS-CoV-2 proteome (CD8 “megapools” (27) yielded lower frequencies with a similar pattern (**Figure 3-S3**).

CD8+ T Cell Responses Broadly Target Nucleocapsid, Spike, and Matrix, but Not Envelope, and Nucleocapsid Is Immunodominant

The CD8+ T cell responses were studied at higher resolution using IFN-ɣ ELISpot assays for responses to smaller pools of overlapping peptides spanning spike (12 pools), nucleocapsid (four pools), matrix (two pools), and envelope (one pool) proteins. Cells used in this assay were polyclonally expanded in culture from PBMC with a bispecific αCD3:CD4 antibody, which will be referred to simply as expanded CD8+ T cells hereafter. This assay yielded spike-specific responses correlating to intracellular

cytokine staining IFN-ɣ responses to stimulation with the spike/CD4+ T cell megapools (**Figure 3-S4**). Across individuals, all pools were targeted except envelope (**Figure 3-3**). The average total responses against spike, nucleocapsid, matrix, and envelope were 396, 901, 296, and 0 spot-forming cells (SFC) per million CD8+ T cells, respectively. Targeting density considered in relationship to target protein size yielded means of 0.31, 2.15, and 1.33 SFC/million CD8+ T cells/ amino acid against spike, nucleocapsid, and matrix, respectively (**Figure 3-S5A**). Targeting of nucleocapsid was significantly greater than spike ($p<0.0001$) but not significantly greater than matrix ($p=0.15$), while matrix targeting was also significantly greater than spike ($p=0.012$).

A similar hierarchy was noted for numbers of responses against pools, a surrogate for breadth of epitope targeting. On average, each person targeted 1.43, 1.50, 0.59, and 0 pools in spike, nucleocapsid, matrix, and envelope, respectively. Assuming that each recognized pool corresponded to one recognized epitope, this equated to 0.0011, 0.0036, and 0.0027 epitopes targeted per amino acid for spike, nucleocapsid, and matrix, respectively (**Figure 3-S5B**). Epitope targeting of nucleocapsid was significantly greater than spike ($p<0.0001$) but not significantly greater than matrix ($p=0.11$), while matrix targeting was also significantly greater than spike ($p=0.0029$). Finally, comparisons of CD8+T cell targeting to anti-RBD antibody levels revealed no correlation (**Figure 3-S6**). Overall, these findings demonstrated highly dominant CD8+ T cell targeting of nucleocapsid over spike, likely intermediate targeting of matrix, and no targeting of envelope.

CD8+ T Cell Responses Against Spike, Nucleocapsid, and Matrix Generally Wane Over Time, and Responses Against Nucleocapsid Are More Persistent

For 29 persons with longitudinal measurements after early infection, responses in expanded $CD8^+$ T cells were tracked for stability. There were 23 (**Figure 3-4A**), 24 (**Figure 3-4B**), and 16 (**Figure 3-4C**) responders available to evaluate for spike, nucleocapsid, and matrix responses, respectively. These responses generally waned over time, with drops in 21/23 (91%), 23/24 (96%), and 15/16 (94%), respectively. Because they often fell to undetectable levels by the second measurement, calculated decay rates were minimal estimates; the observed mean slopes were -0.026, -0.010, and -0.037 $\log_{10}$ SFC/million $CD8^+$ T cells/day for spike, nucleocapsid, and matrix, respectively. Comparing these slopes, loss of anti-nucleocapsid responses was slower than anti-spike ($p=0.042$) and anti-matrix ($p=0.018$) responses. Thus, $CD8^+$ T cell responses against nucleocapsid were not only immunodominant, but more persistent.

SARS-CoV-2 Vaccines Boost Memory $CD8^+$ T Cell Responses Against Spike

mRNA and adenovirus-based COVID-19 vaccines would be expected to access the human leukocyte antigen class I pathway to elicit $CD8^+$ T cell responses. Anti-spike responses in 17 persons with past SARS-CoV-2 infection were evaluated pre- and post-vaccination, measured by IFN-ɣ ELISpot using expanded $CD8^+$ T cells. Vaccination occurred a mean of 225 days from symptom onset (range 64 to 394 days), with eight persons receiving BNT162b2, seven persons receiving mRNA-1273, and two persons receiving Ad26.COV2.S vaccines. In 13/17 persons (76%), the magnitude of anti-spike responses increased after vaccination (**Figure 3-4D**). Responses against nucleocapsid

and matrix fell in 12/17 persons (71%). Increases in responses against nucleocapsid and matrix tended to be observed at the low end of assay sensitivity (~100 SFC/million $CD8^+$ T cells), suggesting assay noise. Among the four persons in whom spike responses did not increase after vaccination, two had no detectable responses at baseline before vaccination, and all four received BNT162b2. Comparison of peptide pool targeting pre- and post vaccination (**Figure 3-4E**) demonstrated significantly greater Sørenson similarity indices within individuals than between individuals (means 0.86 and 0.78, respectively, p=0.010). These findings confirmed that vaccination yields spike targeting similar to prior infection, indicative of boosting memory responses.

SARS-CoV-2 Vaccines Elicit Spike Specific $CD8^+$ T Cell Responses With Similar Targeting in Previously Uninfected Persons Compared to Natural Infection

IFN-ɣ ELISpot assays for $CD8^+$ T cell responses against spike were performed for 22 persons without prior SARS-CoV-2 infection who were vaccinated (15 with BNT162b2 and 7 with mRNA-1273 vaccines) using expanded $CD8^+$ T cells. Responses were evaluated a mean of 11.3 days after the first vaccination (range 8 to 16 days) showed targeting against all peptide pools (**Figure 3-5**), and the average total spike targeting was 2,463 SFC/ million $CD8^+$ T cells. Each person recognized a mean of 4.2 spike pools (range 1 to 10). Comparison to natural infection (**Figure 3-3**) in terms of the distribution of targeting (mean percentage of SFC against each pool versus entire spike, **Figure 3-6A**) or the frequency of targeting (percentage of persons recognizing each pool, **Figure 3-6B**) showed direct correlation, indicating that targeting induced by vaccination is similar to targeting induced by natural infection.

DISCUSSION

The protective contribution of SARS-CoV-2-specific $CD8^+$ T cells is increasingly apparent (16–19), consistent with their known importance for clearing infected cells in other viral infections. Most studies have focused on the phenotypic characteristics of cellular immunity in bulk, such as cytokine production in response to pooled predicted epitope peptides, without detail on targeting of responses. We confirm Th1 bias in both $CD4^+$ and $CD8^+$ virus-specific T cells (11–14), using intracellular staining for IFN-ɣ, IL-2, IL-4, IL-17, and IL-10 in PBMC.

IFN-ɣ production dominated for both T cell subsets, followed by IL-2, with more $CD4^+$ T cells than $CD8^+$ T cells producing IL-2. Most IFN-ɣ-producing cells did not produce IL-2, particularly the $CD8^+$ subset, supporting prior findings (28–30). Minimal production of IL-10 or IL-17 were observed; IL-10 (31) and IL 17 (32) production have been linked to disease progression, but our participants were mostly limited to those who recovered from mild illness.

A few individuals had significant populations of IL-4- producing $CD8^+$ T cells of unclear significance, not previously reported in SARS-CoV-2 infection to our knowledge. IL-4- producing $CD8^+$ T cells have been suggested to be noncytolytic helper cells that do not produce IFN-ɣ (33), associated with humoral immunity in old age (34), asthma in children (35), and autoimmune arthritis (36). Whether they might play a protective (anti-inflammatory), pathogenic (immunosuppressive), or mixed role in COVID-19 is unclear.

Our observations agree with others' observations that most infected persons develop SARS-CoV-2-targeted cellular immune responses (29,37–40). By intracellular cytokine staining flow cytometry in PBMC after incubation with spike/CD4 epitope

megapools (27), 72% and 80% of persons had IFN-ɣ and/or IL-2 responses in the $CD4^+$ and $CD8^+$ T cell subsets, respectively. Considering all tested cytokines and both peptide megapool conditions, all persons had both $CD4^+$ and $CD8^+$ T cell responses (not shown). By IFN-ɣ ELISpot for spike, nucleocapsid, matrix, and envelope in expanded $CD8^+$ T cells, 93% of persons had detectable $CD8^+$ T cell responses against at least one protein.

Others have observed preferential targeting of structural proteins (12,14,27–29,37,38,41–43), using either predicted epitopes (12,27,38,41,43) or overlapping peptides (14,28,29,37,42) combined into single pools. Two studies from Le Bert *et al.* (14) and Peng *et al.* (29) used multiple smaller pools in IFN-ɣ ELISpot assays to assess targeting breadth, but did not separate $CD4^+$ from $CD8^+$ T cell populations. Le Bert et al. found that responses against matrix were most targeted, followed by those against spike or nucleocapsid (envelope was not tested) (14), but Peng *et al.* found that spike was most highly targeted, while nucleocapsid and matrix were similar, and many persons had envelope targeting (29). However, the contributions of $CD4^+$ versus $CD8^+$ T cells to these patterns were not defined.

We follow up in greater detail using expanded $CD8^+$ T cells with small pools of overlapping peptides spanning spike, nucleocapsid, matrix, and envelope in IFN-ɣ ELISpot assays of infected participants. In contrast to Le Bert *et al.* and Peng *et al.* using unseparated PBMC, we clearly identify nucleocapsid as the dominant target of $CD8^+$ T cells. Matrix targeting is quantitatively similar to spike, but more densely targeted, and we observe no targeting of envelope. Similar to Le Bert *et al.* using unseparated PBMC, we find that T cell targeting is distributed across spike, and most

persons target at least one spike epitope. Moreover, we observe modestly higher frequency of receptor binding domain (RBD) targeting, accounting for about a third of responses despite being about a sixth of spike. Even so, the few mutations mostly in the RBD defining various spike variants seem unlikely to affect recognition by $CD8^+$ T cells (44). Overall, differences from the findings of Le Bert *et al.* and Peng *et al.* may result primarily from evaluation of isolated $CD8^+$ T cells versus bulk PBMC (in which $CD4^+$ T cells typically predominate); other studies grossly comparing $CD4^+$ T cells to $CD8^+$ T cells have shown that the former tend to predominate (12,39,42,45–47), and that the two do not correlate (48). Finally, our results suggest that nucleocapsid might be a useful target for vaccine inclusion to elicit broader and more durable CD8+ T cell responses, which is also supported by a recent study suggesting that immunodominant targeting of nucleocapsid is associated with better outcome after SARS-CoV-2 infection (49).

Various studies reported differing results on longevity of virus-specific T cell responses (CD4+, CD8+ or combined) after SARS-CoV-2 infection, with observations of both persistence (30,38,40,46–48,50,51) and decay (14,40,52,53). We observed decay of CD8+ T cell responses similar to our observations of anti-RBD antibodies (54,55), and most rapid waning of matrix responses, in agreement with Le Bert *et al.* (14). The reasons for discrepant findings between studies are unclear, but may relate to methodologies (intracellular cytokine staining versus ELISpot), CD4+ versus CD8+ versus unseparated subsets, targeting of responses measured, and differences in illness severity. As opposed to antibodies (and B cell memory) being required for immediate viral neutralization during exposure or early infection, T cells probably have a

more prolonged effector role in containing and clearing infection, so it is unclear whether our observed peripheral blood decay of the CD8+ T cell response is functionally relevant. Data showing ongoing vaccine protection from severe illness or death despite waning protection from infection (26,56) are further evidence that the falling level of circulating antiviral CD8+ T cells we observe do not preclude an effective recall response.

Some groups have observed either correlation (29,57) or lack of correlation (40) of T cell responses to antibodies. We saw no correlation of either CD4+ or CD8+ T cell responses by intracellular cytokine staining, or CD8+ T cell responses by IFN-ɣ ELISpot to anti-RBD antibodies. These discrepancies again may be related to methodologies or clinical characteristics of the participants. Of note, our cohort included mostly persons who had mild infection (not requiring supplemental oxygen or hospitalization). Because antibody levels vary greatly by disease severity (54,58–60), our dynamic range might have been too limited to see a correlation.

Our data also address spike targeting induced by vaccination. While initial pilot studies of the two mRNA vaccines demonstrated cellular immunity (61,62), these were measurements of whole PBMC by intracellular cytokine staining using a single peptide pool. We provide greater detail, showing vaccination elicits an average of over four targeted epitopes with summed frequency over 1,000 per million CD8+ T cells. While this breadth and frequency was higher than we observed for natural infection, our measurement after vaccination was at the peak, and infected persons were assessed past the peak during infection. A prior study provided results consistent with our suggestion that vaccination boosts prior memory responses against spike; in persons

receiving the BNT162b2 vaccine, those with prior infection reached a level of spike targeting after a single dose that was attained after two doses in persons without prior infection (63). Qualitatively, however, we observed that vaccination and infection generated similar spike responses.

Our study has caveats. Evaluation of cytokine production and T cell "polyfunctionality" was limited to few cytokines and performed with too few PBMC for accurate quantitation or sensitivity below ~0.01%. Our evaluation of CD8+ T cells utilized a cell-sparing expansion method, although results with expanded cells have been shown to correlate well to bulk unexpanded CD8+ T cells (64,65). Responses were evaluated only against spike, nucleocapsid, matrix, and envelope, and could miss dominant responses against other proteins. We did not map to the level of individual peptides/epitopes; thus, we likely underestimated the breadth and depth of targeting. The time points after infection were not frequent enough for precise estimation of decay rates, but only provide minimal boundaries for decay. Most of the COVID-19 participants had mild illness, and there were too few severely ill subjects for comparisons. Finally, the numbers of participants were too small to compare responses between different vaccines.

In summary, we find a Th1-biased IFN-ɣ dominant cellular immune response after SARS-CoV-2 infection in both CD4+ and CD8+ subsets, although some persons have an unusual IL-4- producing CD8+ T cell population of unclear significance. CD8+ T cells predominately target nucleocapsid and those responses appear to be more durable compared to targeting of spike or matrix; no responses were seen against envelope. Vaccination of previously infected persons specifically boosts memory

responses against spike and generates new responses in previously uninfected persons that resemble those from infection. These results provide greater clarity on CD8+ T cell targeting, breadth, and persistence. Inclusion of nucleocapsid in vaccines may allow even broader and longer-lived cellular immune protection against COVID-19 to combat ongoing viral evolution in the pandemic.

MATERIALS & METHODS

Study Participants and Samples

Participants with known immunocompromising conditions (including diabetes mellitus, immunosuppressive medications, HIV-1 infection) were excluded. All COVID-19 recovered persons were infected no later than January 2021, and the majority had mild infection (not requiring supplemental oxygenation or hospitalization). PBMC were isolated from whole blood by density gradient centrifugation and viably cryopreserved until use.

SARS-CoV-2 Synthetic Peptides for Intracellular Cytokine Staining Assays

For intracellular cytokine staining assays, synthetic peptide “megapools” (27) were generously provided by D. Weiskopf and A. Sette. The sets of predicted CD4+ T cell epitopes and overlapping spike peptides were combined in one pool, and the two sets of predicted CD8+ T cell epitopes were combined in a second pool. The final concentration of each peptide during PBMC stimulation was 1µg/ml.

Intracellular Cytokine Staining (ICS) Flow Cytometry

ICS was performed as described (66) with modifications. Cryopreserved PBMC were thawed and plated at ~$5x10^5$ cells per well in 96 well U-bottom plates, with brefeldin A (#00-450651, eBioscience, San Diego, CA) and monensin (#00-4505-51, eBioscience, San Diego, CA) per manufacturer's directions. Each PBMC sample had four wells with: spike plus CD4+ T cell epitope megapools, CD8+ T cell epitope megapools, no additive, or 1µg/ml ionomycin and 500ng/ml PMA (#407951 and #524400, Calbiochem, San Diego, CA). After 6 hours at 37°C, cells were transferred to 5ml polystyrene tubes, washed in PBS with 2% heat inactivated fetal calf serum (wash buffer), and resuspended in wash buffer including antibodies against CD3, CD8, CD4, and Fixable Aqua viability dye for 30 minutes at 4°C (Supplementary Table S1). After washing, cells were permeabilized with Foxp3/ Transcription Factor Staining Buffer (#00-5523-00, eBioscience, San Diego, CA) according to manufacturer's instructions, then stained with antibodies against IL-4, IL-2, IL-10, IFN-ɣ, and IL-17 (Supplementary Table S1) at room temperature for 30 minutes. After washing, the cells were fixed in PBS with 1% paraformaldehyde for analysis (**Figure 3-S1**) on an Attune NxT flow cytometer (ThermoFisher Scientific, West Hills, CA). A minimum of 54,000 live cell events were analyzed. Analysis was performed using FlowJo version 10 software (BD Biosciences).

Determination of Serum Anti-RBD IgG Levels

Anti-RBD IgG levels were assessed as described (54). Briefly, 96-well microtiter plates were coated with 2 mg/mL recombinant RBD protein and blocked with 3% dried milk (Bioworld, Dublin, OH). Serum was added in duplicate serial dilutions, and bound antibodies were detected using goat anti-human IgG conjugated with horseradish peroxidase (Bethyl Laboratories, Montgomery, TX), followed by tetramethylbenzidine substrate solution (ThermoFisher Scientific, Waltham, MA) for measurements at 450 and 650 nm (Spark 10M, Tecan, Baldwin Park, CA). Each plate contained a control titration of the anti-RBD monoclonal antibody CR3022 (Creative Biolabs, Shirley, NY) to provide a standard curve. Serum anti-RBD IgG binding activity was expressed as an equivalent to a concentration of CR3022.

SARS-CoV-2 Synthetic Peptides for IFN-γ ELISpot Assays

Synthetic overlapping peptides spanning SARS-CoV-2 spike, nucleocapsid, matrix, and envelope were obtained from BEI Resources (NR-52402, NR-52404, NR-52403, NR-52405). Lyophilized peptides were initially suspended in DMSO at 20mg/ml, then diluted 10x with water to 2mg/ml. Peptide pools were generated as in **Supplementary Table 3-S2** at 100µg/ml each peptide, and the final concentration of each peptide during the ELISpot assay was 5µg/ml.

IFN-γ ELISpot Assays for CD8+ T Cell Responses

These assays were performed as previously described for measuring HIV-1-specific responses using polyclonally expanded CD8+ T cells (64,67–69), which we and

others have shown to correlate well to unexpanded fresh CD8+ T cells (64,65). In brief, thawed cryopreserved PBMC were plated at 1 to 2 million cells/well in RPMI medium supplemented with IL-2 at 50U/ml (NIH AIDS Reagent Repository Program) with a CD3:CD4 bi-specific monoclonal antibody (gift of Dr. J. Wong) and cultured for approximately 14 days to yield purified polyclonal CD8+ T cells. These cells were viably cryopreserved until the day of ELISpot assay. Cells were added to a 96-well filter plate that had been precoated with an anti-IFN-ɣ antibody (#3420-3-1000, Mabtech, Nacka Strand, Sweden) with the addition of a peptide pool, medium alone (three wells), or medium with PHA (#L1668, Sigma Aldrich, St. Louis, MO) at 25µg/ml. After overnight incubation in a humidified CO2 incubator, the plate was washed and stained with biotinylated anti-IFN-ɣ antibody (#3420-6-250, Mabtech, Nacka Strand, Sweden) for visualization using a streptavidin-peroxidase reagent and counting on an automated ELISpot reader (AID, Autoimmun Diagnostika GMBH, Strassberg, Germany). The response against each peptide pool was expressed as the raw count minus the mean of the triplicate negative control wells, adjusted for the number of cells plated to back-calculate the number of responding cells per million. A positive response against a peptide pool was defined as both ≥50 SFC/million cells and ≥ the mean of the negative control wells plus three standard deviations.

Statistics

Statistical comparisons (two-tailed heteroscedastic Student's t-test) and graphs utilized Microsoft Excel for Mac version 16.50. Sørenson similarity indices between

ELISpot assays were calculated as: the total number of shared spike pool responses (defined as above) ÷ the total number of spike peptide pools (twelve).

Study Approval

Prior to participation, all participants gave written informed consent under an institutional review board-approved protocol at the University of California Los Angeles.

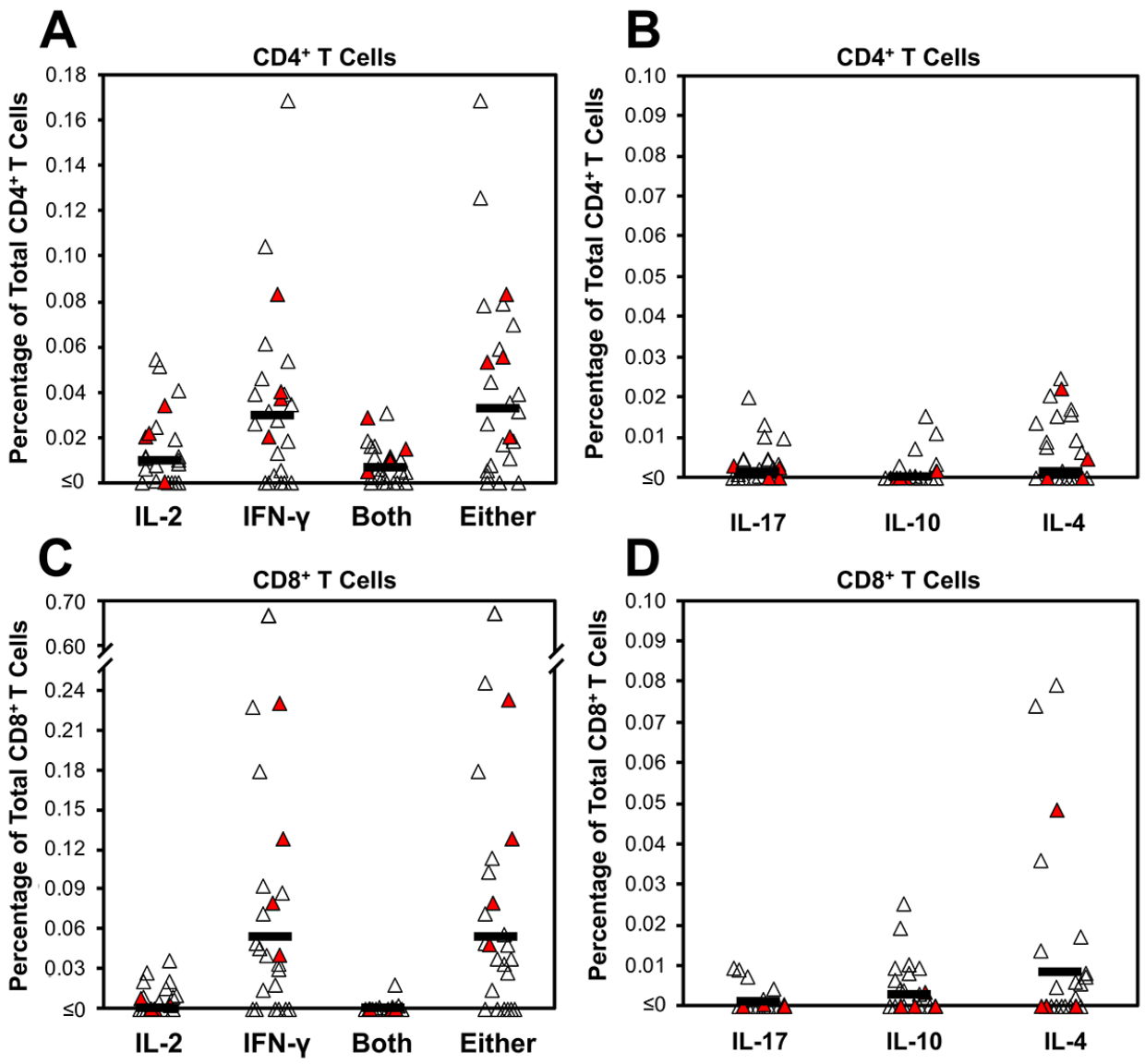

FIGURE 3-1: Intracellular cytokine staining for T cell responses against SARS-CoV-2 early after infection demonstrates bias for IFN-ɣ production. Cytokine production was determined in PBMC by intracellular cytokine staining for $CD4^+$ and $CD8^+$ T cell subsets after stimulation with a pool of overlapping peptides spanning spike combined with predicted $CD4^+$ epitopes from across the proteome (**Supplementary Figure 3-S1**) for 25 persons (21 with mild infection, 4 with severe infection) a mean of 29.8 days from COVID-19 symptom onset (range 15 to 49 days). Filled symbols indicate

persons who had severe infection. **(A)** The background-subtracted frequencies of $CD4^+$ T cells producing IL-2, IFN-ɣ, both cytokines, or either cytokine are plotted. Dark horizontal bars indicate means, which were 0.010%, 0.030%, 0.007%, and 0.033%, respectively. Defining responses as being ≥0.01% above background, responders for these four cytokine response groupings were 12/25 (48%), 17/25 (68%), 10/25 (40%), and 18/25 (72%), respectively. **(B)** The background-subtracted frequencies of $CD4^+$ T cells producing IL-17, IL-10, or IL-4 are plotted. Dark horizontal bars indicate means, which were 0.003%, 0.002%, and 0.007%, respectively. Defining responses as being ≥0.01% above background, responders for these three cytokine responses were 3/26 (11.5%), 2/26 (7.7%), 10/25 (40%), and 7/26 (26.9%), respectively. **(C)** The background-subtracted frequencies of $CD8^+$ T cells producing IL-2, IFN-ɣ, both cytokines, or either cytokine are plotted. Dark horizontal bars indicate means, which were 0.001%, 0.053%, 0.000%, and 0.054%, respectively. Defining responses as being ≥0.01% above background, responders for these four cytokine response groupings were 6/25 (24%),17/25 (68%), 1/25 (4%), and 20/25 (80%), respectively. **(D)** The background-subtracted frequencies of $CD8^+$ T cells producing IL-17, IL-10, or IL-4 are plotted. Dark horizontal bars indicate means, which were 0.002%, 0.004%, and 0.012% respectively. Defining responses as being ≥0.01% above background, responders for these three cytokine responses were 0/26 (0%), 3/26 (11.5%), 10/25 (40%), and 6/26 (23.1%), respectively.

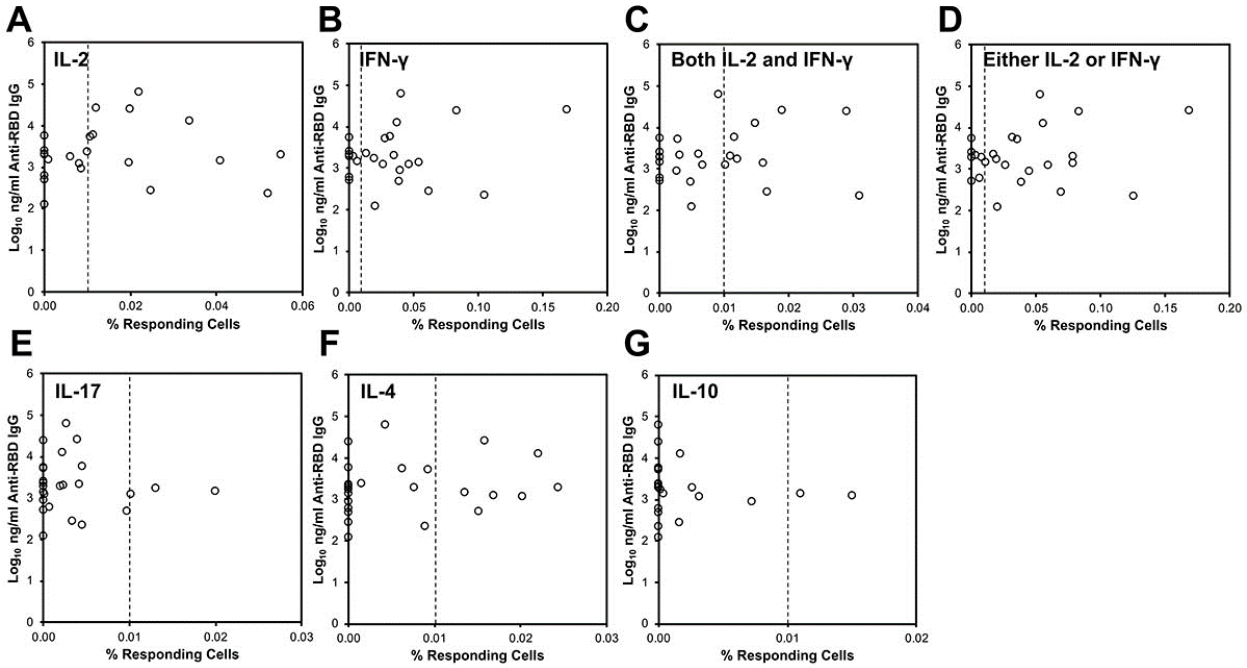

FIGURE 3-2: CD4$^+$ T cell cytokine responses against SARS-CoV-2 do not correlate to serum anti-RBD antibody levels. SARS-CoV-2-specific responses defined as in Figure 1 (x-axis) were compared to serum anti-RBD IgG antibody levels (y-axis). The vertical dotted line indicates 0.01% responding cells producing the indicated cytokine(s). **(A)** Relationship to IL-2-producing cells. **(B)** Relationship to IFN-g-producing cells. **(C)** Relationship to cells producing both IL-2 and IFN-ɣ. **(D)** Relationship to cells producing either IL-2 or IFN-g or both. **(E)** Relationship to IL-17-producing cells. **(F)** Relationship to IL-4-producing cells. **(G)** Relationship to IL-10-producing cells.

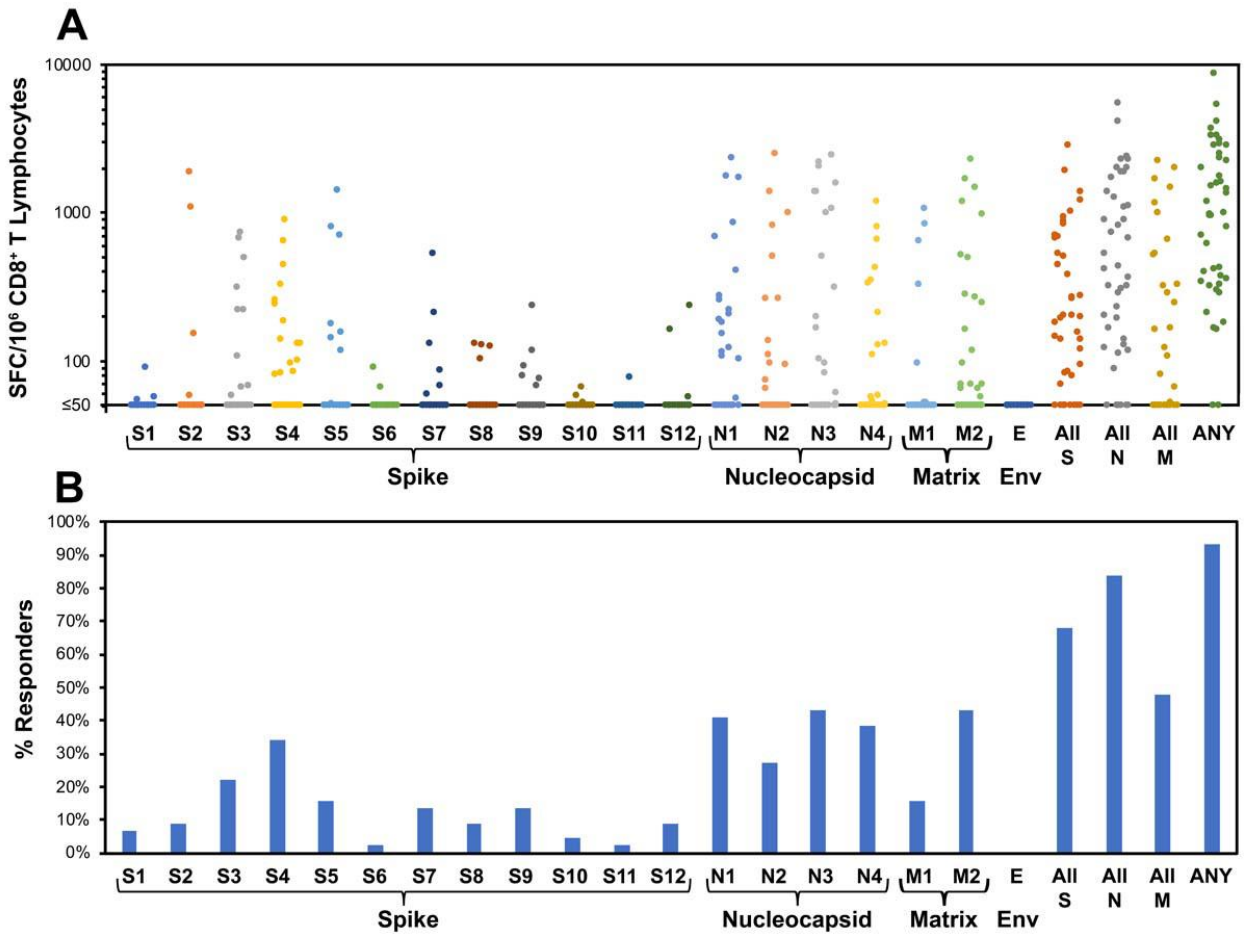

FIGURE 3-3: Evaluation of CD8⁺ T cell targeting of SARS-CoV-2 by ELISpot using peptide pools demonstrates broad targeting of spike, nucleocapsid, and matrix, with dominance of nucleocapsid targeting. For 44 persons after recent SARS-CoV-2 infection (36 with mild infection, 8 with severe infection, mean 31.1 days, range 11 to 47 days after symptom onset), IFN-ɣ ELISpot was performed on polyclonally expanded CD8⁺ T cells using peptides spanning spike, nucleocapsid, matrix, and envelope proteins, which were combined in pools of 16 or fewer **(Supplementary Table 1)**. Spike was contained in 12 pools (S1 to S12), nucleocapsid in four pools (N1 to N4), matrix in two pools (M1 to M2), and envelope in one pool **(E). (A)** Frequencies of responses

against each pool are plotted for each participant. The mean total responses against spike, nucleocapsid, matrix, and envelope were 396 SFC/million $CD8^+$ T cells, 901 SFC/million $CD8^+$ T cells, 296 SFC/million $CD8^+$ T cells, and 0 SFC/million $CD8^+$ T cells, respectively. **(B)** Percentages of persons responding against each pool are plotted. Targeting of spike, nucleocapsid, matrix, and envelope was an average of 1.4, 1.5, 0.6, and 0.0 peptide pools per person, respectively. Response against pools S4 and S5, comprising the receptor binding domain of spike, was an average 0.5 peptide pools per person.

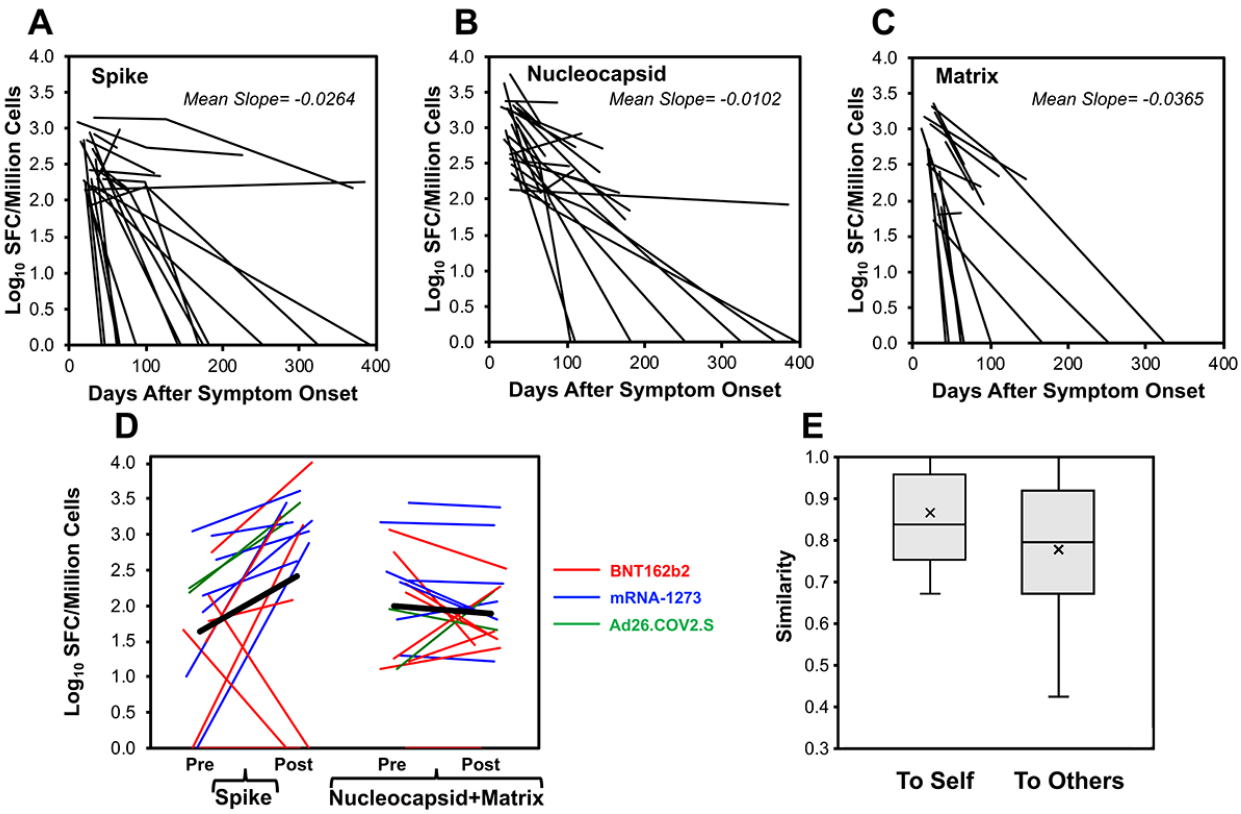

FIGURE 3-4: CD8⁺ T cell responses decay after SARS-CoV-2 infection but vaccination boosts memory against spike protein. CD8⁺ T cell responses were measured longitudinally in expanded CD8+ T cells by IFN-ɣ ELISpot assay in 29 persons monitored starting early SARS-CoV-2 infection (23 with mild infection, 6 with severe infection, starting <45 days after symptom onset). Serial measurements are plotted for 23 total spike responses **(A),** 24 total nucleocapsid responses **(B),** and 16 total matrix responses **(C). (D)** For 17 persons with prior COVID-19 who were vaccinated with an available pre-vaccination measurement within 65 days (14 with mild infection, 3 with severe infection including one who had critical infection, vaccinated mean of 225 days post onset of symptoms, range 64 to 394 days), baseline pre-vaccination (mean of -21.9 days, range -63 to +3 days before vaccination) and resulting

post-vaccination (first dose, mean of 12.8 days, range 5 to 29 days after vaccination) total response levels against spike and combined nucleocapsid plus matrix are plotted. Eight vaccinees received BNT162b2 (red), seven vaccinees received mRNA-1273 (blue), and two vaccinees received Ad26.COV2.S (green). Two non-responders had no detectable response at baseline and received BNT162b2. One non-responder had prior severe illness and the remainder had mild illness. **(E)** For the vaccinated persons, Sørenson similarity values were calculated between pre- and post- vaccination recognized spike pools within each person (self) and across all combinations with other persons (others). Box plots indicate 25th to 75th quartiles and medians, with medians (horizontal line) and means (x) marked. The high background similarity between individuals resulted from the high number of unrecognized pools (average 10.2/12 pools) and thus multiple shared unrecognized pools across persons.

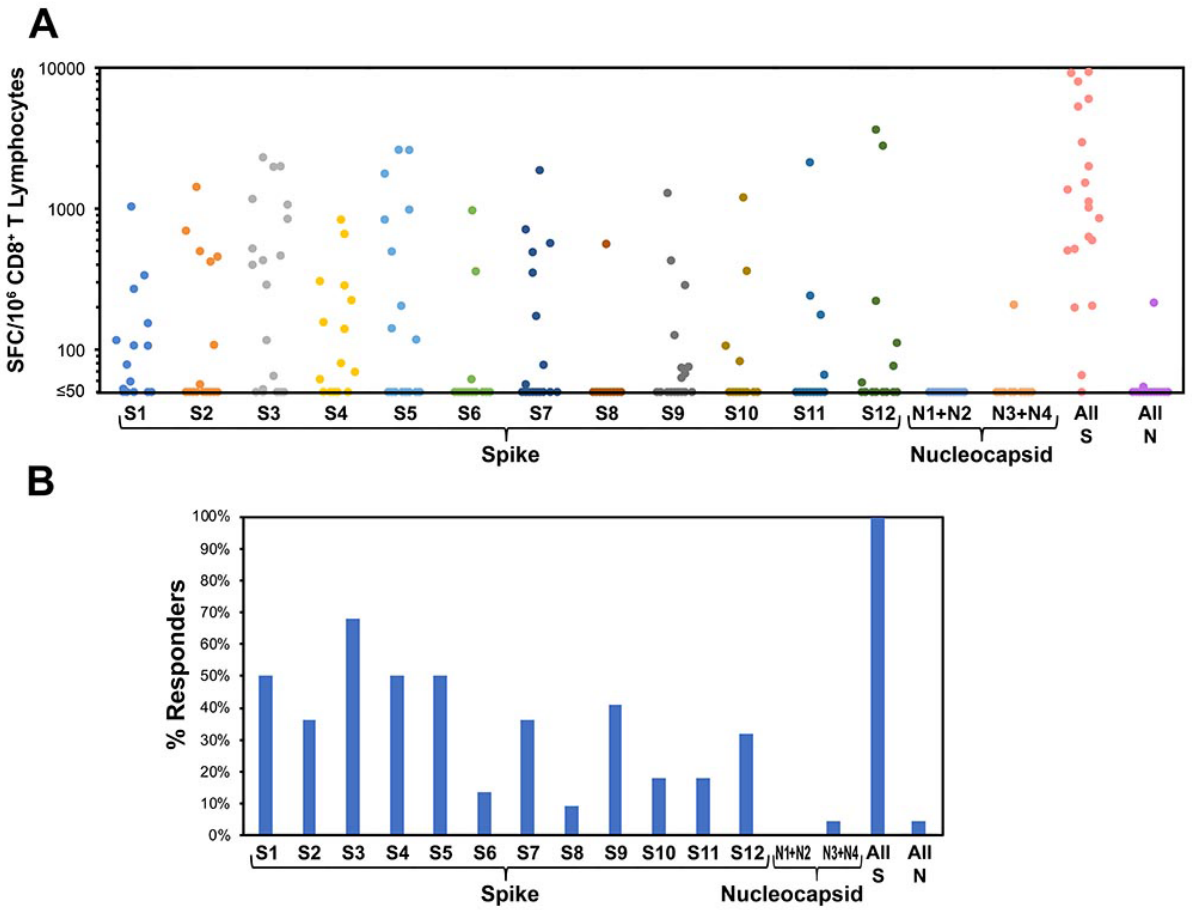

FIGURE 3-5: Spike targeting after vaccination of persons without prior SARS-CoV-2 infection is broadly distributed. 22 persons without a history of SARS-CoV-2 infection were monitored for responses in expanded $CD8^+$ T cells against spike and nucleocapsid (negative control) by IFN-ɣ ELISpot assay after vaccination with BNT162b2 (15 persons) or mRNA 1273 (7 persons). Responses were evaluated a mean of 11.3 days after the first vaccine dose (range 8 to 16 days). **(A)** Frequencies of responses against each pool are plotted for each participant. The mean total response against spike was 2,463 SFC/million $CD8^+$ T cells. **(B)** Percentages of persons responding against each pool are plotted. Targeting of spike was an average of 4.2 pools per person. Response against pools S4 and S5, comprising the receptor binding domain of spike, was an average 1.0 peptide pools per person.

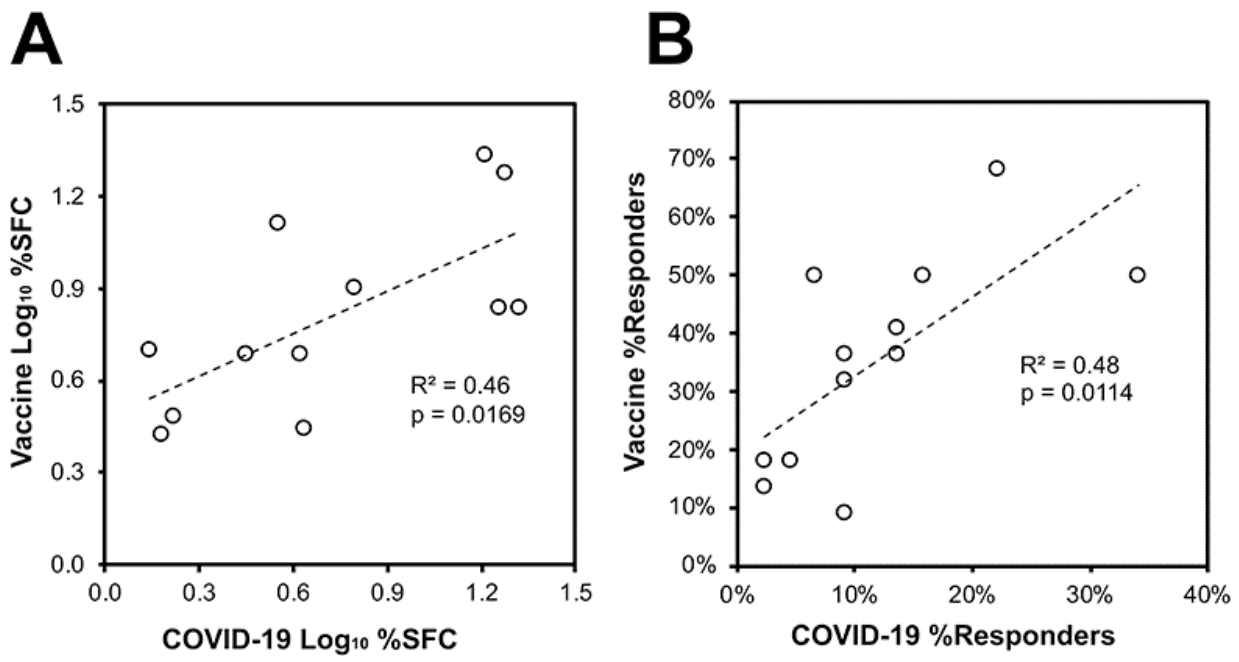

FIGURE 3-6: Vaccination of persons without prior SARS-CoV-2 infection elicits CD8⁺ T cell targeting of spike similar to natural infection. Across the 44 persons with recent SARS-CoV-2 infection **(Figure 3-3)** and 22 persons after vaccination without prior SARS-CoV-2 infection **(Figure 3-5),** spike-specific $CD8^+$ T cell responses were compared (as determined by IFN-ɣ ELISpot using expanded CD8+ T cells). Pearson correlation p values are indicated. **(A)** The mean percentage contribution of each pool to the total spike response (log_{10} transformed) is plotted between the two groups. **(B)** The percentage of persons responding against each pool is plotted between the two groups.

Initial Surface/Viability Stain Panel		
Target	**Label**	**Catalog#, Company**
CD3	Super Bright 436	#62-0037-42, eBioscience, San Diego, CA
CD8	Super Bright 600	#63-0088-42, eBioscience, San Diego, CA
CD4	PE-Cy7	#25-0049-42, eBioscience, San Diego, CA
(Viability)	Fixable Aqua	#L34957, Invitrogen, Waltham, MA
Intracellular Cytokine Stain Panel		
Target	**Label**	**Catalog#, Company**
IL-4	PE	#130-091-647, Miltenyi Biotec, Bergisch Gladbach, Germany
IL-2	PerCP-Cy5.5	#506504, BioLegend, San Diego, CA
IL-10	APC	# 506807, BioLegend, San Diego, CA
IL-17	APC-eFluor	# 47-7179-42, eBioscience, San Diego, CA
IFN-ɣ	FITC	#506504, BioLegend, San Diego, CA

Table 3-S1: Antibodies utilized for surface and intracellular cytokine staining flow cytometry.

			Peptide Number		Amino Acid Number	
	Pool	# Peptides	First	Last	First	Last
Spike Pools	S1	15	1	15	1	115
	S2	15	16	30	106	220
	S3	15	31	45	211	325
	S4	15	46	60	316	430
	S5	15	61	75	421	535
	S6	15	76	90	526	640
	S7	15	91	105	631	745
	S8	15	106	120	736	850
	S9	15	121	135	841	955
	S10	15	136	150	946	1060
	S11	15	151	165	1051	1165
	S12	16	166	181	1156	1273
	Note: RBD is amino acids 319-541					
Nucleocapsid Pools	N1	15	1	15	1	115
	N2	15	16	30	106	220
	N3	15	31	45	211	325
	N4	14	46	59	316	419
Matrix Pools	M1	15	1	15	1	115
	M2	16	16	31	106	199
Envelope Pool	E	10	1	10	1	75

Table 3-S2: Peptide pools utilized for ELISpot mapping.

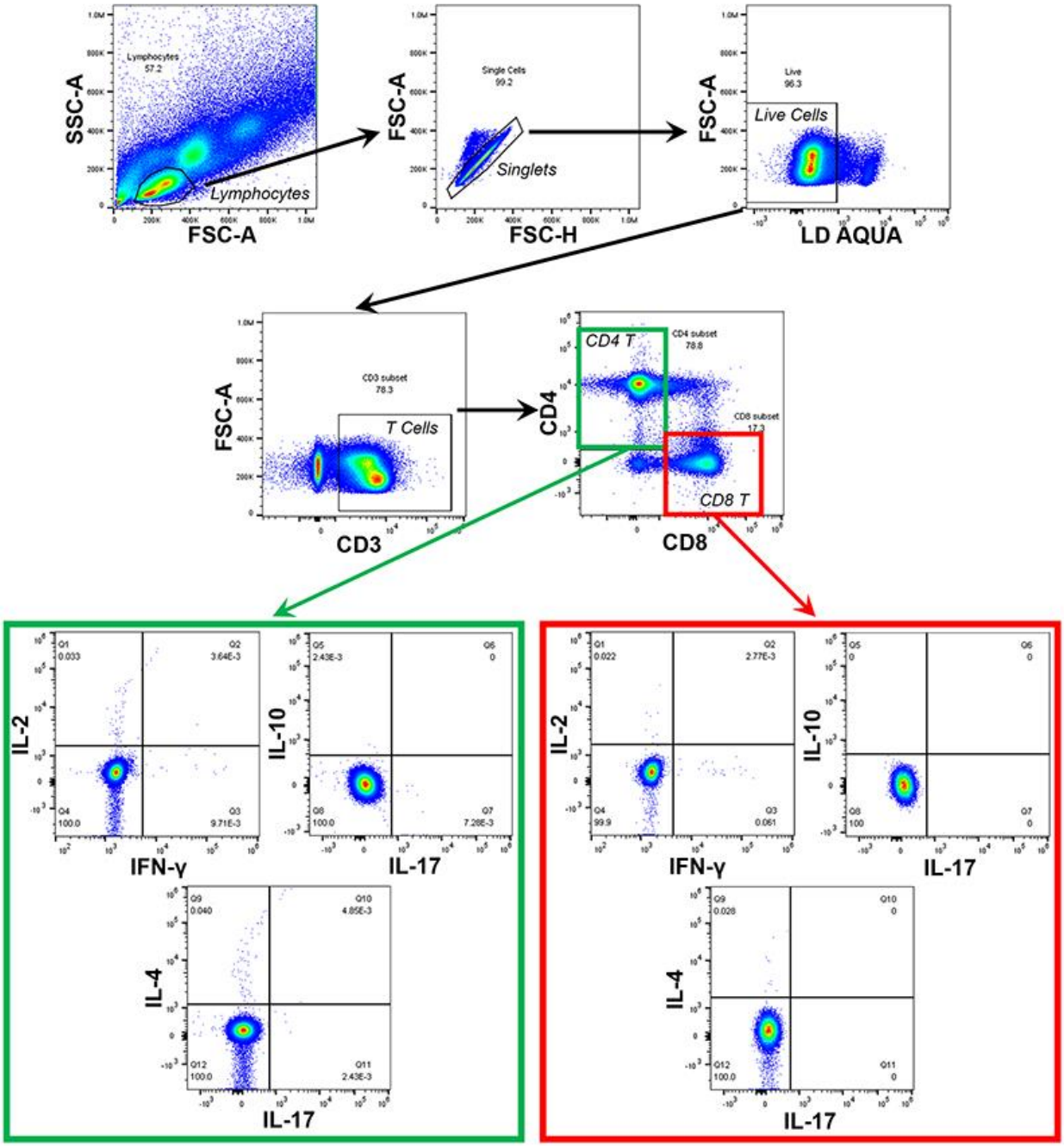
A
SSC-A
FSC-A
Lymphocytes
57.2
Lymphocytes
FSC-A
FSC-H
Single Cells
99.2
Singlets
FSC-A
LD AQUA
Live
96.3
Live Cells
FSC-A
CD3
CD3 subset
78.3
T Cells
CD4
CD8
CD4 subset
78.8
CD4 T
CD8 subset
17.3
CD8 T
IL-2
IFN-γ
IL-10
IL-17
IL-4
IL-17
IL-2
IFN-γ
IL-10
IL-17
IL-4
IL-17

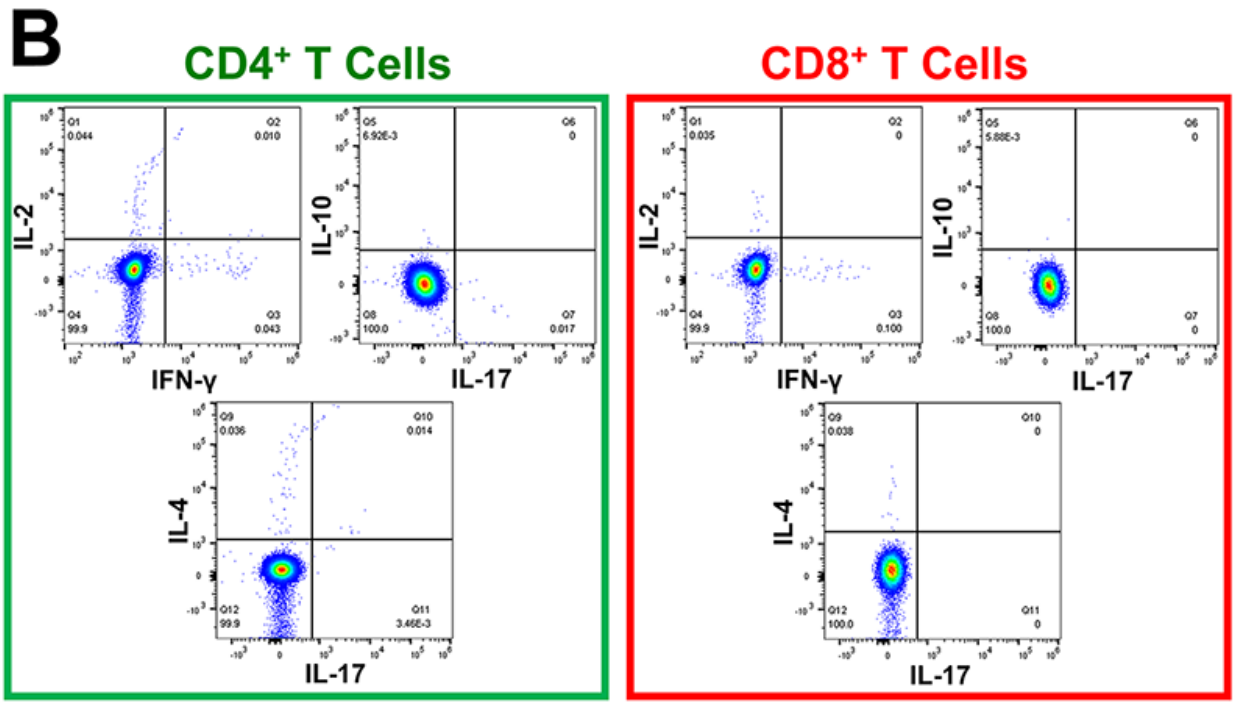

Figure 3-S1: Flow cytometry gating strategy in PBMC and sample data. (A) T cells were defined as $CD3^+$ cells within the live cell singlet lymphocyte population and gated into $CD4^+$ and $CD8^+$ subsets for evaluation. Unstimulated cell results are shown in the colored boxes reflecting the final gated cells. **(B)** Representative megapool-stimulated cell results are shown.

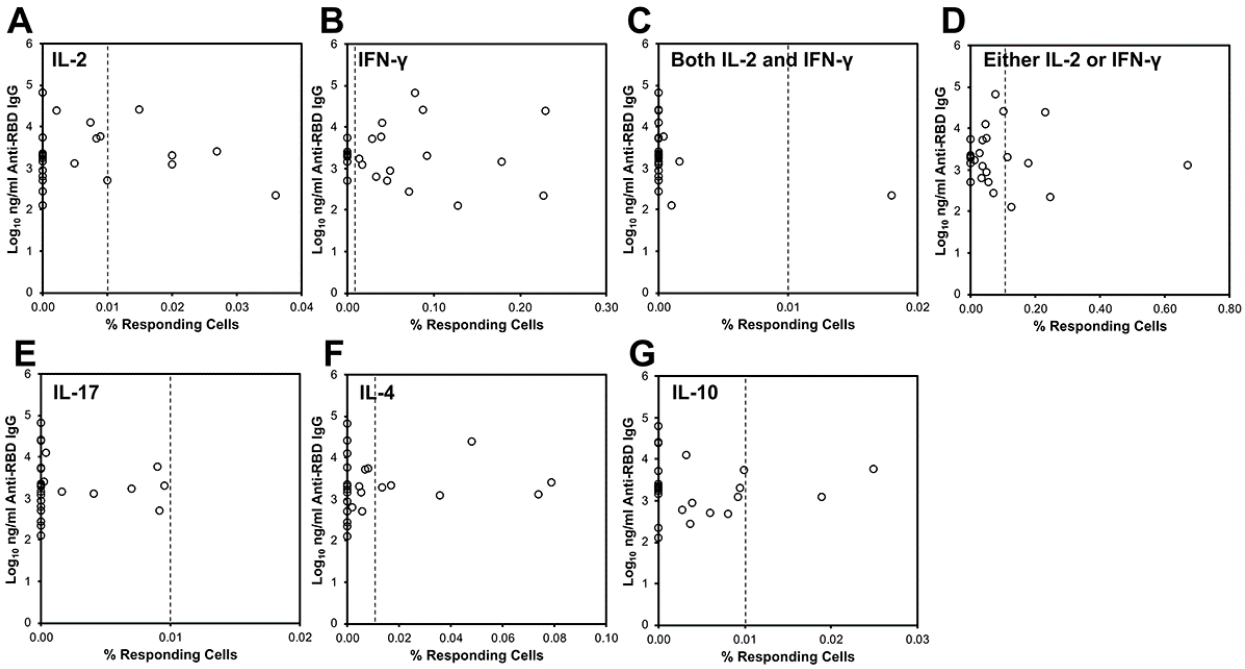

Figure 3-S2: Comparison of CD8+ T cell cytokine responses against SARS- CoV-2 to serum anti-RBD antibody levels demonstrates no correlation. SARS-CoV-2-specific responses defined as in Figure 1 (x-axis) were compared to serum anti-RBD IgG antibody levels (y-axis). The vertical dotted line indicates the cutoff of 0.01% background-subtracted responding cells producing the indicated cytokine(s).

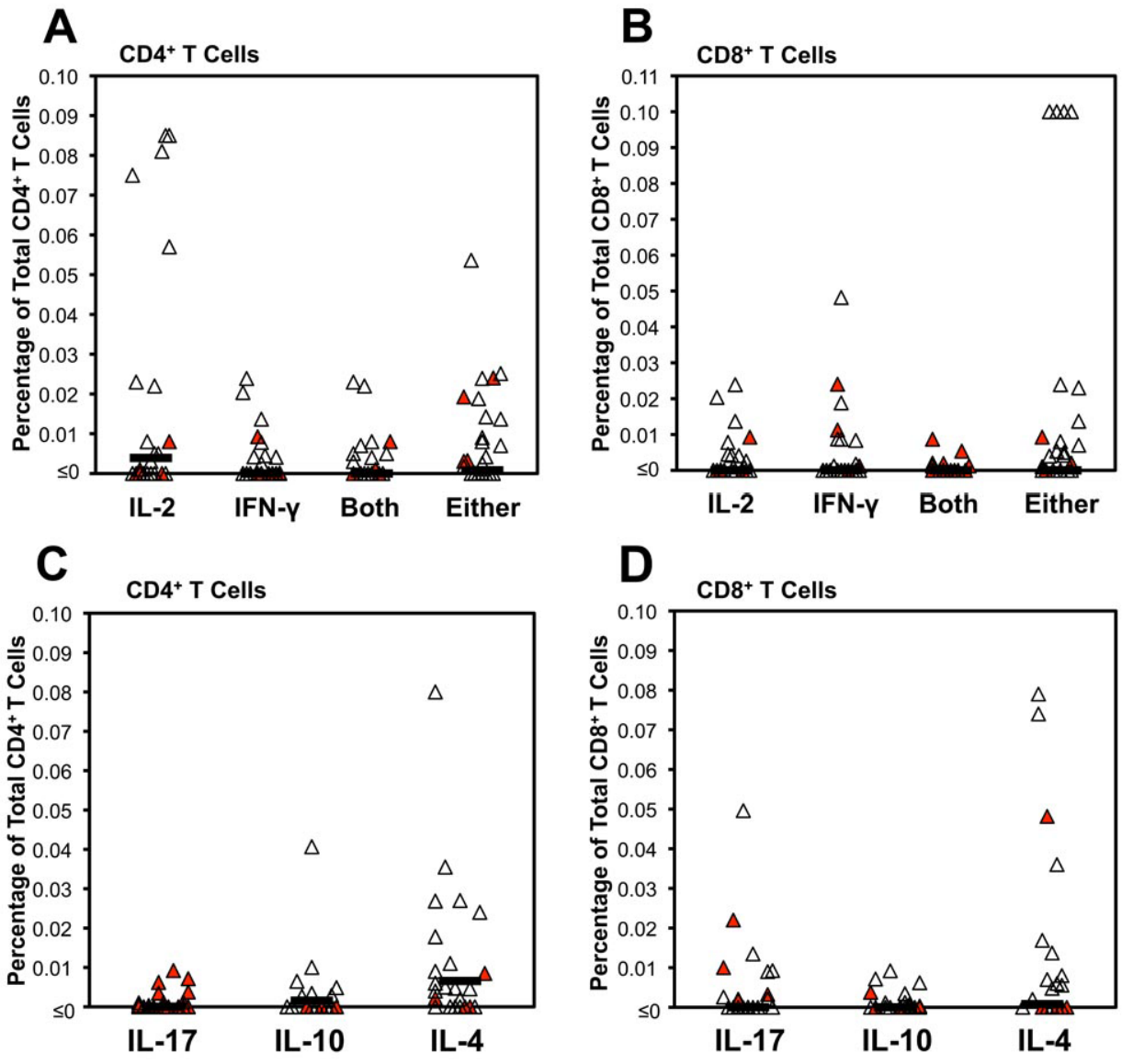

Figure 3-S3: Intracellular cytokine staining in PBMC for T cell responses against SARS- CoV-2 early after infection (using pooled predicted CD8+ T cell epitopes) for IL-2, IFN-γ, L-17, IL-10, and IL-4 yields similar results to those in Figure 3-1. Cytokine responses were defined as in Figure 1, except using pooled predicted CD8+ T cell epitope peptides. Symbols filled with red indicate persons with severe infection.

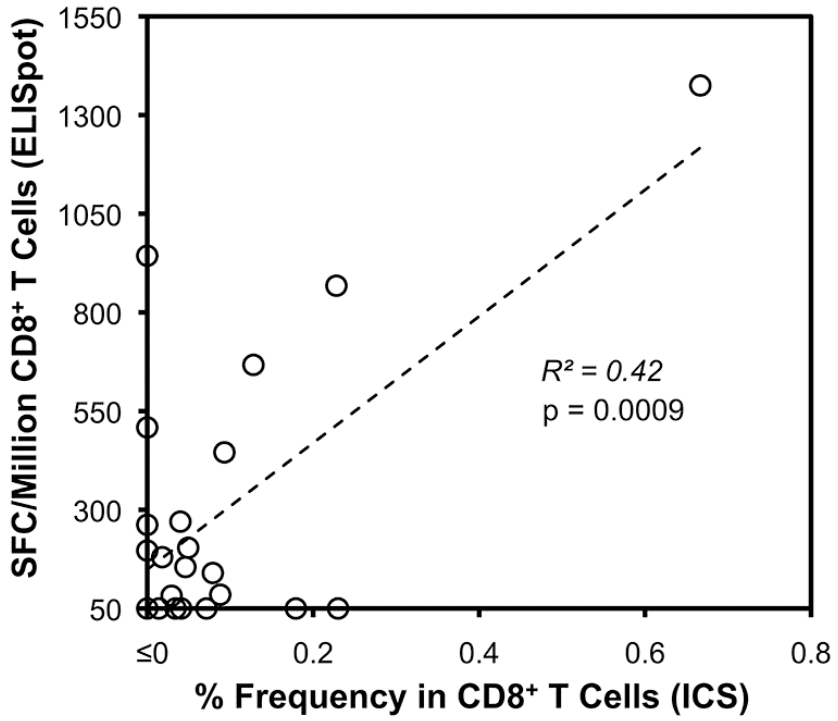

Figure 3-S4: Intracellular cytokine staining and ELISpot CD8+ T cell responses correlate. Results of intracellular IFN-γ staining (in PBMC, shown in Figure 3-1) are plotted against results of IFN-γ ELISpot using spike-spanning peptide pools (using expanded CD8+ T cells, shown in Figure 3-3) for 24 persons whose responses were evaluated by both methods. The Pearson correlation p-value is indicated.

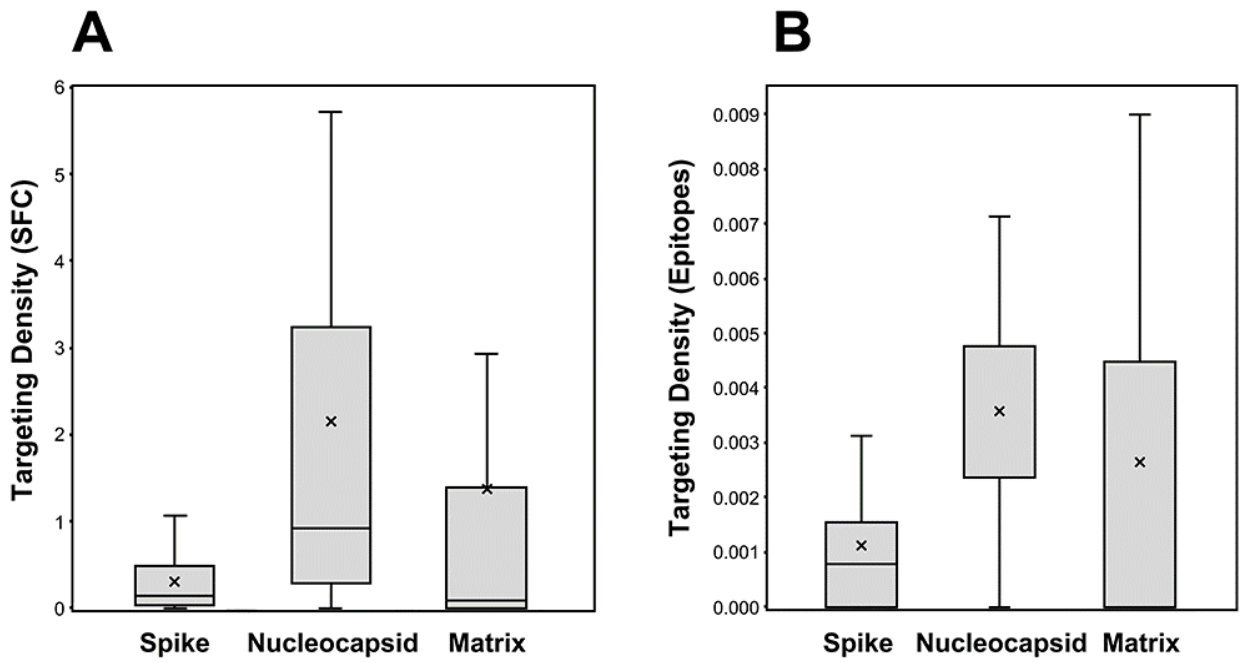

Figure 3-S5: The targeting density of SARS-CoV-2 CD8+ T cell responses is highest against nucleocapsid. For the 44 persons in whom IFN-ɣ ELISpot responses were defined against spike, nucleocapsid, and matrix proteins (Figure 3), the densities of targeting in the context of protein size (1273 amino acids for spike, 419 amino acids for nucleocapsid, 222 amino acids for matrix) were calculated. **Panel A:** Targeting density was defined as the ratio of SFC/10^6 expanded CD8+ T cells / # amino acids. **Panel B:** Targeting density was defined as the ratio of epitopes (approximated by recognized peptide pools) / # amino acids.

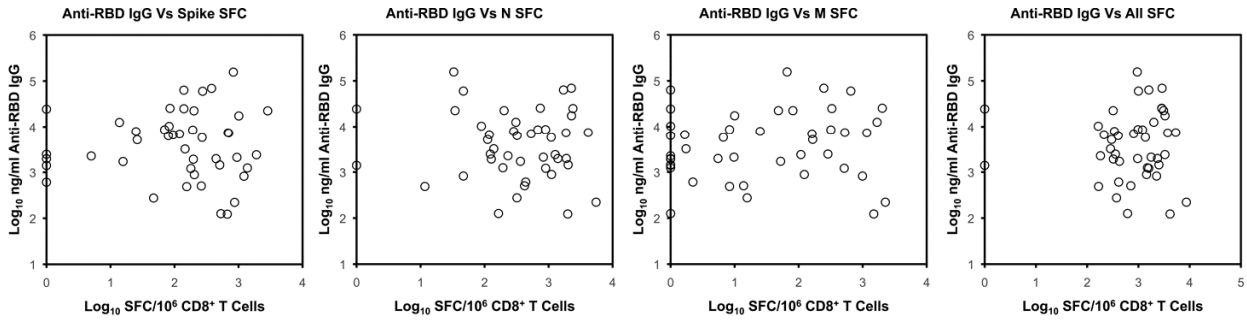

Figure 3-S6: CD8+ T cell responses by IFN-γ ELISpot against SARS-CoV-2 do not correlate to serum anti-RBD antibody levels. CD8+ T cell responses against spike, nucleocapsid (N), and matrix (M) (depicted in Figure 3-3) were plotted against anti-RBD IgG levels.

REFERENCES

1. Cromer D, Juno JA, Khoury D, Reynaldi A, Wheatley AK, Kent SJ, et al. Prospects for durable immune control of SARS-CoV-2 and prevention of reinfection. Nat Rev Immunol. 2021 Jun;21(6):395–404.

2. Sadarangani M, Marchant A, Kollmann TR. Immunological mechanisms of vaccine-induced protection against COVID-19 in humans. Nat Rev Immunol. 2021 Jul 1;1–10.

3. Dougan M, Nirula A, Azizad M, Mocherla B, Gottlieb RL, Chen P, et al. Bamlanivimab plus Etesevimab in Mild or Moderate Covid-19. N Engl J Med. 2021 Oct 7;385(15):1382–92.

4. Libster R, Pérez Marc G, Wappner D, Coviello S, Bianchi A, Braem V, et al. Early High-Titer Plasma Therapy to Prevent Severe Covid-19 in Older Adults. N Engl J Med. 2021 Feb 18;384(7):610–8.

5. O'Brien MP, Forleo-Neto E, Musser BJ, Isa F, Chan KC, Sarkar N, et al. Subcutaneous REGEN-COV Antibody Combination to Prevent Covid-19. N Engl J Med. 2021 Sep 23;385(13):1184–95.

6. Agarwal A, Mukherjee A, Kumar G, Chatterjee P, Bhatnagar T, Malhotra P, et al. Convalescent plasma in the management of moderate covid-19 in adults in India: open label phase II multicentre randomised controlled trial (PLACID Trial). BMJ. 2020 Oct 22;371:m3939.

7. Simonovich VA, Burgos Pratx LD, Scibona P, Beruto MV, Vallone MG, Vázquez C, et al. A Randomized Trial of Convalescent Plasma in Covid-19 Severe Pneumonia. N Engl J Med. 2021 Feb 18;384(7):619–29.

8. Janiaud P, Axfors C, Schmitt AM, Gloy V, Ebrahimi F, Hepprich M, et al. Association of Convalescent Plasma Treatment With Clinical Outcomes in Patients With COVID-19: A Systematic Review and Meta-analysis. JAMA. 2021 Mar 23;325(12):1185–95.

9. Stankov MV, Cossmann A, Bonifacius A, Dopfer-Jablonka A, Ramos GM, Gödecke N, et al. Humoral and cellular immune responses against SARS-CoV-2 variants and human coronaviruses after single BNT162b2 vaccination. Clin Infect Dis Off Publ Infect Dis Soc Am. 2021 Jun 16;ciab555.

10. Chen G, Wu D, Guo W, Cao Y, Huang D, Wang H, et al. Clinical and immunological features of severe and moderate coronavirus disease 2019. J Clin Invest. 2020 May 1;130(5):2620–9.

11. Braun J, Loyal L, Frentsch M, Wendisch D, Georg P, Kurth F, et al. SARS-CoV-2-reactive T cells in healthy donors and patients with COVID-19. Nature. 2020 Nov;587(7833):270–4.

12. Grifoni A, Weiskopf D, Ramirez SI, Mateus J, Dan JM, Moderbacher CR, et al. Targets of T Cell Responses to SARS-CoV-2 Coronavirus in Humans with COVID-19 Disease and Unexposed Individuals. Cell. 2020 Jun 25;181(7):1489-1501.e15.

13. Weiskopf D, Schmitz KS, Raadsen MP, Grifoni A, Okba NMA, Endeman H, et al. Phenotype and kinetics of SARS-CoV-2-specific T cells in COVID-19 patients with acute respiratory distress syndrome. Sci Immunol. 2020 Jun 26;5(48):eabd2071.

14. Le Bert N, Clapham HE, Tan AT, Chia WN, Tham CYL, Lim JM, et al. Highly functional virus-specific cellular immune response in asymptomatic SARS-CoV-2 infection. J Exp Med. 2021 May 3;218(5):e20202617.

15. Wyllie D, Jones HE, Mulchandani R, Trickey A, Taylor-Phillips S, Brooks T, et al. SARS-CoV-2 responsive T cell numbers and anti-Spike IgG levels are both associated with protection from COVID-19: A prospective cohort study in keyworkers [Internet]. medRxiv; 2021 [cited 2022 Jul 24]. p. 2020.11.02.20222778. Available from: https://www.medrxiv.org/content/10.1101/2020.11.02.20222778v2

16. Liao M, Liu Y, Yuan J, Wen Y, Xu G, Zhao J, et al. Single-cell landscape of bronchoalveolar immune cells in patients with COVID-19. Nat Med. 2020 Jun;26(6):842–4.

17. McMahan K, Yu J, Mercado NB, Loos C, Tostanoski LH, Chandrashekar A, et al. Correlates of protection against SARS-CoV-2 in rhesus macaques. Nature. 2021 Feb;590(7847):630–4.

18. Kared H, Redd AD, Bloch EM, Bonny TS, Sumatoh H, Kairi F, et al. SARS-CoV-2-specific CD8+ T cell responses in convalescent COVID-19 individuals. J Clin Invest. 2021 Mar 1;131(5):145476.

19. Tan AT, Linster M, Tan CW, Le Bert N, Chia WN, Kunasegaran K, et al. Early induction of functional SARS-CoV-2-specific T cells associates with rapid viral clearance and mild disease in COVID-19 patients. Cell Rep. 2021 Feb 9;34(6):108728.

20. Polack FP, Thomas SJ, Kitchin N, Absalon J, Gurtman A, Lockhart S, et al. Safety and Efficacy of the BNT162b2 mRNA Covid-19 Vaccine. N Engl J Med. 2020 Dec 31;383(27):2603–15.

21. Baden LR, El Sahly HM, Essink B, Kotloff K, Frey S, Novak R, et al. Efficacy and Safety of the mRNA-1273 SARS-CoV-2 Vaccine. N Engl J Med. 2021 Feb 4;384(5):403–16.

22. Abu-Raddad LJ, Chemaitelly H, Butt AA, National Study Group for COVID-19 Vaccination. Effectiveness of the BNT162b2 Covid-19 Vaccine against the B.1.1.7 and B.1.351 Variants. N Engl J Med. 2021 Jul 8;385(2):187–9.

23. Greaney AJ, Loes AN, Crawford KHD, Starr TN, Malone KD, Chu HY, et al. Comprehensive mapping of mutations in the SARS-CoV-2 receptor-binding domain that affect recognition by polyclonal human plasma antibodies. Cell Host Microbe. 2021 Mar 10;29(3):463-476.e6.

24. Kustin T, Harel N, Finkel U, Perchik S, Harari S, Tahor M, et al. Evidence for increased breakthrough rates of SARS-CoV-2 variants of concern in BNT162b2-mRNA-vaccinated individuals. Nat Med. 2021 Jun 14;1–6.

25. Madhi SA, Baillie V, Cutland CL, Voysey M, Koen AL, Fairlie L, et al. Efficacy of the ChAdOx1 nCoV-19 Covid-19 Vaccine against the B.1.351 Variant. N Engl J Med. 2021 May 20;384(20):1885–98.

26. Haas EJ, Angulo FJ, McLaughlin JM, Anis E, Singer SR, Khan F, et al. Impact and effectiveness of mRNA BNT162b2 vaccine against SARS-CoV-2 infections and COVID-19 cases, hospitalisations, and deaths following a nationwide vaccination campaign in Israel: an observational study using national surveillance data. Lancet Lond Engl. 2021 May 15;397(10287):1819–29.

27. Grifoni A, Sidney J, Zhang Y, Scheuermann RH, Peters B, Sette A. A Sequence Homology and Bioinformatic Approach Can Predict Candidate Targets for Immune Responses to SARS-CoV-2. Cell Host Microbe. 2020 Apr 8;27(4):671-680.e2.

28. Lineburg KE, Srihari S, Altaf M, Swaminathan S, Panikkar A, Raju J, et al. Rapid detection of SARS-CoV-2-specific memory T-cell immunity in recovered COVID-19 cases. Clin Transl Immunol. 2020;9(12):e1219.

29. Peng Y, Mentzer AJ, Liu G, Yao X, Yin Z, Dong D, et al. Broad and strong memory CD4+ and CD8+ T cells induced by SARS-CoV-2 in UK convalescent individuals following COVID-19. Nat Immunol. 2020 Nov;21(11):1336–45.

30. Bonifacius A, Tischer-Zimmermann S, Dragon AC, Gussarow D, Vogel A, Krettek U, et al. COVID-19 immune signatures reveal stable antiviral T cell function despite declining humoral responses. Immunity. 2021 Feb 9;54(2):340-354.e6.

31. Laing AG, Lorenc A, del Molino del Barrio I, Das A, Fish M, Monin L, et al. A dynamic COVID-19 immune signature includes associations with poor prognosis. Nat Med. 2020 Aug 17;1–13.

32. Sadeghi A, Tahmasebi S, Mahmood A, Kuznetsova M, Valizadeh H, Taghizadieh A, et al. Th17 and Treg cells function in SARS-CoV2 patients compared with healthy controls. J Cell Physiol. 2021 Apr;236(4):2829–39.

33. Le Gros G, Erard F. Non-cytotoxic, IL-4, IL-5, IL-10 producing CD8+ T cells: their activation and effector functions. Curr Opin Immunol. 1994 Jun;6(3):453–7.

34. Schwaiger S, Wolf AM, Robatscher P, Jenewein B, Grubeck-Loebenstein B. IL-4-producing CD8+ T cells with a CD62L++(bright) phenotype accumulate in a subgroup of older adults and are associated with the maintenance of intact humoral immunity in old age. J Immunol Baltim Md 1950. 2003 Jan 1;170(1):613–9.

35. Machura E, Mazur B, Rusek-Zychma M, Barć-Czarnecka M. Cytokine production by peripheral blood CD4+ and CD8+ T cells in atopic childhood asthma. Clin Dev Immunol. 2010;2010:606139.

36. Baek HJ, Zhang L, Jarvis LB, Gaston JSH. Increased IL-4+ CD8+ T cells in peripheral blood and autoreactive CD8+ T cell lines of patients with inflammatory arthritis. Rheumatol Oxf Engl. 2008 Jun;47(6):795–803.

37. Le Bert N, Tan AT, Kunasegaran K, Tham CYL, Hafezi M, Chia A, et al. SARS-CoV-2-specific T cell immunity in cases of COVID-19 and SARS, and uninfected controls. Nature. 2020 Aug;584(7821):457–62.

38. Ansari A, Arya R, Sachan S, Jha SN, Kalia A, Lall A, et al. Immune Memory in Mild COVID-19 Patients and Unexposed Donors Reveals Persistent T Cell Responses After SARS-CoV-2 Infection. Front Immunol. 2021;12:636768.

39. Cassaniti I, Percivalle E, Bergami F, Piralla A, Comolli G, Bruno R, et al. SARS-CoV-2 specific T-cell immunity in COVID-19 convalescent patients and unexposed controls measured by ex vivo ELISpot assay. Clin Microbiol Infect [Internet]. 2021 Apr 2 [cited 2021 Jul 5]; Available from: https://www.ncbi.nlm.nih.gov/pmc/articles/PMC8016542/

40. Dan JM, Mateus J, Kato Y, Hastie KM, Yu ED, Faliti CE, et al. Immunological memory to SARS-CoV-2 assessed for up to 8 months after infection. Science. 2021 Feb 5;371(6529):eabf4063.

41. Ferretti AP, Kula T, Wang Y, Nguyen DMV, Weinheimer A, Dunlap GS, et al. Unbiased Screens Show CD8+ T Cells of COVID-19 Patients Recognize Shared Epitopes in SARS-CoV-2 that Largely Reside outside the Spike Protein. Immunity. 2020 Nov 17;53(5):1095-1107.e3.

42. Thieme CJ, Anft M, Paniskaki K, Blazquez-Navarro A, Doevelaar A, Seibert FS, et al. Robust T Cell Response Toward Spike, Membrane, and Nucleocapsid SARS-

CoV-2 Proteins Is Not Associated with Recovery in Critical COVID-19 Patients. Cell Rep Med. 2020 Sep 22;1(6):100092.

43. Schulien I, Kemming J, Oberhardt V, Wild K, Seidel LM, Killmer S, et al. Characterization of pre-existing and induced SARS-CoV-2-specific CD8+ T cells. Nat Med. 2021 Jan;27(1):78–85.

44. Redd AD, Nardin A, Kared H, Bloch EM, Pekosz A, Laeyendecker O, et al. CD8+ T-Cell Responses in COVID-19 Convalescent Individuals Target Conserved Epitopes From Multiple Prominent SARS-CoV-2 Circulating Variants. Open Forum Infect Dis. 2021 Jul;8(7):ofab143.

45. Sekine T, Perez-Potti A, Rivera-Ballesteros O, Strålin K, Gorin JB, Olsson A, et al. Robust T Cell Immunity in Convalescent Individuals with Asymptomatic or Mild COVID-19. Cell. 2020 01;183(1):158-168.e14.

46. Brand I, Gilberg L, Bruger J, Garí M, Wieser A, Eser TM, et al. Broad T Cell Targeting of Structural Proteins After SARS-CoV-2 Infection: High Throughput Assessment of T Cell Reactivity Using an Automated Interferon Gamma Release Assay. Front Immunol. 2021;12:688436.

47. Zuo J, Dowell AC, Pearce H, Verma K, Long HM, Begum J, et al. Robust SARS-CoV-2-specific T cell immunity is maintained at 6 months following primary infection. Nat Immunol. 2021 May;22(5):620–6.

48. Breton G, Mendoza P, Hägglöf T, Oliveira TY, Schaefer-Babajew D, Gaebler C, et al. Persistent cellular immunity to SARS-CoV-2 infection. J Exp Med. 2021 Apr 5;218(4):e20202515.

49. Peng Y, Felce SL, Dong D, Penkava F, Mentzer AJ, Yao X, et al. An immunodominant NP105-113-B*07:02 cytotoxic T cell response controls viral replication and is associated with less severe COVID-19 disease. Nat Immunol. 2022 Jan;23(1):50–61.

50. Bilich T, Nelde A, Heitmann JS, Maringer Y, Roerden M, Bauer J, et al. T cell and antibody kinetics delineate SARS-CoV-2 peptides mediating long-term immune responses in COVID-19 convalescent individuals. Sci Transl Med. 2021 Apr 21;13(590):eabf7517.

51. Ma T, Ryu H, McGregor M, Babcock B, Neidleman J, Xie G, et al. Protracted yet coordinated differentiation of long-lived SARS-CoV-2-specific CD8+ T cells during COVID-19 convalescence. BioRxiv Prepr Serv Biol. 2021 Apr 29;2021.04.28.441880.

52. Bacher P, Rosati E, Esser D, Martini GR, Saggau C, Schiminsky E, et al. Low-Avidity CD4+ T Cell Responses to SARS-CoV-2 in Unexposed Individuals and Humans with Severe COVID-19. Immunity. 2020 Dec 15;53(6):1258-1271.e5.

53. Casado JL, Vizcarra P, Velasco H, Hammerle J, McGee A, Fernandez-Escribano M, et al. Progressive and parallel decline of humoral and T cell immunity in convalescent health care workers with asymptomatic or mild-moderate SARS-CoV-2 infection. J Infect Dis. 2021 May 7;jiab242.

54. Ibarrondo FJ, Hofmann C, Fulcher JA, Goodman-Meza D, Mu W, Hausner MA, et al. Primary, Recall, and Decay Kinetics of SARS-CoV-2 Vaccine Antibody Responses. ACS Nano. 2021 Jul 27;15(7):11180–91.

55. Ibarrondo FJ, Fulcher JA, Goodman-Meza D, Elliott J, Hofmann C, Hausner MA, et al. Rapid Decay of Anti-SARS-CoV-2 Antibodies in Persons with Mild Covid-19. N Engl J Med. 2020 Sep 10;383(11):1085–7.

56. Thomas SJ, Moreira ED, Kitchin N, Absalon J, Gurtman A, Lockhart S, et al. Six Month Safety and Efficacy of the BNT162b2 mRNA COVID-19 Vaccine [Internet]. medRxiv; 2021 [cited 2022 Jul 24]. p. 2021.07.28.21261159. Available from: https://www.medrxiv.org/content/10.1101/2021.07.28.21261159v1

57. Agrati C, Castilletti C, Goletti D, Meschi S, Sacchi A, Matusali G, et al. Coordinate Induction of Humoral and Spike Specific T-Cell Response in a Cohort of Italian Health Care Workers Receiving BNT162b2 mRNA Vaccine. Microorganisms. 2021 Jun 16;9(6):1315.

58. Long QX, Tang XJ, Shi QL, Li Q, Deng HJ, Yuan J, et al. Clinical and immunological assessment of asymptomatic SARS-CoV-2 infections. Nat Med. 2020 Aug;26(8):1200–4.

59. Qu J, Wu C, Li X, Zhang G, Jiang Z, Li X, et al. Profile of Immunoglobulin G and IgM Antibodies Against Severe Acute Respiratory Syndrome Coronavirus 2 (SARS-CoV-2). Clin Infect Dis Off Publ Infect Dis Soc Am. 2020 Nov 19;71(16):2255–8.

60. Röltgen K, Powell AE, Wirz OF, Stevens BA, Hogan CA, Najeeb J, et al. Defining the features and duration of antibody responses to SARS-CoV-2 infection associated with disease severity and outcome. Sci Immunol. 2020 Dec 7;5(54):eabe0240.

61. Jackson LA, Anderson EJ, Rouphael NG, Roberts PC, Makhene M, Coler RN, et al. An mRNA Vaccine against SARS-CoV-2 — Preliminary Report. N Engl J Med [Internet]. 2020 Jul 14 [cited 2020 Nov 12]; Available from: https://www.ncbi.nlm.nih.gov/pmc/articles/PMC7377258/

62. Sahin U, Muik A, Derhovanessian E, Vogler I, Kranz LM, Vormehr M, et al. COVID-19 vaccine BNT162b1 elicits human antibody and TH1 T cell responses. Nature. 2020 Oct;586(7830):594–9.

63. Angyal A, Longet S, Moore SC, Payne RP, Harding A, Tipton T, et al. T-cell and antibody responses to first BNT162b2 vaccine dose in previously infected and SARS-CoV-2-naive UK health-care workers: a multicentre prospective cohort study. Lancet Microbe. 2022 Jan;3(1):e21–31.

64. Ibarrondo FJ, Anton PA, Fuerst M, Ng HL, Wong JT, Matud J, et al. Parallel human immunodeficiency virus type 1-specific CD8+ T-lymphocyte responses in blood and mucosa during chronic infection. J Virol. 2005 Apr;79(7):4289–97.

65. Jones N, Agrawal D, Elrefaei M, Hanson A, Novitsky V, Wong JT, et al. Evaluation of antigen-specific responses using in vitro enriched T cells. J Immunol Methods. 2003 Mar 1;274(1–2):139–47.

66. Ibarrondo FJ, Wilson SB, Hultin LE, Shih R, Hausner MA, Hultin PM, et al. Preferential depletion of gut CD4-expressing iNKT cells contributes to systemic immune activation in HIV-1 infection. Mucosal Immunol. 2013 May;6(3):591–600.

67. Sabado RL, Kilpatrick S, Ali A, Dagarag M, Ng HL, Cao H, et al. Detection of HIV-1-specific CTL responses in Clade B infection with Clade C Peptides and not Clade B consensus peptides. J Immunol Methods. 2005 Jan;296(1–2):1–10.

68. Yang OO, Daar ES, Jamieson BD, Balamurugan A, Smith DM, Pitt JA, et al. Human Immunodeficiency Virus Type 1 Clade B Superinfection: Evidence for Differential Immune Containment of Distinct Clade B Strains. J Virol. 2005 Jan;79(2):860–8.

69. Yang OO, Daar ES, Ng HL, Shih R, Jamieson BD. Increasing CTL targeting of conserved sequences during early HIV-1 infection is correlated to decreasing viremia. AIDS Res Hum Retroviruses. 2011 Apr;27(4):391–8.

Chapter 4: Persistence of Spike-Specific Circulating Memory T Cells After SARS-CoV-2 mRNA Vaccination Despite Sharper Decline Relative to Infection

INTRODUCTION

Both humoral and cellular adaptive immune responses are elicited in the majority of people after infection with the SARS-CoV-2 virus (1–3) as well as immunization across several vaccine platforms (4–7). Correlates of protection against SARS-CoV-2 infection were established early-to-mid 2021 based on neutralizing activity of antibodies from vaccinated and COVID-19-convalescent subjects (8). However, rapid waning of antibody titers after infection (9,10) and/or vaccination (11,12) means that such protection is short-lived. Additionally, the values determined to correlate with protection may prove unreliable against continually emerging SARS-CoV-2 variants (13,14). On the other hand, vaccine efficacy (VE) against symptomatic COVID-19 wanes more slowly (compared to efficacy against any type of infection), and protection against severe disease, hospitalization, and death remain higher over a much longer period of time (12,15,16).

CD8+ Cytotoxic T Lymphocytes (CTL) are one of the fundamental components of the adaptive immune system and are particularly important in fighting and clearing viral infections. In an otherwise healthy individual, a typical CTL response to a new viral pathogen will drive naïve virus-specific T cells to mature and undergo exponential clonal expansion. As the infection is cleared and stimuli begin to disappear, the responding T cell population contracts to a much smaller, long-lived population of primarily memory cells, though with increased numbers and an elevated activation state compared to the naïve, pre-infection baseline (17). The timeline over which the kinetics of this response play out varies, as does the magnitude of the response (18). Upon repeat exposure to antigen, CTL (as well as CD4+ memory T cells (19)) can become activated more easily

and undergo clonal expansion much more rapidly (20). While the persistence of different memory T cells may vary, there is evidence that antiviral memory CD4+ and CD8+ T cell populations responding to certain pathogens can endure for decades, if not a lifetime (21).

For some pathogens, the duration of a vaccine-induced immune response mirrors that of a natural immune response in infection, although the mechanisms that determine this are poorly understood. While it is clear that adjusting factors like the delivery system, adjuvant, and scheduling can all impact the immune response, the mechanisms behind these changes also remain largely unknown (22–24). As we continue to face challenging pathogens, including strains or variants which are even more difficult to overcome, it is crucial to characterize the ways in which the immune system responds to stimuli.

We previously found that, in COVID-19-convalescent individuals, levels of CTL with specificity across the SARS-CoV-2 structural proteins exhibit decay within weeks in non-specifically expanded CD8+ T cells, as measured by IFN-ɣ ELISpot (25). When investigating the prevalence of spike-specific CTL responses in SARS-CoV-2 naïve individuals after mRNA vaccination, we, and others (25–30), found the that the majority of subjects developed some level of T cell immunity. However, most studies have used samples collected less than a month after vaccination to look for these responses. Given the rapid waning of the circulating SARS-CoV-2-specific CTL population after infection, we sought to investigate the short-term kinetics and longer-term persistence of spike-specific T cells after SARS-CoV-2 mRNA vaccination.

RESULTS

Shorter-lived detection of S-specific $CD8^+$ T cell responses in healthy vaccinated subjects compared to SARS-CoV-2-recovered subjects when evaluated by IFN-γ ELISpot assay

The acute time course of T cell responses elicited by mRNA SARS-CoV-2 vaccines has not been described in detail. For two SARS-CoV-2-naïve persons who received the BNT162b2 vaccine, serial IFN-γ ELISpot assays with pooled overlapping peptides were utilized to evaluate anti-spike responses in expanded $CD8^+$ T cells over time **(Figure 4-1A&B).** Both demonstrated remarkably short-lived detection of responses after each of the two vaccine doses, with sharp peaks of anti-spike $CD8^+$ T cells occurring about 10 days after each vaccination, but decay of these responses to undetectable levels less than 10 days after each peak. Moreover, the second vaccination dose peak was lower than the first in both cases. In contrast, the anti-RBD antibodies in these two subjects followed typical kinetics, with a stable plateau after the first dose followed by a higher plateau after the second dose.

By comparison, another person who was immunized with ChAdOx1-S vaccine **(Figure 4-1C)** showed different acute kinetics, with the initial anti-S $CD8^+$ T cell response peaking slightly later but persisting until the second dose. The second peak was minimal, but the kinetics of anti-RBD antibody levels evolved as expected. Cross-sectional assessment of additional SARS-CoV-2-naïve mRNA vaccinees revealed patterns consistent with the longitudinal evaluations after both the first **(Figure 4-1D)** and second **(Figure 4-1E)** vaccine doses. Cross-sectional evaluation of recently COVID-19-recovered persons, in contrast, suggested more stable anti-S $CD8^+$ T cell

responses over a similar time span **(Figure 4-1F).** Overall, these results suggest that detectable frequencies of anti-S $CD8^+$ T cells elicited by mRNA vaccination are very short-lived compared to natural infection.

Similarly, ICS evaluation of unexpanded PBMC reveals persistent low-level detection of both CD4+ and CD8+ circulating S-specific T cells after SARS-CoV-2 mRNA vaccination relative to natural infection

To confirm the ELISpot findings and extend analyses to $CD4^+$ T cells, intracellular cytokine staining was performed for analysis of anti-spike responses after stimulation with overlapping peptides spanning spike **(Figure 4-2).** By IFN-γ readout, almost no responses were detectable in either $CD4^+$ or $CD8^+$ T cell compartments between 13 and 235 days after the second vaccination dose **(Figure 4-3A&B),** in agreement with the IFN-γ ELISpot assay results for isolated $CD8^+$ T cells. In contrast, analysis of recovered persons up to 49 days after onset of COVID-19 showed that most had detectable responses in both the $CD4^+$ **(Figure 4-3C)** and $CD8^+$ **(Figure 4-3D)** T cell compartments, and there was no trend for decay over that time period in this cross-sectional analysis. The frequencies of $CD4^+$ and $CD8^+$ T cell responses were correlated **(Figure 4-3E)** in the COVID-19-recovered persons. In parallel, analyses of vaccine-elicited IL-4 **(Figure 4-S1A&B)** and IL-10 **(Figure 4-S2A&B)** responses to spike showed few detectable responses, but in COVID-19-recovered persons detectable IL-4 but not IL-10 responses **(Figure 4-S3).** As a whole, these findings demonstrated that $CD4^+$ and $CD8^+$ T cell responses (as defined by IFN-γ production) generated by vaccination typically dropped below the limit of detection (0.01%) in unexpanded PBMC

soon after completing vaccination, while responses from natural infection generally remained detectable in most subjects for at least the first month after onset of symptoms.

Enrichment of S-responsive T cells after *in vitro* exposure to a lipid nanoparticle mRNA spike vaccine indicates vigorous and persistent memory responses in the vaccinees despite the low frequency of circulating IFN-γ-responsive cells

Given that T cell responses had largely become undetectable, both by IFN-γ ELISpot of expanded CD8+ T cells and by ICS using unexpanded PBMC, we needed to evaluate whether the rapid drop in detection of spike-specific T cell responses reflected a true loss of cellular immunity. To do so, PBMCs from the SARS-CoV-2-naïve vaccinees were tested in a novel assay for circulating memory T cells by antigen-specific boosting. PBMCs were cultured with mRNA-1273 vaccine under a variety of conditions to maximize expansion of spike-specific T cells while minimizing toxicity **(Figure 4-S4 & Figure 4-4).** Ultimately, the optimal conditions proved to be an initial addition of the mRNA-1273 vaccine at a concentration of 120ng/ml, with approximately two weeks of expansion prior to assessment.

Despite the overall lack of responses detected in unenriched PBMC from vaccinees **(Figure 4-3A & B),** the same PBMC samples (ranging from 13 to 235 days after completed vaccination) demonstrated clearly detectable spike-specific responses in the majority of subjects after culture with mRNA-1273 **(Figure 4-5)**. This was true for both the $CD4^+$ **(Fig. 4-5A)** and $CD8^+$ T cell compartments **(Fig. 4-5B),** where frequencies of responding T cells in these populations were generally well correlated

(Fig. 4-5C). As a whole, these results indicated that vaccine-elicited anti-spike T cell responses persist despite rapidly dropping to undetectable levels by standard ELISpot or ICS assays soon after vaccination.

DISCUSSION

The SARS-CoV-2 virus contains 4 structural proteins: spike (S), nucleocapsid (N), membrane (M), and envelope (E). The most prevalent COVID-19 vaccines administered in the United States all include the spike glycoprotein, but they also all exclude the remainder of the viral proteins. The S protein contains the receptor-binding domain (RBD), which is critical for a virion to infect a cell. Therefore, a subset of antibodies specific for the RBD can effectively bind to a virion and prevent it from establishing an infection. The optimal outcome of vaccination—especially from a public health perspective—is protection from detectable infection, but this has not yet been attained durably in SARS-CoV-2 vaccination. Despite early evidence of extremely high vaccine efficacy against infection (symptomatic or asymptomatic), it became clear within months that this absolute protection diminishes rapidly (11,12,16).

When determining the success or failure of a vaccination strategy, prevention of detectable infection is not the only outcome that can be considered successful. In the case of SARS-CoV-2, current vaccines are unable to produce long-term complete protection against infection, especially with the frequent arrival of new variants. Attempting to maintain such a level of immune protection in a large swath of the population, if even possible, would be extremely impractical. Thus, from a public health perspective, it seems appropriate to focus attention on factors that provide longer-term

protection against severe COVID-19 and death, which, if achieved broadly, should also be considered a successful vaccination strategy.

In this chapter, we began with mapping out the early kinetics of de novo CTL responses to spike protein in SARS-CoV-2-naïve subjects after vaccination. In those who received mRNA vaccines, we observed a sharp rise and precipitous drop, mapped in detail for two subjects in Fig. 4-1A&B. Though not mapped out with an equal level of detail, the same pattern was observed through cross-sectional analysis of additional SARS-CoV-2-naïve subjects after each dose of mRNA vaccine. On the other hand, the kinetics of the CTL response in a subject who received an adenoviral-vectored vaccine were prolonged, with CTL levels remaining detectable for the entire period between vaccine doses. These contrasting CTL patterns occur in the context of anti-RBD antibody responses that exhibit similar patterns.

The kinetics of the CTL responses elicited by mRNA vaccination that we showed here also differ greatly from what we saw previously following SARS-CoV-2 infection. While we had observed consistent decay of longitudinal CTL responses in most subjects (25), this occurred over a more drawn-out timeline: the calculated average time from symptom onset to a 10-fold reduction in CTL levels was less than 40 days for S-specific CTL, and less than 105 days for N-specific CTL.

Looking at bulk $CD4^+$ and $CD8^+$ T cell responses by ICS, the patterns contrasted even more greatly. Even the relatively early timepoints of vaccinees did not show responding cells for either $CD4^+$ or $CD8^+$ T cell compartment in unenriched PBMCs, while the majority of SARS-CoV-2-convalescent subjects had clearly positive responses for both (by IFN-ɣ). After enriching the PBMC of SARS-CoV-2-vaccinees with the

mRNA-1273 vaccine in culture, we saw strong responses to spike peptides from both $CD4^+$ and $CD8^+$ T cells in the majority of subjects, with several subjects responding five months out or later from their second dose of SARS-CoV-2 mRNA vaccine. As it is extremely difficult to elicit antigen-specific *de novo* T cells in culture, these responding T cells are likely attributable to expansion of memory cells that had been elicited by the vaccine.

In seminal research by Murali-Krishna *et al*. using an acute LCMV mouse model, levels of virus-specific $CD8^+$ T cells began to decay after peaking at approximately 8 days (17). Ultimately, this population shrank down over the course of a month to a sustained memory pool with a frequency of about 5% of levels seen at the peak. The kinetics seen in response to the SARS-CoV-2 adenoviral vector vaccine align with this, but the decay of CTL levels after mRNA vaccination is stunningly rapid. A memory pool representing a 95% reduction of peak values would be undetectable by our assays using unenriched PBMC given the maximum levels of response that were seen. It is unclear what causes the responding population to contract so quickly, or if there are functional consequences to this.

Given how rapidly S-specific CTL arise after the second dose of SARS-CoV-2 mRNA vaccination, as well as their ability to expand exponentially in response to antigen *in vitro*, the memory cells that are induced appear to be highly functional. Though our lab has shown that responding to high levels of peptide *in vitro* does not necessarily translate to antiviral functionality (31,32), clinical observations months after SARS-CoV-2 mRNA vaccination suggest that there is still some benefit from this

vaccination that is preserved even after vaccinees become susceptible to infection again.

While most studies examining T cell responses to SARS-CoV-2 have used variations of ICS-flow cytometry and IFN-ɣ ELISpot, there are still no standardized techniques across the field. This has produced inconsistent results between studies, impeding constructive comparisons of different data sets. Most reports of IFN-ɣ ELISpot data assessing cellular immunity to SARS-CoV-2 vaccination have either used unseparated PBMC (27,38) or whole blood (39,40). Studies have also shown inconsistencies with results from commercial ELISpot assays (41,42), likely further confounding the data on T cell responses to the vaccine. To date, we have not been able to find any publications that have analyzed responses to SARS-CoV-2 mRNA vaccination in isolated $CD8^+$ T cells.

There are several studies which have used ICS to separately analyze total $CD4^+$ and $CD8^+$ T cell responses after vaccination, as we have here. However, most studies have varied from one another in technical aspects, and the readouts from those studies are similarly inconsistent. Geers *et al.* stimulated PBMC with spike peptide pools for 20 hours before evaluating responses by activation-induced marker (AIM) (43). Samples were collected from SARS-CoV-2-naïve subjects 2-3 weeks after the first dose and 3-4 weeks after the second dose of BNT162b2 vaccination. Significant increases were seen for S-reactive CD4+ T cells but not for CD8+ T cells. These results agree with our data showing a general lack of CTL responses in the time periods they tested. However, they did see evidence of S-reactive CD4+ T cells, which may be attributable to the much longer incubation period (20 hours instead of the 6-hour incubation that we used).

Zhang *et al.* also used PBMC and had a similarly long incubation period of 24 hours with spike megapool (identical to what we used in our ICS assays), after which they measured CD8+ and CD4+ T cell responses by both AIM and ICS (47). Their results between AIM and ICS were generally concordant, finding 60-67% of subjects having CD8+ T cell responses and 100% of subjects having CD4+ T cell responses to spike megapool at six months post mRNA vaccination. They also report that these data represent a reduction in the magnitude of responses as well as the percentage of subjects with CD8+ T cell responses between early timepoints and six months out. They suggest that a reason for variable levels of detection between different studies is the incubation period. Specifically, they reference Atmar *et al.* (44), who found 10-30% of mRNA-vaccinated subjects to have spike responses by ICS and a 6-8 hour incubation at least 12 weeks out from completing their mRNA vaccination series.

Interestingly, a study that pre-incubated samples did not seem to enrich for S-reactive CTL, as was seen in our study. Lozano-Rodriguez *et al.* (45) collected samples at days 14 and 230 after completion of a two-dose mRNA vaccine regimen and incubated freshly collected PBMC with spike peptides for 5 days prior to analysis by ICS. At both timepoints they observed minimal CD8+ T cell responses.

Most studies also appear to have planned collections around theoretically optimal timepoints based on antibody responses, which our data suggest is well after the peak $CD8^+$ T cell response for most subjects. Gil-Manso *et al.* (46) mapped out bulk T cell responses in stimulated fresh whole-blood at collections 3, 7, and 14 days after the second dose of mRNA vaccination. While they show IFN-ɣ and IL-2 responses as early as day 3, their results show responses to be generally higher at day 14. This could be

due to differences in the short-term kinetics between CD4+ and CD8+ T cells. While we only have analyzed the detailed kinetics of very early timepoints for CD8+ T cells, the results of this study could suggest that CD4+ T cells peak at a later timepoint and mask the timing of the CD8+ T cell response when analyzed in bulk.

This also brings up the question of which particular cell populations are being detected depending on timing, assay conditions, and other factors that likely all contributed to the inconsistencies between the studies above as well as our own. While we were able to detect IFN-ɣ-producing cells by ICS in unenriched PBMC for weeks following COVID-19 but not after mRNA vaccination, this could theoretically be attributable to induction of different types of T cell immunity. Detecting expanded CTL responses by the same assay in the weeks following COVID-19 and in the days following mRNA vaccination might suggest that we are seeing the same immune response play out over an expedited timeline, but that might not be the full picture. The mRNA vaccine platform is still quite new, and the inconsistencies shown in these studies emphasize just how crucial it is to be asking the right questions.

While the diminution of vaccine efficacy in protecting against SARS-CoV-2 infection can be attributed to a loss of protection from decreased antibody levels (8,13), we cannot definitively attribute the sustained protection against severe disease and death solely to T cells. However, as antibodies have shown to have little to no effect on the course of a SARS-CoV-2 infection once it establishes (33–35), the memory T cell population elicited by the vaccine likely plays a role in attenuating disease severity in the months following.

The mRNA COVID vaccines lose protection against asymptomatic and non-severe symptomatic infection relatively quickly, especially in the face of new variants. However, in terms of saving lives and reducing suffering, they have been extremely successful. Given our prior study showing the immunodominance of CTL responses for the N protein, as well as prolonged maintenance of circulating levels after SARS-CoV-2 infection, it could be valuable to immunize against other SARS-CoV-2 proteins. An increased breadth of targeting would likely further extend the benefits that have already been seen and help to reduce the threat of SARS-CoV-2.

MATERIALS & METHODS

Study participants and samples

Prior to participation, all subjects gave written, informed consent under an institutional review board-approved protocol at the University of California Los Angeles. Participants with known immunocompromising conditions (including diabetes mellitus, immunosuppressive medications, and HIV-1 infection) were excluded. All COVID-19-recovered persons were infected no later than January, 2021. Vaccinees were healthy individuals with no prior history of COVID-19 and were negative for antibodies against the SARS-CoV-2 spike receptor-binding domain (RBD) by ELISA at baseline. PBMC were separated by density gradient centrifugation and viably cryopreserved until use.

$CD8^+$ T cell IFN-γ ELISpot assays

Measurements of spike-specific $CD8^+$ T cell responses were performed as described in detail (25), using polyclonally expanded $CD8^+$ T cells in a method shown to

correlate well to unexpanded freshly purified peripheral blood $CD8^+$ T cells (36,37). In brief, peripheral blood mononuclear cells (PBMC) were non-specifically expanded for approximately 14 days using a CD3:CD4 bi-specific antibody (generous gift of Dr. Johnson Wong), which leads to a primarily CD8+ T cell population. These cells were screened in a standard IFN-ɣ ELISpot assay against 12 peptide pools comprised of overlapping 15-mer synthetic peptides spanning the SARS-CoV-2 spike protein (BEI Resources NR-52402) (see **Table 3-S2**, pools S1-S12). Triplicate negative control wells included no peptide, and two positive control wells included phytohemagglutinin (PHA) (#L1668, Sigma Aldrich, St. Louis, MO) at 25µg/ml. Counts from each well were background-subtracted using the average count from the negative control wells, and the total spike response was determined as the sum of all 12 peptide pool wells. Results totaling ≤ 50 spot forming cells (SFC) per million $CD8^+$ T cells were considered negative.

Anti-RBD antibody measurements

Serum immunoglobulin G (IgG) SARS-CoV-2 spike RBD-specific antibodies were quantified as described in detail (11). In brief, 96-well microtiter plates were coated with 2 µg/mL recombinant RBD protein. Serum was added in duplicate serial dilutions and bound antibodies were detected using goat anti-human IgG conjugated with horseradish peroxidase, followed by tetramethylbenzidine substrate solution and measurements at 450 and 650 nm. Each plate contained a control titration of the anti-RBD monoclonal antibody CR3022 (Creative Biolabs, Shirley, NY) to provide a standard curve. Serum

anti-RBD IgG binding activity was expressed as an equivalent to a concentration of CR3022.

Intracellular cytokine staining (ICS) to detect T cells targeting spike

ICS staining and flow cytometry were performed as described in detail (25), differing only in the particular peptide “megapools” which were used as stimuli. In brief, PBMC were incubated with brefeldin A and monensin and the addition of either media only (‘unstimulated’ condition used to subtract non-specific cytokine expression), a single combined pool of overlapping 15-mer peptides spanning SARS-CoV-2 spike (5) at a final concentration of 1µg/ml per individual peptide (the spike or S megapool), or with PMA and ionomycin as a positive control. The 6-hour incubation was followed by surface staining (CD3, CD8, CD4, and Fixable Aqua viability dye), permeabilization, and intracellular cytokine staining (IFN-ɣ, IL-2, IL-4, IL-10) for flow cytometric analysis on an Attune NxT.

In vitro enrichment of memory T cells against spike

In parallel with ICS evaluation for anti-spike T cell responses immediately upon thawing, a portion of the PBMC was cultured with the mRNA-1273 vaccine *in vitro*. PBMC were plated at 1-2x10^6 cells per well in 24-well flat-bottom tissue culture plates in RPMI-1640 (supplemented with L-glutamine, HEPES buffer, and antibiotic) with recombinant human IL-2 at 50U/ml (NIH AIDS Reagent Repository Program) and the initial addition of mRNA-1273 vaccine (Moderna) at a final concentration of 120ng/ml, unless otherwise specified. The cultures were repleted with fresh medium every three to

four days and transferred to T-25 flasks if confluent. The resulting cells were utilized for ICS evaluation of anti-spike T cell responses after approximately 14 days of culture. Aliquots were viably cryopreserved; if ICS staining yielded fewer than 10,000 events in the $CD4^+$ or $CD8^+$ T cell compartments, the ICS was repeated on another aliquot and the results were combined with weighted averaging.

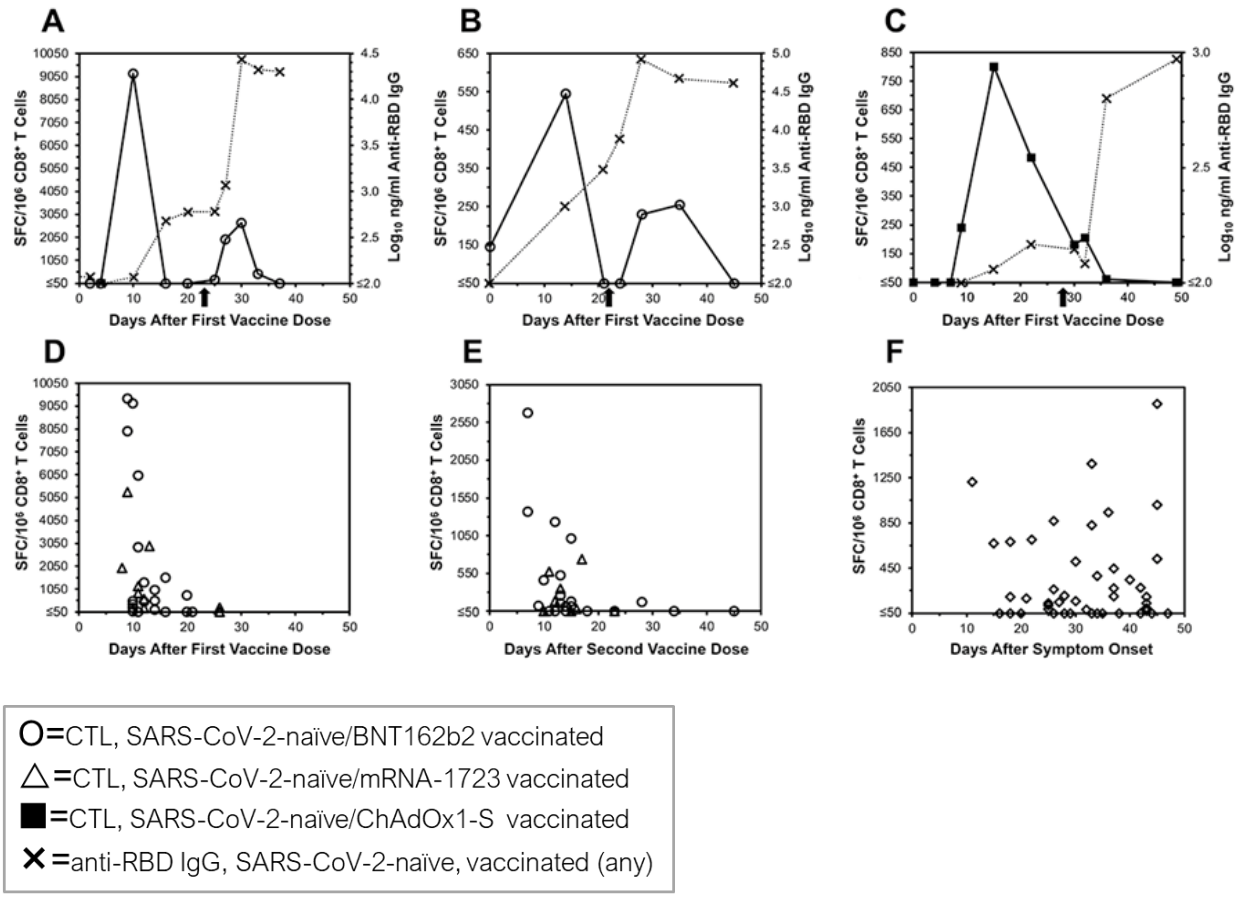

Figure 4-1: Detection of circulating SARS-CoV-2-specific CD8⁺ T cells by IFN-γ ELISpot after mRNA vaccination or infection. IFN-γ ELISpot assay was utilized to assess the magnitude of the circulating CD8⁺ T cell response to overlapping peptides spanning the SARS-CoV-2 spike protein. IFN-γ ELISpot assays utilized polyclonally expanded CD8+ T cells. **Panels A & B:** Longitudinal anti-spike CD8⁺ T cells (open circles/○) and anti-RBD IgG (✕ symbol) are plotted for two SARS-CoV-2-naïve persons after BNT162b2 vaccination. Arrows indicate the timing of the second vaccine dose. **Panel C:** Longitudinal anti-spike CD8⁺ T cells (closed squares/■) and anti-RBD IgG (✕ symbol) are plotted for a SARS-CoV-2-naïve person after ChAdOx1-S vaccination. Arrow indicates the timing of the second vaccine dose. **Panel D:** Cross-sectional anti-spike CD8⁺ T cell responses plotted for 25 SARS-CoV-2-naïve persons

after the first dose of BNT162b2 (20 points from 16 persons, circles/○) or mRNA-1273 (9 points from 9 persons, triangles/△). Collection timepoints range from 8-26 (mean of 13) days after vaccine dose 1. **Panel E:** Cross-sectional anti-spike $CD8^+$ T cell responses are plotted for 24 persons after the second dose of BNT162b2 (20 points from 15 persons, circles/○) or mRNA-1273 (9 points from 9 persons, triangles/△). Collection timepoints range from 7-45 (mean of 16) days after vaccine dose 2. **Panel F:** Cross-sectional anti-spike $CD8^+$ T cell responses are plotted for 47 samples from 45 persons after recovery from COVID-19, collected 11-47 (mean 32) days after symptom onset.

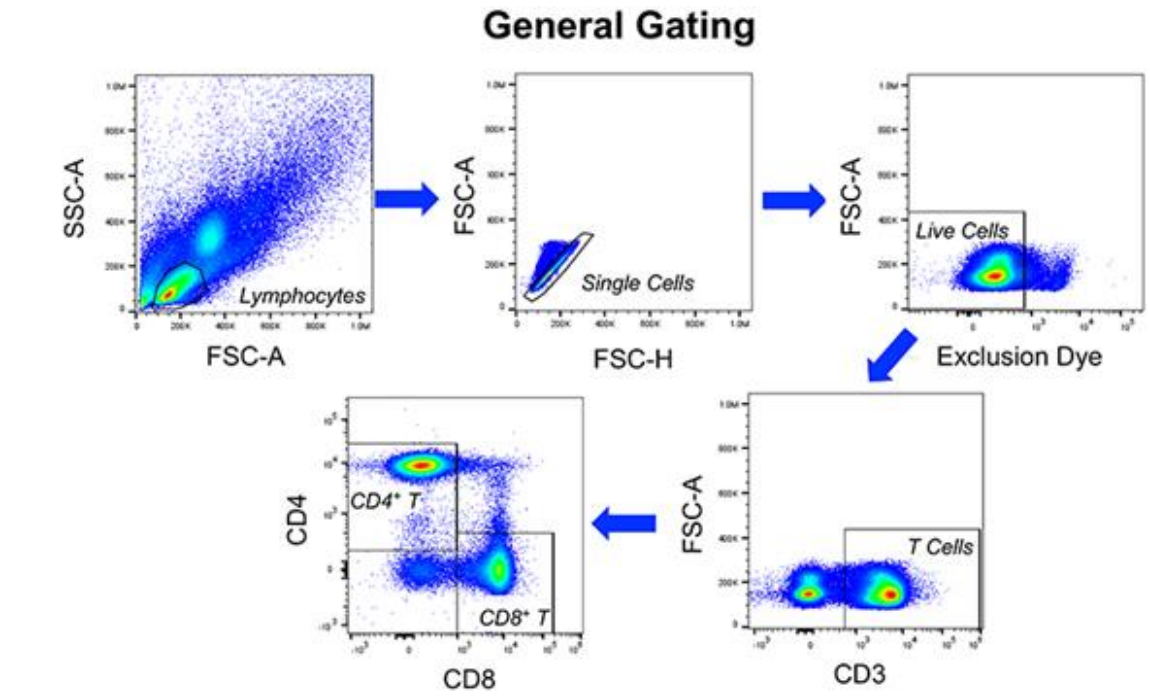
General Gating
SSC-A
FSC-A
Lymphocytes
FSC-A
FSC-H
Single Cells
FSC-A
Live Cells
Exclusion Dye
FSC-A
CD3
T Cells
CD4
CD8
CD4+ T
CD8+ T

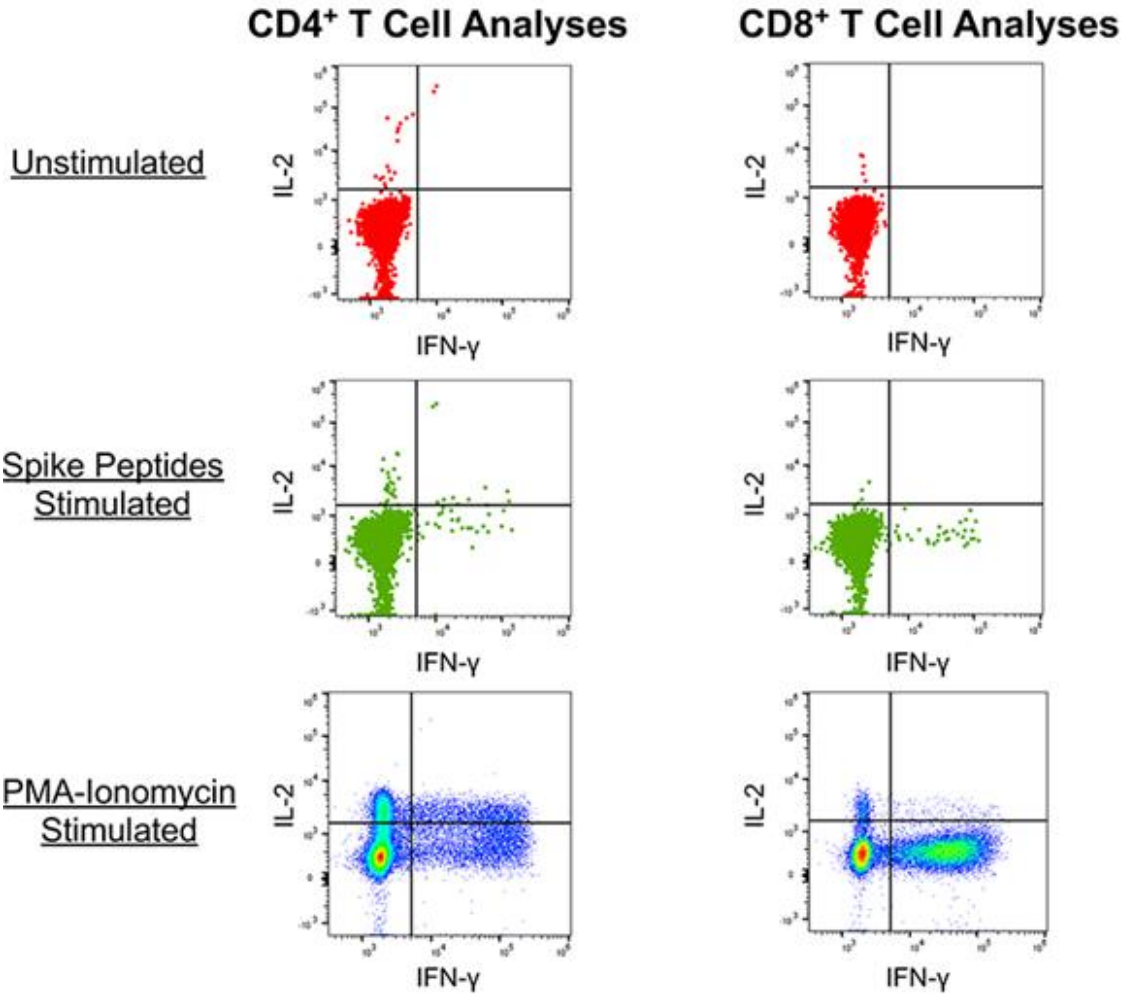
CD4+ T Cell Analyses
CD8+ T Cell Analyses
Unstimulated
Spike Peptides Stimulated
PMA-Ionomycin Stimulated
IL-2
IFN-γ

Figure 4-2: Gating and representative plots of intracellular cytokine staining for $CD4^+$ and $CD8^+$ T cell responses against SARS-CoV-2 spike megapool in PBMC from COVID-19-Convalescent Subjects. PBMC collected from a person 13 days post-COVID-19 symptom onset were incubated in the presence or absence of overlapping 15-mer synthetic peptides spanning the SARS-CoV-2 spike protein. After six hours, production of IFN-γ, IL-2, IL-10 (not shown) and IL-4 (not shown) was assessed by intracellular cytokine staining and flow cytometry. PMA-ionomycin stimulation was included as a positive control. Sequential gates were drawn as follows: the lymphocyte population; single cells; live cells; $CD3^+$ cells (T cells). Within the $CD3^+$ population, $CD4^+/CD8^-$ and $CD8^+/CD4^-$ cells were gated and analyzed separately for intracellular staining of cytokines in $CD4^+$ and $CD8^+$ T cell populations, respectively.

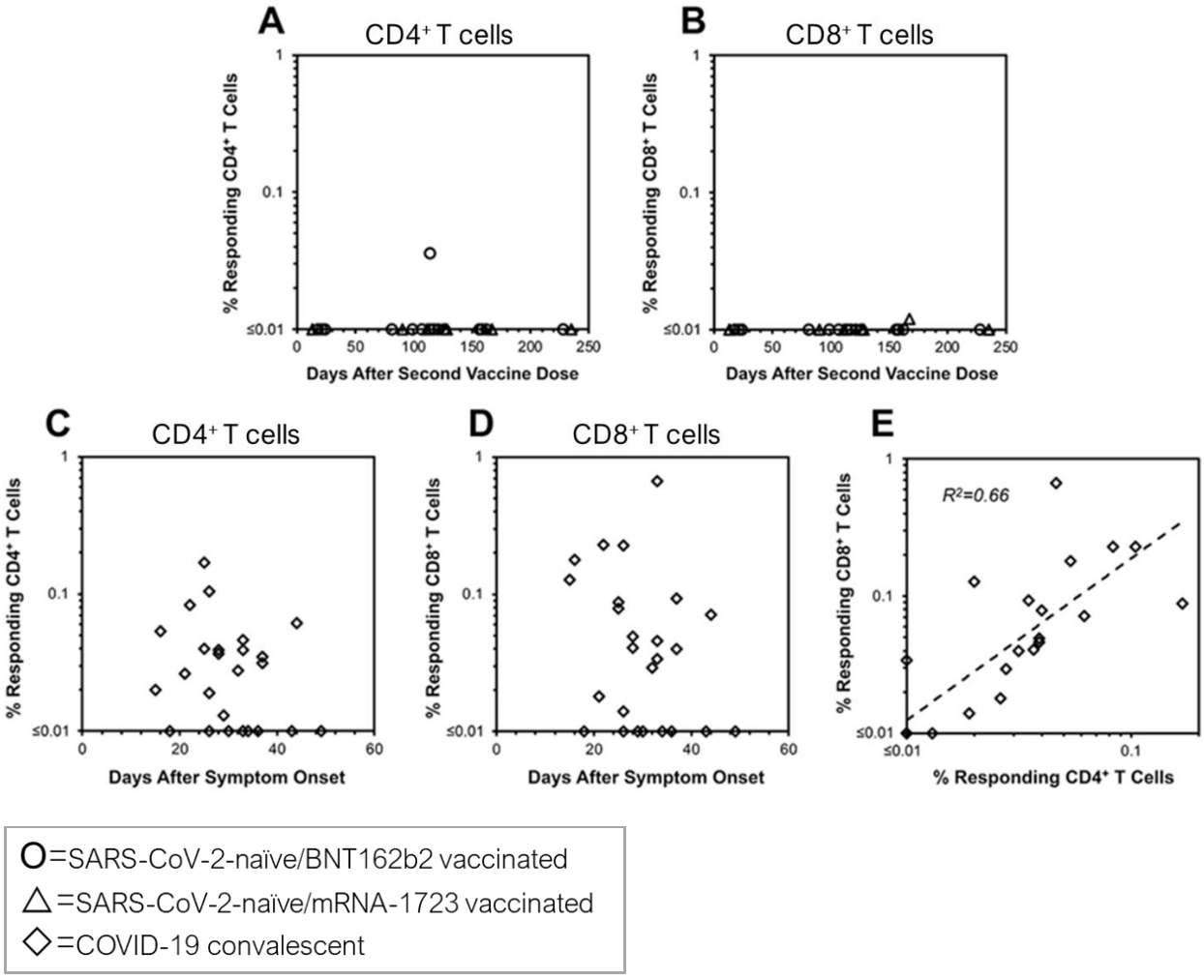

Figure 4-3: Detection by IFN-γ ICS of circulating spike-specific CD4⁺ and CD8⁺ T cells in unexpanded PBMC. (A-E) PBMC were assessed by intracellular cytokine staining flow cytometry for CD4⁺ and CD8⁺ T cell IFN-γ production in response to overlapping peptides spanning spike, as shown in Figure 4-2. Background-subtracted values are plotted. **Panels A & B:** Data are plotted for 22 persons vaccinated with BNT162b2 (18 points from 16 persons, circles/O) or mRNA-1273 (7 points from 6 persons, triangles/△) for CD4⁺ **(A)** and CD8⁺ **(B)** T cells. Time points ranged from 13 to 235 days (mean 115 days) after the second vaccine dose. For each subset, there was only one response greater than the 0.01% IFN-γ+ threshold. **Panels C-E:** Data are

plotted for 25 COVID-19 (diamonds/◇) recovered persons for $CD4^+$ **(C)** and $CD8^+$ **(D)** T cells ranging from 15 to 49 days (mean 30.2 days) after symptom onset. For each subset, 17/25 (68.0%) had responses greater than 0.01%. **(E)** The relationship between the frequency of spike-responding $CD4^+$ and $CD8^+$ T cells in each subject.

A

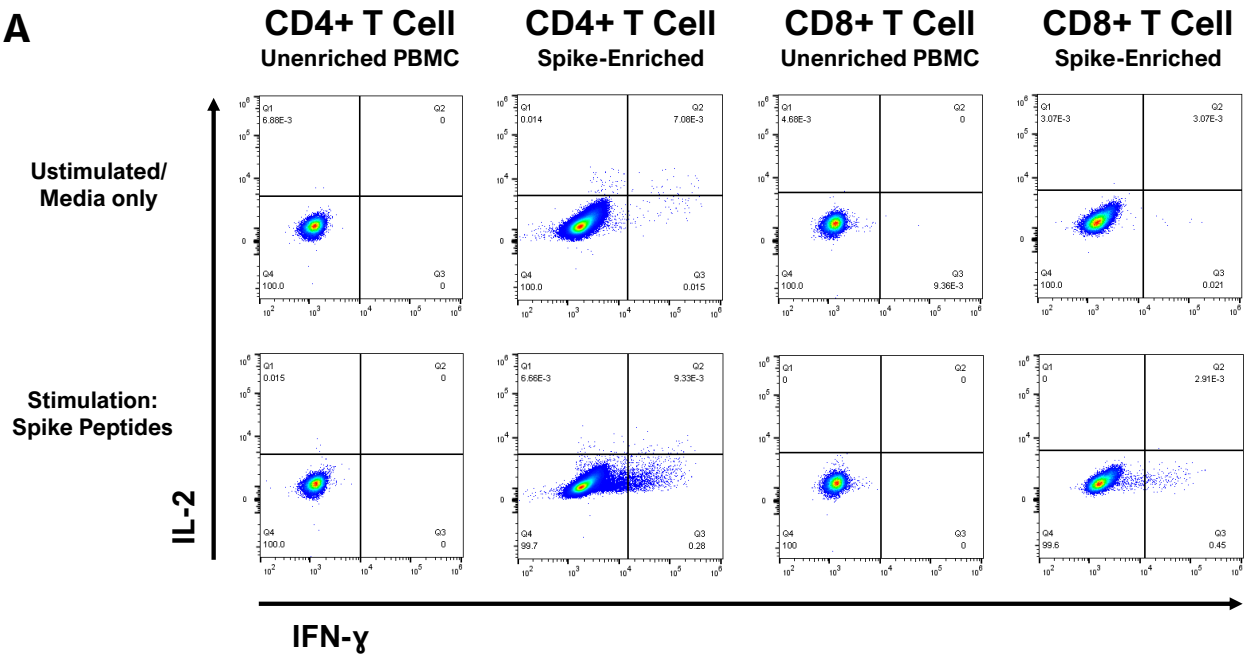

B

CD4⁺ T cells	CD4⁺ T cells	CD8⁺ T cells	CD8⁺ T cells
Condition: Unstimulated PBMC: Unenriched	Condition: Unstimulated mRNA-1273 **enriched**	Condition: Unstimulated PBMC: Unenriched	Condition: Unstimulated mRNA-1273 **enriched**
Condition: +S peptides PBMC: Unenriched	Condition: +S peptides mRNA-1273 **enriched**	Condition: +S peptides PBMC: Unenriched	Condition: +S peptides mRNA-1273 **enriched**

Figure 4-4: Persistence of memory CD4⁺ and CD8⁺ T cell responses against spike revealed by *in vitro* enrichment after culturing PBMC with mRNA-1273 vaccine.

PBMCs were collected from a SARS-CoV-2-naïve subject 128 days after the second dose of the mRNA-1273 vaccine in the two-dose regimen. Unexpanded PBMC were directly tested (first and third columns representing gated CD4⁺ and CD8⁺ T cell populations, respectively) for reactivity against the spike megapool as detailed in Figure 4-2. Additionally, PBMC from the same sample were cultured *in vitro* with the mRNA-1273 vaccine for approximately two weeks to elicit proliferation of spike-specific T cells, which were then assayed in parallel to the unenriched PBMC (second and third columns representing gated CD4⁺ and CD8⁺ T cell populations, respectively) **(A).** Flow conditions from panel A mapped onto a table **(B).**

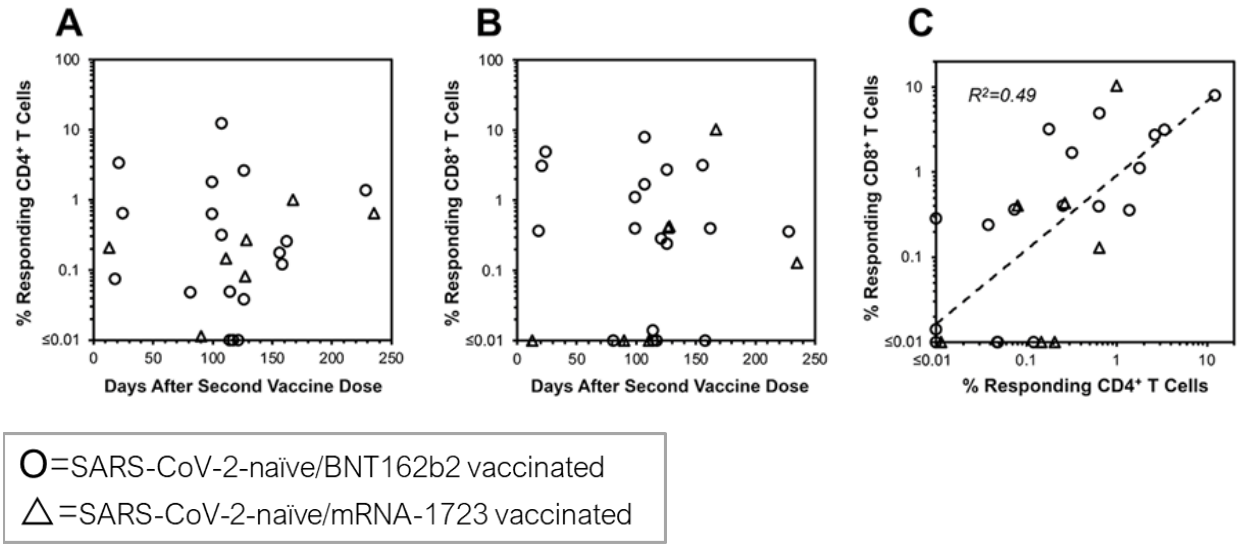

Figure 4-5: Persistent vaccine-elicited CD4⁺ and CD8⁺ T cell memory responses against spike in SARS-CoV-2-naïve persons. (A-C) Samples are derived from the PBMC of the same 22 subjects and 25 timepoints used in Fig. 4-3 A&B, here after *in vitro* culturing with the mRNA-1273 vaccine to enrich for memory T cell responses. Intracellular cytokine staining flow cytometry in response to spike peptides, to characterize memory CD4+ and CD8+ for production of IFN-ɣ (**A&B**, respectively), IL-4 (**Fig. 4-S1, C&D**, respectively), and IL-10 (**Fig. 4-S2, C&D**, respectively). CD4⁺ T cell subset: 22/25 (88.0%) samples greater than 0.01% IFN-ɣ+ (14/18 BNT162b2 vaccinees, circles/O, and 7/7 mRNA-1273 vaccinees, triangles/△). CD8⁺ T cell subset: 18/25 (76.0%) samples greater than 0.01% IFN-ɣ+ (15/18 BNT162b2 vaccinees, circles/O, and 4/7 mRNA-1273 vaccinees, triangles/△). **Panel C:** The relationship between the frequency of CD4+ and CD8+ T cells responding to spike by individual subject.

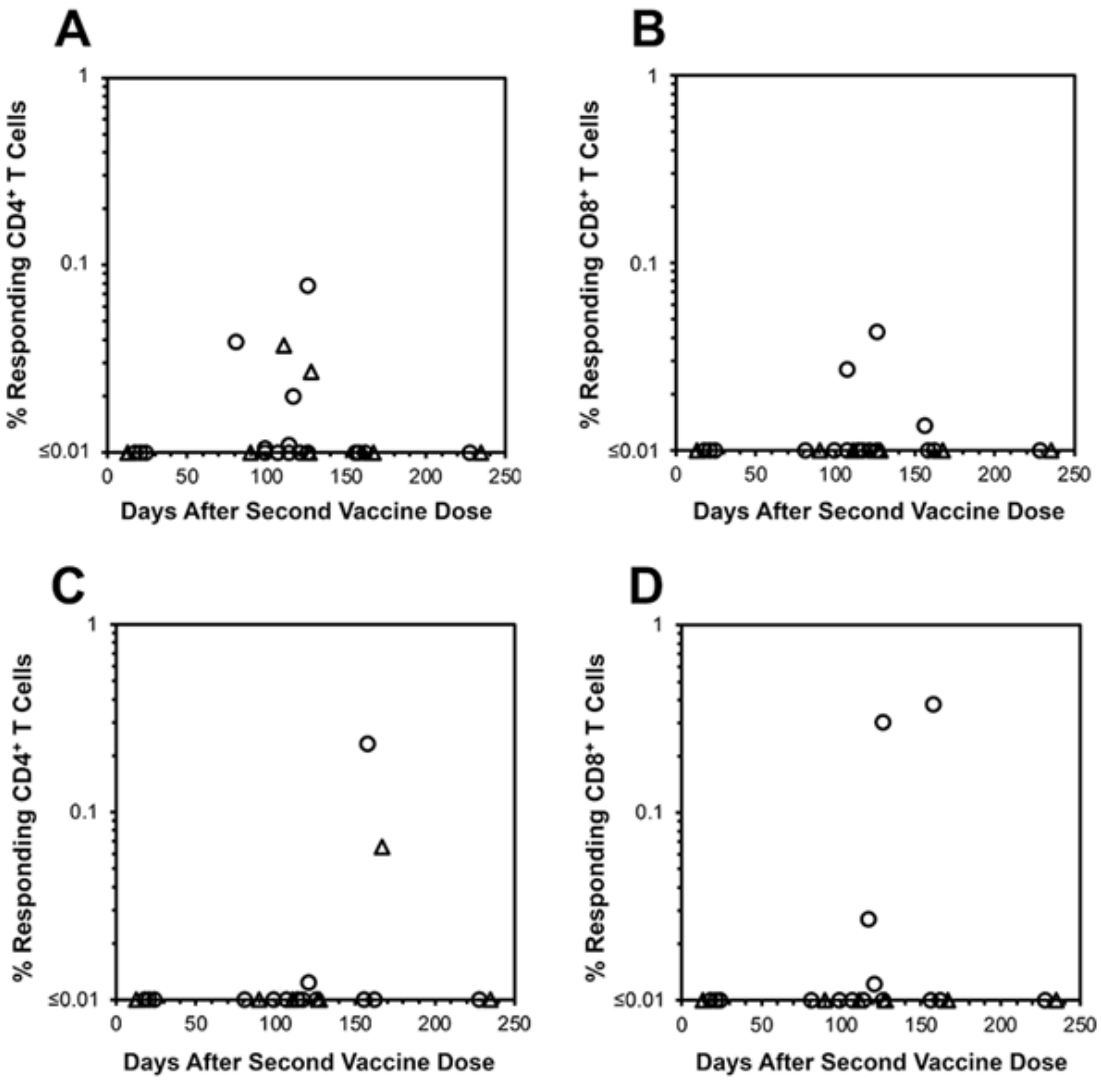

Supplemental Figure 4-S1: Vaccine-elicited CD4$^+$ and CD8$^+$ T cell responses against SARS-CoV-2 spike measured by IL-4 intracellular cytokine staining. In parallel with Fig. 4-3; PBMC from SARS-CoV-2-naïve persons after mRNA vaccination were assessed by intracellular cytokine staining flow cytometry for IL-4 production by CD4$^+$ and CD8$^+$ T cells in response to overlapping peptides spanning spike (spike megapool). Background-subtracted values are plotted. Data are plotted for 22 persons vaccinated with BNT162b2 (18 points from 16 persons, circles/O) or mRNA-1273 (7 points from 6 persons, triangles/△). Time points ranged from 13 to 235 days after the

second vaccine dose. **Panels A & B:** percentage of $CD4^+$ **(A)** and $CD8^+$ **(B)** T cells responding in unenriched PBMC. **Panels C & D:** performed in parallel with Fig. 4-5; percentage of $CD4^+$ **(C)** and $CD8^+$ **(D)** T cells responding after *in vitro* enrichment of PBMC in culture with mRNA-1273.

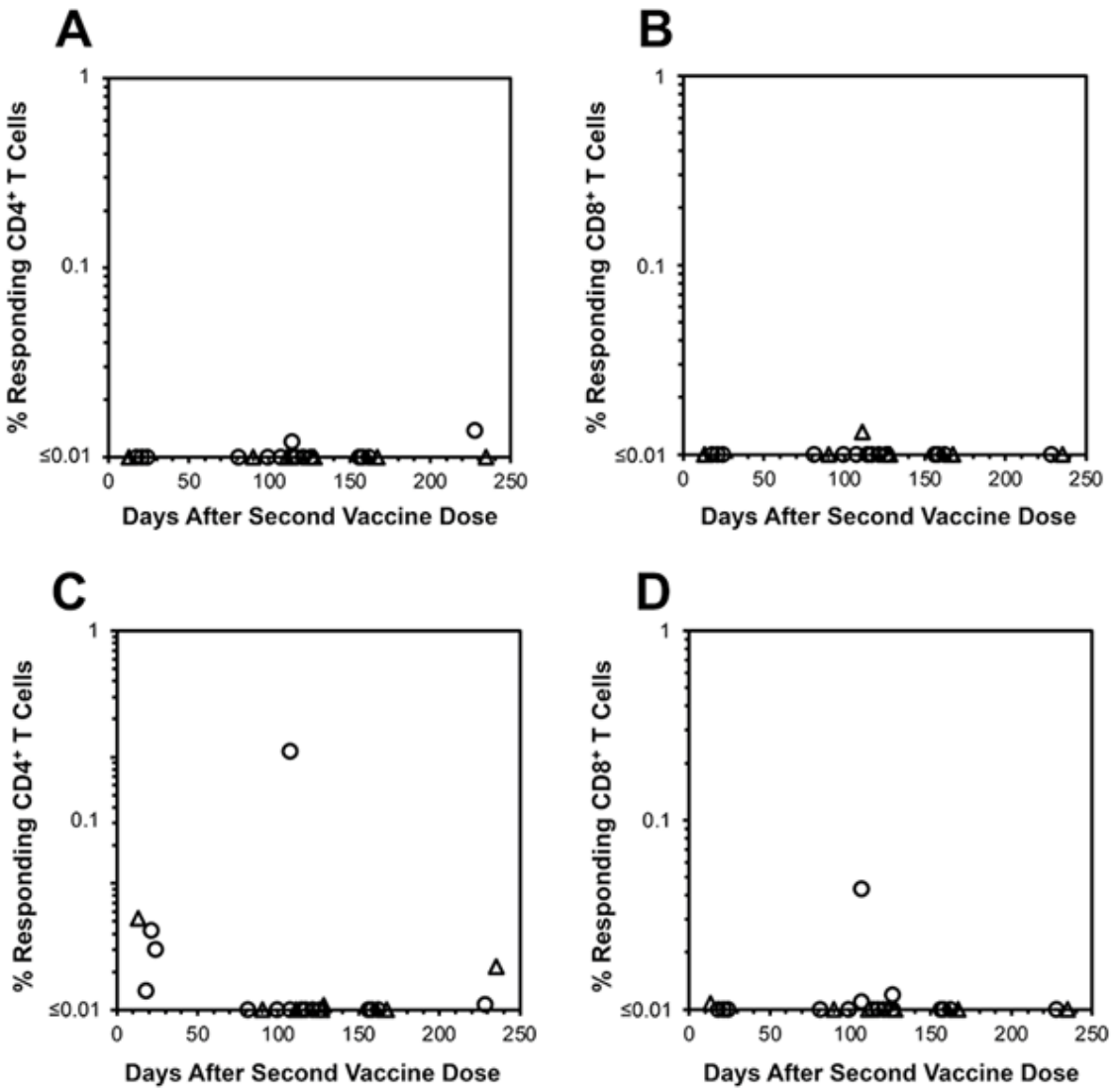

Supplemental Figure 4-S2: Vaccine-elicited CD4⁺ and CD8⁺ T cell responses against SARS-CoV-2 spike measured by IL-10 intracellular cytokine staining.

PBMC from SARS-CoV-2-naïve persons after mRNA vaccination were assessed by intracellular cytokine staining flow cytometry for CD4⁺ and CD8⁺ T cell IL-10 production in response to overlapping peptides spanning spike, in parallel with Fig. 4-3. Background-subtracted values are plotted. Data are plotted for 22 persons vaccinated with BNT162b2 (18 points from 16 persons, circles) or mRNA-1273 (7 points from 6 persons, triangles). Time points ranged from 13 to 235 days after the second vaccine

dose. **Panels A & B:** percentage of $CD4^+$ **(A)** and $CD8^+$ **(B)** T cells responding in unenriched PBMC. **Panels C & D:** performed in parallel with Fig. 4-5; percentage of $CD4^+$ **(C)** and $CD8^+$ **(D)** T cells responding after *in vitro* enrichment of PBMC in culture with mRNA-1273.

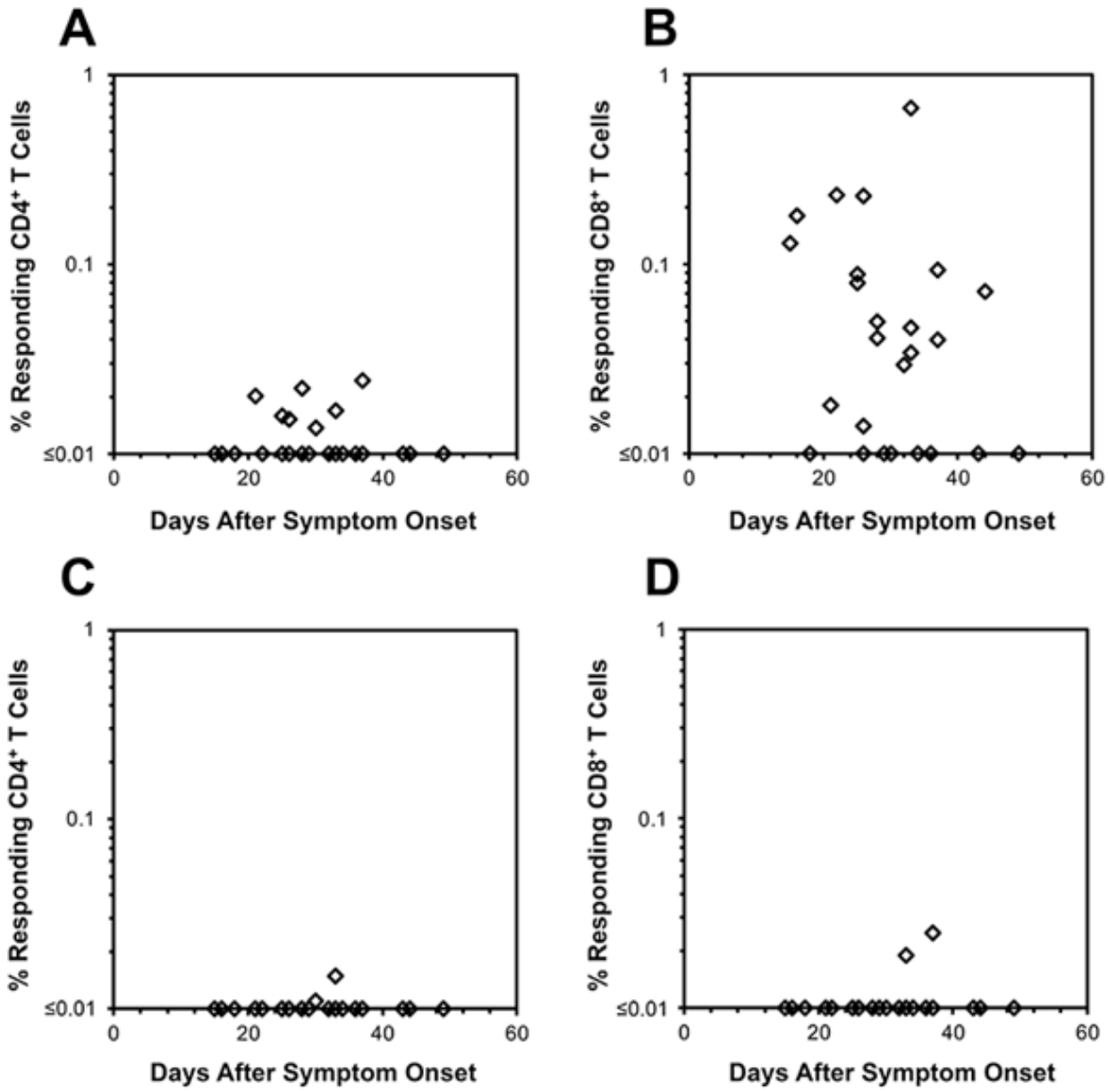

Supplemental Figure 4-S3: CD4$^+$ and CD8$^+$ T cell responses against spike measured by IL-4 and IL-10 intracellular cytokine staining in persons after COVID-19. In parallel with Fig. 4-3; unenriched PBMCs from 25 COVID-19-recovered persons were assessed by ICS flow cytometry for IL-4 and IL-10 production by CD4$^+$ and CD8$^+$ T cells in response to overlapping peptides spanning spike. Background-subtracted values are plotted. **Panels A & B:** IL-4 responses are plotted for CD4$^+$ **(A)** and CD8$^+$ T **(B)** cells. **Panels C & D:** IL-10 responses are plotted for CD4$^+$ **(C)** and CD8$^+$ T **(D)** cells.

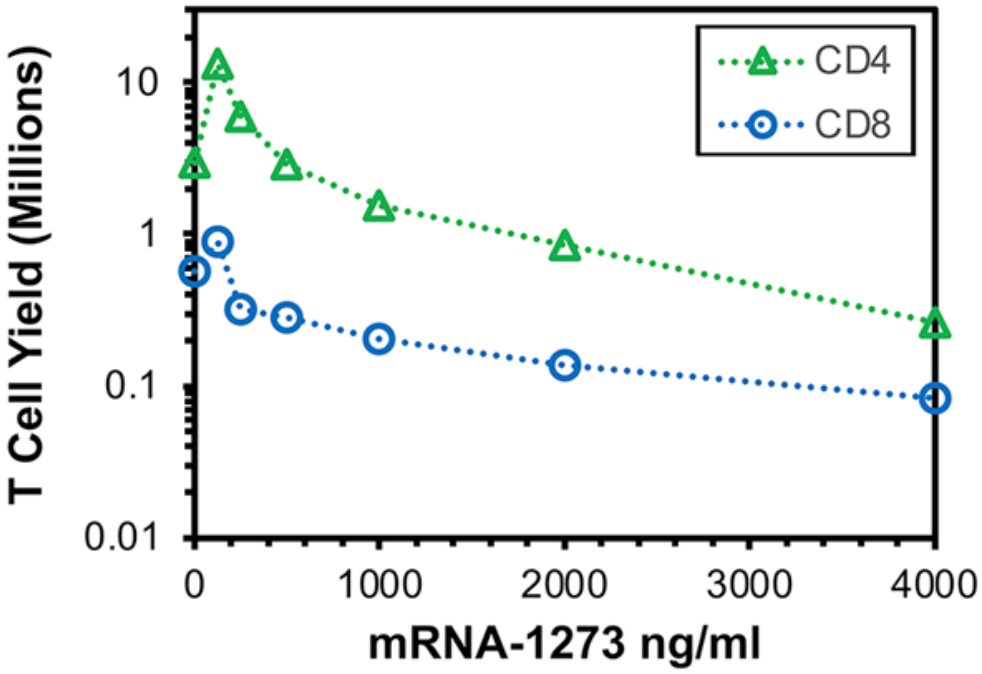

Supplemental Figure 4-S4. Titration of mRNA-1273 culture concentration to enrich spike-responsive memory T cells in PBMC. PBMCs from a SARS-CoV-2-naïve subject who had completed the two dose vaccination series with the BNT162b2 vaccine six months prior were cultured for 14 days with varying concentrations of mRNA-1273 vaccine, starting with 2 x 10^6 cells per condition. Total cell counts and flow cytometry for fractions of $CD4^+$ and $CD8^+$ T cells were then obtained to calculate the yields of these cells. The highest yield was seen for 125 ng/ml added vaccine, with 13.3 x 10^6 $CD4^+$ T cells and 0.9 x 10^6 $CD8^+$ T cells, compared to control cells without stimulus that yielded 3.0 x 10^6 $CD4^+$ T cells and 0.6 x 10^6 $CD8^+$ T cells. A parallel positive control stimulation with an anti-CD3 monoclonal antibody yielded 2.3 x 10^6 $CD4^+$ T cells and 20.0 x 10^6 $CD8^+$ T cells (not plotted), a different pattern of $CD4^+$ T cell expansion relative to $CD8^+$, supporting the specificity of stimulation with mRNA-1273. Evaluation of the resulting cells by IFN-γ ELISpot assays for spike were performed using 2 x 10^5 cells per well (as

described in Methods) on cells stimulated at 125 ng/ml, 250 ng/ml, and 500 ng/ml of mRNA-1273. All of these mRNA-1273-stimulated wells had too many spots to quantify at >400 SFC/well (>2,000 SFC/million cells) although the well with cells stimulated by 125 ng/ml appeared the most saturated; data not shown.

REFERENCES

1. Dan JM, Mateus J, Kato Y, Hastie KM, Yu ED, Faliti CE, et al. Immunological memory to SARS-CoV-2 assessed for up to 8 months after infection. Science. 2021 Feb 5;371(6529):eabf4063.

2. Kared H, Redd AD, Bloch EM, Bonny TS, Sumatoh H, Kairi F, et al. SARS-CoV-2-specific CD8+ T cell responses in convalescent COVID-19 individuals. J Clin Invest. 2021 Mar 1;131(5):145476.

3. Sekine T, Perez-Potti A, Rivera-Ballesteros O, Strålin K, Gorin JB, Olsson A, et al. Robust T Cell Immunity in Convalescent Individuals with Asymptomatic or Mild COVID-19. Cell. 2020 01;183(1):158-168.e14.

4. Zhang Z, Mateus J, Coelho CH, Dan JM, Moderbacher CR, Gálvez RI, et al. Humoral and cellular immune memory to four COVID-19 vaccines. Cell. 2022 Jul 7;185(14):2434-2451.e17.

5. Kingstad-Bakke B, Lee W, Chandrasekar SS, Gasper DJ, Salas-Quinchucua C, Cleven T, et al. Vaccine-induced systemic and mucosal T cell immunity to SARS-CoV-2 viral variants. Proc Natl Acad Sci U S A. 2022 May 17;119(20):e2118312119.

6. Sahin U, Muik A, Vogler I, Derhovanessian E, Kranz LM, Vormehr M, et al. BNT162b2 vaccine induces neutralizing antibodies and poly-specific T cells in humans. Nature. 2021 Jul;595(7868):572–7.

7. Ewer KJ, Barrett JR, Belij-Rammerstorfer S, Sharpe H, Makinson R, Morter R, et al. T cell and antibody responses induced by a single dose of ChAdOx1 nCoV-19 (AZD1222) vaccine in a phase 1/2 clinical trial. Nat Med. 2021 Feb;27(2):270–8.

8. Khoury DS, Cromer D, Reynaldi A, Schlub TE, Wheatley AK, Juno JA, et al. Neutralizing antibody levels are highly predictive of immune protection from symptomatic SARS-CoV-2 infection. Nat Med. 2021 Jul;27(7):1205–11.

9. Ibarrondo FJ, Fulcher JA, Goodman-Meza D, Elliott J, Hofmann C, Hausner MA, et al. Rapid Decay of Anti-SARS-CoV-2 Antibodies in Persons with Mild Covid-19. N Engl J Med. 2020 Sep 10;383(11):1085–7.

10. Iyer AS, Jones FK, Nodoushani A, Kelly M, Becker M, Slater D, et al. Persistence and decay of human antibody responses to the receptor binding domain of SARS-CoV-2 spike protein in COVID-19 patients. Sci Immunol. 2020 Oct 8;5(52):eabe0367.

11. Ibarrondo FJ, Hofmann C, Fulcher JA, Goodman-Meza D, Mu W, Hausner MA, et al. Primary, Recall, and Decay Kinetics of SARS-CoV-2 Vaccine Antibody Responses. ACS Nano. 2021 Jul 27;15(7):11180–91.

12. Goldberg Y, Mandel M, Bar-On YM, Bodenheimer O, Freedman L, Haas EJ, et al. Waning Immunity after the BNT162b2 Vaccine in Israel. N Engl J Med. 2021 Dec 9;385(24):e85.

13. Koutsakos M, Lee WS, Reynaldi A, Tan HX, Gare G, Kinsella P, et al. The magnitude and timing of recalled immunity after breakthrough infection is shaped by SARS-CoV-2 variants. Immunity. 2022 Jul 12;55(7):1316-1326.e4.

14. Beaudoin-Bussières G, Laumaea A, Anand SP, Prévost J, Gasser R, Goyette G, et al. Decline of Humoral Responses against SARS-CoV-2 Spike in Convalescent Individuals. mBio. 2020 Oct 16;11(5):e02590-20.

15. Ssentongo P, Ssentongo AE, Voleti N, Groff D, Sun A, Ba DM, et al. SARS-CoV-2 vaccine effectiveness against infection, symptomatic and severe COVID-19: a systematic review and meta-analysis. BMC Infect Dis. 2022 May 7;22(1):439.

16. Chemaitelly H, Tang P, Hasan MR, AlMukdad S, Yassine HM, Benslimane FM, et al. Waning of BNT162b2 Vaccine Protection against SARS-CoV-2 Infection in Qatar. N Engl J Med. 2021 Dec 9;385(24):e83.

17. Murali-Krishna K, Altman JD, Suresh M, Sourdive DJD, Zajac AJ, Miller JD, et al. Counting Antigen-Specific CD8 T Cells: A Reevaluation of Bystander Activation during Viral Infection. Immunity. 1998 Feb 1;8(2):177–87.

18. Akondy RS, Monson ND, Miller JD, Edupuganti S, Teuwen D, Wu H, et al. The Yellow Fever Virus Vaccine Induces a Broad and Polyfunctional Human Memory CD8+ T Cell Response. J Immunol Baltim Md 1950. 2009 Dec 15;183(12):7919–30.

19. Rogers PR, Dubey C, Swain SL. Qualitative changes accompany memory T cell generation: faster, more effective responses at lower doses of antigen. J Immunol Baltim Md 1950. 2000 Mar 1;164(5):2338–46.

20. Wherry EJ, Teichgräber V, Becker TC, Masopust D, Kaech SM, Antia R, et al. Lineage relationship and protective immunity of memory CD8 T cell subsets. Nat Immunol. 2003 Mar;4(3):225–34.

21. Hammarlund E, Lewis MW, Hansen SG, Strelow LI, Nelson JA, Sexton GJ, et al. Duration of antiviral immunity after smallpox vaccination. Nat Med. 2003 Sep;9(9):1131–7.

22. Kumar A, Meldgaard TS, Bertholet S. Novel Platforms for the Development of a Universal Influenza Vaccine. Front Immunol. 2018;9:600.

23. Natoli G, Ostuni R. Adaptation and memory in immune responses. Nat Immunol. 2019 Jul;20(7):783–92.

24. Bhattacharya D. Instructing durable humoral immunity for COVID-19 and other vaccinable diseases. Immunity. 2022 Jun 14;55(6):945–64.

25. Taus E, Hofmann C, Ibarrondo FJ, Hausner MA, Fulcher JA, Krogstad P, et al. Dominant CD8+ T Cell Nucleocapsid Targeting in SARS-CoV-2 Infection and Broad Spike Targeting From Vaccination. Front Immunol [Internet]. 2022 [cited 2022 Apr 18];13. Available from: https://www.frontiersin.org/article/10.3389/fimmu.2022.835830

26. Stankov MV, Cossmann A, Bonifacius A, Dopfer-Jablonka A, Ramos GM, Gödecke N, et al. Humoral and cellular immune responses against SARS-CoV-2 variants and human coronaviruses after single BNT162b2 vaccination. Clin Infect Dis Off Publ Infect Dis Soc Am. 2021 Jun 16;ciab555.

27. Angyal A, Longet S, Moore SC, Payne RP, Harding A, Tipton T, et al. T-cell and antibody responses to first BNT162b2 vaccine dose in previously infected and SARS-CoV-2-naive UK health-care workers: a multicentre prospective cohort study. Lancet Microbe. 2022 Jan;3(1):e21–31.

28. Oberhardt V, Luxenburger H, Kemming J, Schulien I, Ciminski K, Giese S, et al. Rapid and stable mobilization of CD8+ T cells by SARS-CoV-2 mRNA vaccine. Nature. 2021 Sep;597(7875):268–73.

29. Tarke A, Coelho CH, Zhang Z, Dan JM, Yu ED, Methot N, et al. SARS-CoV-2 vaccination induces immunological T cell memory able to cross-recognize variants from Alpha to Omicron. Cell. 2022 Mar 3;185(5):847-859.e11.

30. Mateus J, Dan JM, Zhang Z, Rydyznski Moderbacher C, Lammers M, Goodwin B, et al. Low-dose mRNA-1273 COVID-19 vaccine generates durable memory enhanced by cross-reactive T cells. Science. 2021 Oct 22;374(6566):eabj9853.

31. Bennett MS, Ng HL, Dagarag M, Ali A, Yang OO. Epitope-Dependent Avidity Thresholds for Cytotoxic T-Lymphocyte Clearance of Virus-Infected Cells. J Virol. 2007 May 15;81(10):4973–80.

32. Bennett MS, Joseph A, Ng HL, Goldstein H, Yang OO. Fine-tuning of T-cell receptor avidity to increase Hiv epitope variant recognition by cytotoxic T lymphocytes. Aids. 2010 Nov 13;24(17):2619–28.

33. Agarwal A, Mukherjee A, Kumar G, Chatterjee P, Bhatnagar T, Malhotra P, et al. Convalescent plasma in the management of moderate covid-19 in adults in India: open label phase II multicentre randomised controlled trial (PLACID Trial). BMJ. 2020 Oct 22;371:m3939.

34. Simonovich VA, Burgos Pratx LD, Scibona P, Beruto MV, Vallone MG, Vázquez C, et al. A Randomized Trial of Convalescent Plasma in Covid-19 Severe Pneumonia. N Engl J Med. 2021 Feb 18;384(7):619–29.

35. Janiaud P, Axfors C, Schmitt AM, Gloy V, Ebrahimi F, Hepprich M, et al. Association of Convalescent Plasma Treatment With Clinical Outcomes in Patients With COVID-19: A Systematic Review and Meta-analysis. JAMA. 2021 Mar 23;325(12):1185–95.

36. Ibarrondo FJ, Anton PA, Fuerst M, Ng HL, Wong JT, Matud J, et al. Parallel human immunodeficiency virus type 1-specific CD8+ T-lymphocyte responses in blood and mucosa during chronic infection. J Virol. 2005 Apr;79(7):4289–97.

37. Jones N, Agrawal D, Elrefaei M, Hanson A, Novitsky V, Wong JT, et al. Evaluation of antigen-specific responses using in vitro enriched T cells. J Immunol Methods. 2003 Mar 1;274(1–2):139–47.

38. Jäger M, Sonnleitner ST, Dichtl S, Lafon E, Diem G, Walder G, et al. Immune Responses Against SARS-CoV-2 WT and Delta Variant in Elderly BNT162b2 Vaccinees. Front Immunol. 2022;13:868361.

39. Agrati C, Castilletti C, Goletti D, Meschi S, Sacchi A, Matusali G, et al. Coordinate Induction of Humoral and Spike Specific T-Cell Response in a Cohort of Italian Health Care Workers Receiving BNT162b2 mRNA Vaccine. Microorganisms. 2021 Jun 16;9(6):1315.

40. Yamashita K, Suzuki A, Takebayashi S, Toguchi A, Ogitani K, Niizeki N, et al. Differential Dynamics of Humoral and Cell-Mediated Immunity with Three Doses of BNT162b2 SARS-CoV-2 Vaccine in Healthcare Workers in Japan: A Prospective Cohort Study. Vaccines (Basel). 2022 Jun 30;10(7):1050.

41. Phillips E, Adele S, Malone T, Deeks A, Stafford L, Dobson SL, et al. Comparison of two T-cell assays to evaluate T-cell responses to SARS-CoV-2 following vaccination in naïve and convalescent healthcare workers. Clin Exp Immunol. 2022 Jul 22;209(1):90–8.

42. Aiello A, Coppola A, Vanini V, Petrone L, Cuzzi G, Salmi A, et al. Accuracy of QuantiFERON SARS-CoV-2 RUO assay and characterization of the CD4+ and CD8+ T-cell-SARS-CoV-2 response: comparison with a homemade IFN-γ release assay. Int J Infect Dis. 2022 Jul 22;S1201-9712(22)00444-1.

43. Geers D, Shamier MC, Bogers S, den Hartog G, Gommers L, Nieuwkoop NN, et al. SARS-CoV-2 variants of concern partially escape humoral but not T-cell responses in COVID-19 convalescent donors and vaccinees. Sci Immunol. 2021 May 25;6(59):eabj1750.

44. Atmar RL, Lyke KE, Deming ME, Jackson LA, Branche AR, El Sahly HM, et al. Homologous and Heterologous Covid-19 Booster Vaccinations. N Engl J Med. 2022 Mar 17;386(11):1046–57.

45. Lozano-Rodríguez R, Valentín-Quiroga J, Avendaño-Ortiz J, Martín-Quirós A, Pascual-Iglesias A, Terrón-Arcos V, et al. Cellular and humoral functional responses after BNT162b2 mRNA vaccination differ longitudinally between naive and subjects recovered from COVID-19. Cell Rep. 2022 Jan 11;38(2):110235.

46. Gil-Manso S, Carbonell D, López-Fernández L, Miguens I, Alonso R, Buño I, et al. Induction of High Levels of Specific Humoral and Cellular Responses to SARS-CoV-2 After the Administration of Covid-19 mRNA Vaccines Requires Several Days. Front Immunol. 2021;12:726960.

47. Zhang Z, Mateus J, Coelho CH, Dan JM, Moderbacher CR, Gálvez RI, et al. Humoral and cellular immune memory to four COVID-19 vaccines. Cell. 2022 Jul 7;185(14):2434-2451.e17.

Chapter 5: Conclusions and Discussion

SUMMARY & KEY FINDINGS

In this dissertation, we sought to more deeply understand the behaviors and characteristics of T cells arising from vaccination and natural infection. In chapter 2, we presented an analysis of clonal CD8+ T cell responses elicited in a T cell-based vaccine for HIV-1. In chapters 3 and 4 we reported our characterization of T cell responses following SARS-CoV-2 infection and in response to SARS-CoV-2 mRNA vaccination in healthy subjects.

Antiviral activity of CTL clones from an HIV-1 vaccine trial

We began by assessing CD8+ cytotoxic T lymphocyte (CTL) clones elicited by the Mrk/Ad5 vaccine, which had been intended to provide cell-based immunity against the human immunodeficiency virus (HIV-1) (4). In an effort to help elucidate the reasons behind the failure of the vaccine, we evaluated CTL clones for antiviral capabilities and cross-reactivity to common variants of their cognate epitope.

While the antiviral effects of CTL may not be exclusively cytolytic, cytotoxicity is the main mechanism by which CTL help contain and clear viral infections(5–7). Therefore, we first tested whether clones were able to kill HLA-matched target cells infected with replicative virus bearing the vaccine variant of their cognate epitope. All CTL clones were able to kill target cells under these conditions and mostly exhibited high killing efficiency, although three clones targeting A*24-restricted KW9 Gag (KYKLKHIVW) exhibited a gradient of killing efficiencies.

When tested against additional common epitope variants, all clones displayed a low degree of cross-reactivity, with most clones responding to either the virus bearing

the vaccine sequence only, or the vaccine sequence and one additional variant. We saw a pattern generally consistent with this narrow reactivity when we assessed the CTL clones for virus inhibition. The three clones targeting KW9 exhibited a gradient of suppressive capacity that corresponded to their killing efficiencies. Overall, these results suggested that the Mrk/Ad5 vaccine elicited CTL clones capable of antiviral functions, but that these clones exhibited limited cross-reactivity to epitope variants and differed in efficiency of antiviral functions.

T cell responses after SARS-CoV-2 infection or mRNA vaccination

In the two following chapters, we characterized the $CD4^+$ and $CD8^+$ T cell responses in SARS-CoV-2-convalescent subjects and in healthy, SARS-CoV-2-naïve individuals after mRNA vaccination.

We first evaluated T cell responses in COVID-19-convalescent individuals shortly after SARS-CoV-2 infection and in the months following. Most subjects in the study had clinically mild disease, meaning supplemental oxygen was not required, although a few subjects with severe disease were also included. Testing responses *in vitro* to peptide 'megapools' (8) by intracellular cytokine staining (ICS) flow cytometry, we found that the majority of subjects developed both $CD4^+$ and $CD8^+$ T cells responses, and that T cell help was generally characterized by a Th1 bias, in agreement with several other reports (9,10). We then analyzed the $CD8^+$ T cell compartment in greater detail by testing polyclonally expanded CD8+ T cells in IFN-ɣ ELISpot against smaller peptide pools covering the SARS-CoV-2 structural proteins spike, nucleocapsid, membrane, and envelope. Between all subjects, we found CD8+ T cells responded to all pools, except

envelope, and that CTL nucleocapsid responses were immunodominant in terms of density (number of subjects responding per pool) and intensity (strength of response to each pool). When responses were analyzed longitudinally, we found distinct decay rates of CTL based on protein specificity, and that CTL responding to N persisted longest on average. In subjects who were subsequently vaccinated, responses to N and M pools were generally stable or declined, while CTL responses against spike pools increased. Comparing similarity in targeted pools after vaccination suggested specific boosting of prior responses by the vaccines.

We then performed IFN-ɣ ELISpot on polyclonally expanded $CD8^+$ T cells derived from samples collected shortly after initial vaccination in SARS-CoV-2-naïve individuals. We found that all subjects had CTL responses to at least one pool, with an average of over 4 pools per person, and that targeting was broadly distributed across the spike protein. When we compared spike-specific CTL responses after natural infection with responses elicited by SARS-CoV-2 vaccination, we saw similar patterns of immunogenicity and immunodominance.

We next expanded this testing to additional timepoints to examine the kinetics of CTL responses to spike after SARS-CoV-2 mRNA vaccination in healthy, SARS-CoV-2-naïve individuals. Assessing detailed timepoints around and during vaccination for two subjects revealed rapid rise and sharp drops in spike-specific CTL levels shortly after vaccination. In contrast, analysis on a similarly detailed timeline of CTL responses in a person who received a recombinant adenovirus-vectored vaccine showed a more gradual rise and decline in spike-specific CTL levels, while patterns of anti-RBD antibodies were similar between all three subjects. Cross sectional analysis from

additional SARS-CoV-2-naïve individuals receiving mRNA agreed with findings that levels of circulating spike-specific CTL rise quickly after vaccination and then drop sharply.

Looking for evidence of memory T cell responses in the months following mRNA vaccination in SARS-CoV-2-naïve individuals, we tested PBMC by ICS for responses to a spike megapool. Most COVID-19-convalesent individuals had detectable responses for both CD4+ and CD8+ T cells in the first 50 days after symptom onset. However, when assessed by the same techniques and cutoffs, samples from mRNA vaccinated SARS-CoV-2-naïve subjects were almost all negative.

In order to test for memory T cells that were present at levels below the limits of detection that we had established previously, we developed a method of enriching spike-specific T cells by culturing PBMC with the mRNA-1273 vaccine. Applying this method to samples spanning several months after vaccination revealed both $CD4^+$ and $CD8^+$ spike-specific T cells in most subjects and timepoints. Overall, these data suggest that circulating T cells elicited by SARS-CoV-2 mRNA vaccines, after an initial peak 1-2 weeks after vaccination, rapidly contract to a memory population that persists for at least several months.

SIGNIFICANCE & IMPLICATIONS

While CTL responses to HIV-1 are not curative, they can be highly effective at suppressing infection (11–13) and have been shown to be capable of providing protective immunity in some non-human primate models (14,15). Whether they can

provide protection on their own is unclear, but they will likely be a key element of any protective immune response.

The Mrk/Ad5 vaccine was intended to elicit a CTL response against HIV-1—one of the most variable pathogens humans have ever faced. However, the clones we tested suggest that the vaccine ultimately elicited CTL with narrow reactivity to epitope variants. While this sample size is very limited, it does bring to focus the care that must be taken in designing future vaccines for HIV-1 and other pathogens that present extreme antigenic diversity. With the introduction of highly effective antiretroviral therapies, the biggest challenge to a curing HIV-1 infection is the latent reservoir. While HIV-1 poses many challenges in terms of protective immunity, the heterogeneity of sequences is likely the main barrier. For CTL responses, it is crucial to understand the potential breadth of targeting antigenic variants, both in terms of clonal responses and polyclonal responses. The Mrk/Ad5 vaccine only used a single variant for the gag, pol, and nef genes it introduced, which likely had functional consequences for the CTL it induced, as shown in chapter 2. There is evidence that it is possible to engineer vaccines to help focus immune responses to more conserved regions (16–19), and other studies have shown the possibility of inducing CTL that can respond more broadly (20–22). An effective CTL-based vaccine will almost certainly require both of these factors to be executed at a high level, ideally inducing CTL that are directed towards epitopes in more conserved regions, and which can respond to the majority of frequent variants in those epitopes.

Relative to the challenge of HIV, developing effective vaccines against SARS-CoV-2 was incredibly simple. Nevertheless, challenges still remain, variants continue to

arise, and the future of the COVID-19 pandemic is not yet determined. While many have remained focused on maintaining immune responses in the population that prevent any form of infection, this simply is not practical given the current availability of highly effective vaccines and therapeutics. The ‘absolute’ protection conferred in the early weeks or months following SARS-CoV-2 vaccination have been correlated with antibody levels. Antibody levels wane rapidly after vaccination and/or infection, and many variants of concern seem to have reduced susceptibility to previously induced antibody responses. Protection against severe disease and death, however, is largely maintained for many months, so it clearly is of value to understand and improve upon all areas of immunity that contribute to this. As T cells are a key component of antiviral immunity, they should be utilized as fully as possible.

The mutation rate of SARS-CoV-2 is laughable in comparison to HIV-1. This relative stability means that even in the face of variants, prior immunity is highly effective at preventing subsequent severe disease or death. This has been achieved while using only a portion of the virus, and the one that is under the most immune pressure. Based on our work published earlier this year (23), CTL responses to the nucleocapsid protein are highly immunodominant and largely persist significantly longer than CTL responses to across spike. While the CTL response to matrix protein pools waned relatively rapidly, matrix was also found to be highly immunogenic. Broadening the T cell response to include additional SARS-CoV-2 proteins outside of spike has the potential to increase the number of people who develop CTL responses, broaden the response across the viral genome to increase the chances of intact immunity in the face of mutated variants, and potentially lead to longer-lasting CTL responses. Even though

SARS-CoV-2 has caused millions of deaths worldwide in a span of less than three years, we are incredibly fortunate to live in a time when the science and technology already exists to allow for the development, testing, and release of extremely effective vaccines in such a short period of time. CTL elicited in SARS-CoV-2 vaccines have likely played an important role preventing suffering and death during this pandemic, and it would likely serve us well to arm ourselves with all the immunity we can.

Additionally, the efficacy we saw in using the mRNA vaccine *in vitro* to enrich a T cell population against a specific antigen is very exciting. This enabled us to detect responding T cells that were in PBMC that we could not detect by other methods. This seems like a very promising technique that might allow for detection and expansion of low frequency cells with a given specificity. While this can be done with exogenously added peptides, having the proteins processed and peptides loaded on MHC will likely prove superior, as the peptides are processed and loaded in fragments of the same length as was used to elicit them (for example, a 15mer might not have a good fit to present a particular 9mer epitope, thereby altering the efficiency of that particular TCR-pMHC complex).

The work presented in chapter 3 has been published with the following citation:

Taus E, Hofmann C, Ibarrondo FJ, Hausner MA, Fulcher JA, Krogstad P, Ferbas KG, Tobin NH, Rimoin AW, Aldrovandi GM, Yang OO. Dominant $CD8^+$ T Cell Nucleocapsid Targeting in SARS-CoV-2 Infection and Broad Spike Targeting From Vaccination. Front Immunol. 2022 Feb 22;13:835830. doi: 10.3389/fimmu.2022.835830. PMID: 35273611; PMCID: PMC8902813.

The work presented in chapter 4 is currently in preparation for submission.

References

1. Angyal A, Longet S, Moore SC, Payne RP, Harding A, Tipton T, et al. T-cell and antibody responses to first BNT162b2 vaccine dose in previously infected and SARS-CoV-2-naive UK health-care workers: a multicentre prospective cohort study. Lancet Microbe. 2022 Jan;3(1):e21–31.

2. Jäger M, Sonnleitner ST, Dichtl S, Lafon E, Diem G, Walder G, et al. Immune Responses Against SARS-CoV-2 WT and Delta Variant in Elderly BNT162b2 Vaccinees. Front Immunol. 2022;13:868361.

3. Agrati C, Castilletti C, Goletti D, Meschi S, Sacchi A, Matusali G, et al. Coordinate Induction of Humoral and Spike Specific T-Cell Response in a Cohort of Italian Health Care Workers Receiving BNT162b2 mRNA Vaccine. Microorganisms. 2021 Jun 16;9(6):1315.

4. Buchbinder SP, Mehrotra DV, Duerr A, Fitzgerald DW, Mogg R, Li D, et al. Efficacy assessment of a cell-mediated immunity HIV-1 vaccine (the Step Study): a double-blind, randomised, placebo-controlled, test-of-concept trial. Lancet. 2008 Nov 29;372(9653):1881–93.

5. Borrow P, Lewicki H, Hahn BH, Shaw GM, Oldstone MB. Virus-specific CD8+ cytotoxic T-lymphocyte activity associated with control of viremia in primary human immunodeficiency virus type 1 infection. J Virol. 1994 Sep;68(9):6103–10.

6. Schmitz JE, Kuroda MJ, Santra S, Sasseville VG, Simon MA, Lifton MA, et al. Control of Viremia in Simian Immunodeficiency Virus Infection by CD8+ Lymphocytes. Science. 1999 Feb 5;283(5403):857–60.

7. Yang OO, Kalams SA, Rosenzweig M, Trocha A, Jones N, Koziel M, et al. Efficient lysis of human immunodeficiency virus type 1-infected cells by cytotoxic T lymphocytes. J Virol. 1996 Sep 1;70(9):5799–806.

8. Grifoni A, Sidney J, Zhang Y, Scheuermann RH, Peters B, Sette A. A Sequence Homology and Bioinformatic Approach Can Predict Candidate Targets for Immune Responses to SARS-CoV-2. Cell Host Microbe. 2020 Apr 8;27(4):671-680.e2.

9. Dan JM, Mateus J, Kato Y, Hastie KM, Yu ED, Faliti CE, et al. Immunological memory to SARS-CoV-2 assessed for up to 8 months after infection. Science. 2021 Feb 5;371(6529):eabf4063.

10. Weiskopf D, Schmitz KS, Raadsen MP, Grifoni A, Okba NMA, Endeman H, et al. Phenotype and kinetics of SARS-CoV-2-specific T cells in COVID-19 patients with acute respiratory distress syndrome. Sci Immunol. 2020 Jun 26;5(48):eabd2071.

11. Kaslow RA, Carrington M, Apple R, Park L, Muñoz A, Saah AJ, et al. Influence of combinations of human major histocompatibility complex genes on the course of HIV-1 infection. Nat Med. 1996 Apr;2(4):405–11.

12. Pereyra F, Heckerman D, Carlson JM, Kadie C, Soghoian DZ, Karel D, et al. HIV control is mediated in part by CD8+ T-cell targeting of specific epitopes. J Virol. 2014 Nov;88(22):12937–48.

13. Betts MR, Nason MC, West SM, De Rosa SC, Migueles SA, Abraham J, et al. HIV nonprogressors preferentially maintain highly functional HIV-specific CD8+ T cells. Blood. 2006 Jun 15;107(12):4781–9.

14. Barouch DH, Liu J, Li H, Maxfield LF, Abbink P, Lynch DM, et al. Vaccine protection against acquisition of neutralization-resistant SIV challenges in rhesus monkeys. Nature. 2012 Jan 4;482(7383):89–93.

15. Adnan S, Reeves RK, Gillis J, Wong FE, Yu Y, Camp JV, et al. Persistent Low-Level Replication of SIVΔnef Drives Maturation of Antibody and CD8 T Cell Responses to Induce Protective Immunity against Vaginal SIV Infection. PLOS Pathog. 2016 Dec 13;12(12):e1006104.

16. Borthwick N, Ahmed T, Ondondo B, Hayes P, Rose A, Ebrahimsa U, et al. Vaccine-elicited human T cells recognizing conserved protein regions inhibit HIV-1. Mol Ther J Am Soc Gene Ther. 2014 Feb;22(2):464–75.

17. Kulkarni V, Valentin A, Rosati M, Alicea C, Singh AK, Jalah R, et al. Altered response hierarchy and increased T-cell breadth upon HIV-1 conserved element DNA vaccination in macaques. PloS One. 2014;9(1):e86254.

18. Yang OO, Ali A, Kasahara N, Faure-Kumar E, Bae JY, Picker LJ, et al. Short Conserved Sequences of HIV-1 Are Highly Immunogenic and Shift Immunodominance. J Virol. 2015 Jan 15;89(2):1195–204.

19. B M, C M, A SB, P C, S ML, Mc P, et al. Therapeutic Vaccination Refocuses T-cell Responses Towards Conserved Regions of HIV-1 in Early Treated Individuals (BCN 01 study). EClinicalMedicine [Internet]. 2019 Jun 5 [cited 2022 Aug 13];11. Available from: https://pubmed.ncbi.nlm.nih.gov/31312806/

20. Korber B, Hraber P, Wagh K, Hahn BH. Polyvalent vaccine approaches to combat HIV-1 diversity. Immunol Rev. 2017 Jan;275(1):230–44.

21. Barouch DH, Tomaka FL, Wegmann F, Stieh DJ, Alter G, Robb ML, et al. Evaluation of a mosaic HIV-1 vaccine in a multicentre, randomised, double-blind, placebo-controlled, phase 1/2a clinical trial (APPROACH) and in rhesus monkeys (NHP 13-19). Lancet Lond Engl. 2018 21;392(10143):232–43.

22. Chen SMY, Wong YC, Yim LY, Zhang H, Wang H, Lui GCY, et al. Enhanced Cross-Reactive and Polyfunctional Effector-Memory T Cell Responses by ICVAX-a Human

PD1-Based Bivalent HIV-1 Gag-p41 Mosaic DNA Vaccine. J Virol. 2022 Apr 13;96(7):e0216121.

23. Taus E, Hofmann C, Ibarrondo FJ, Hausner MA, Fulcher JA, Krogstad P, et al. Dominant CD8+ T Cell Nucleocapsid Targeting in SARS-CoV-2 Infection and Broad Spike Targeting From Vaccination. Front Immunol [Internet]. 2022 [cited 2022 Apr 18];13. Available from: https://www.frontiersin.org/article/10.3389/fimmu.2022.835830